UNIVERSIDADE FEDERAL DE MINAS GERAIS

Programa de Pós-Graduação em Engenharia Metalúrgica, Materiais e de Minas

TESE DE DOUTORADO

Síntese de zeólita analcima de elevada pureza e cristalinidade a partir de pó de vidro e lama de anodização de alumínio pela abordagem estatística de Plackett Burman

Autor: Luciano Fernandes de Magalhães

Orientador: Prof. PhD. Antônio Eduardo Clark Peres

Coorientador: Prof. PhD. Gilberto Rodrigues da Silva

Fevereiro/2022

UNIVERSIDADE FEDERAL DE MINAS GERAIS

Programa de Pós-Graduação em Engenharia Metalúrgica, Materiais e de Minas

Luciano Fernandes de Magalhães

TESE DE DOUTORADO

Síntese de zeólita analcima de elevada pureza e cristalinidade a partir de pó de vidro e lama de anodização de alumínio pela abordagem estatística de Plackett Burman

Tese apresentada ao Programa de Pós-Graduação em Engenharia Metalúrgica, Materiais e de Minas da Escola de Engenharia da Universidade Federal de Minas Gerais, como requisito parcial para obtenção do Grau de Doutor em Engenharia Metalúrgica, Materiais e de Minas

Área de concentração: Tecnologia Mineral

Orientador: Prof. PhD. Antônio Eduardo Clark Peres

Coorientador: Prof. PhD. Gilberto Rodrigues da Silva

Fevereiro/2022

Magalhães, Luciano Fernandes de.
M188s Síntese de zeólita analcima de eleva pureza e cristalinidade a partir de pó de vidro e lama de anodização de alumínio pela abordagem estatística de Plackett Burman [recurso eletrônico] / Luciano Fernandes de Magalhães. – 2022.
1 recurso online (xii, 92 f.: il., color.): pdf.

Orientador: Antônio Eduardo Clark Peres.
Coorientador: Gilberto Rodrigues da Silva.

Tese (doutorado) - Universidade Federal de Minas Gerais, Escola de Engenharia.

Inclui bibliografia.
Exigências do sistema: Adobe Acrobat Reader.

1. Engenharia de Minas - Teses. 2. Tecnologia mineral - Teses. 3. Anodização – Teses. 4. Resíduos industriais – Teses. 5. Zeólitos - Teses I. Peres, Antônio Eduardo Clark. II. Silva, Gilberto Rodrigues da. III. Universidade Federal de Minas Gerais. Escola de Engenharia. IV. Título.

CDU: 622(043)

Ficha catalográfica elaborada pela bibliotecária Letícia Alves Vieira – CRB-6/2337
Biblioteca Prof. Mário Werneck - Escola de Engenharia da UFMG

FOLHA DE APROVAÇÃO

UNIVERSIDADE FEDERAL DE MINAS GERAIS
ESCOLA DE ENGENHARIA
Programa de Pós-Graduação em Engenharia Metalúrgica, Materiais e de Minas

PPGEM

Tese intitulada **"Síntese de Zeólita Analcima de Elevada Pureza e Cristalinidade a Partir de Pó de Vidro e Lama de Anodização de Alumínio Pela Abordagem Estatística de Plackett Burman"**, área de concentração: Tecnologia Mineral, apresentada pelo candidato **Luciano Fernandes de Magalhães**, para obtenção do grau de Doutor em Engenharia Metalúrgica, Materiais e de Minas, aprovada pela comissão examinadora constituída pelos seguintes membros:

Prof. Antônio Eduardo Clark Peres
Orientador - PhD (UFMG)

Prof. Gilberto Rodrigues da Silva
Coorientador - PhD (UFMG)

Prof. Luiz Cláudio Monteiro Montenegro
Dr. (UFMG)

Prof. Afonso Henriques Martins
D.Sc. (UFMG)

Profª Michelly dos Santos Oliveira
Drª (CEFET/MG/Araxá)

Engº. Hélio Cardoso Pereira
Dr. (Consultor)

Coordenador do Programa de Pós-Graduação em Engenharia Metalúrgica, Materiais e de Minas/UFMG

Belo Horizonte, 16 de fevereiro de 2022

AGRADECIMENTOS

Primeiramente agradeço a Deus, pelas oportunidades que me foram dadas ao longo da minha vida, e por me mostrar a grande determinação que eu não imaginava possuir, que me fez superar cada um dos muitos obstáculos que surgiram durante esse percurso.

Agradeço aos meus pais, Irene e José Humberto, e minha irmã, Lidiane, que durante toda minha vida me apoiaram em minhas decisões, e pelo apoio incondicional que me permitiram chegar onde cheguei.

Aos meus grandes amigos Yara, Zanon, Ana Flávia, Tamara, Aryh e Viviane, que durante todo esse tempo estiveram ao meu lado me apoiando, por compreenderem minhas ausências e principalmente por me ajudarem a levantar de cada tombo que levei durante o trajeto.

Aos professores e funcionários do DEMIN, que me receberam de braços abertos na minha chegada na UFMG, e por todos os conhecimentos e experiências compartilhados.

Ao Professor Afonso Henriques Martins, por todos os ensinamentos em análise estatística que foram de grande ajuda no desenvolvimento deste trabalho.

Ao meu orientador, Professor Antônio Eduardo Clark Peres, pela confiança em mim depositada, por todos os ensinamentos e conselhos, e pelo grande susto no dia em que o conheci!

Ao meu coorientador, Gilberto Rodrigues da Silva, pelos inúmeros conhecimentos compartilhados e aconselhamentos que foram fundamentais para o meu aperfeiçoamento, e também pela parceria nas aulas de Processamento Mineral.

Aos meus colegas da Pós-Graduação, pelos momentos de descontração, por toda a ajuda em momentos em que precisei e pelas parcerias formadas.

A CAPES pela concessão da bolsa de doutorado, e o Programa de Pós-Graduação em Engenharia Metalúrgica, Materiais e de Minas, pelo suporte financeiro que foram imprescindíveis para o desenvolvimento da pesquisa.

Por último, mas não menos importante, um imenso agradecimento ao Luiz Ricardo, que durante os últimos 6 anos demonstrou apoio incondicional, principalmente em momentos em que pensei em desistir, por aturar minhas crises, principalmente as de raiva, pelos inúmeros momentos de alegria e por todo o companheirismo construído nesse tempo.

“It is not about how fast I get there,
It is not about what is waiting on the other side,
It’s the climb.”

Jessi Alexander, Jon Mabe

Resumo

Diversas atividades industriais, inclusive a mineração, geram diariamente uma crescente quantidade de efluentes que necessitam de tratamento para que possam ser descartados de forma adequada. A adsorção torna-se uma forma de remover contaminantes de efluentes, e as zeólitas possuem potencial para este tipo de aplicação. Pertencentes à família dos tectossilicatos, esses minerais podem ser sintetizados em laboratório, inclusive a partir de resíduos industriais, o que garante a otimização de suas propriedades. Dois resíduos que apresentam as características necessárias para a síntese são o pó de vidro (PV) e a lama de anodização de alumínio (LAA). Por demonstrarem dificuldades na reciclagem, sua utilização na síntese é uma alternativa para reduzir suas emissões. Neste trabalho foi desenvolvida uma extensa pesquisa, demonstrando as propriedades das zeólitas e sua eficiência na remoção de diversos tipos de efluentes. Também são levantadas lacunas que ainda necessitam de aprofundamento nos sistemas de adsorção analisados. Também foi objeto de estudo neste trabalho a síntese da zeólita analcima de elevada pureza e cristalinidade a partir de PV e LAA. O método estatístico de Plackett Burman foi utilizado para verificar as variáveis de maior relevância estatística no processo. Os resultados demonstram que foi possível a obtenção de analcima pura, com cristalinidade de 75%. Imagens de microscopia eletrônica de varredura revelam que a cristalização ocorreu de forma incompleta, e que a otimização das variáveis de maior relevância estatística pode levar a síntese de analcima com cristalinidade ainda maior. Dessa forma, o presente estudo demonstra que a combinação de PV e LAA é uma alternativa na síntese de zeólita de elevado valor agregado, o que pode contribuir para a redução de emissão de resíduos sólidos, assim como gerar adsorventes eficazes e de baixo custo para o tratamento de efluentes.

Palavras-chave: analcima, zeólita, pó de vidro, anodização de alumínio, síntese, tratamento de efluentes.

Abstract

Several industrial activities, including mining, generate an increasing amount of effluents daily that need treatment so that they can be properly disposed of. Adsorption becomes a way to remove contaminants from effluents, and zeolites have the potential for this type of application. Belonging to the tectosilicate family, these minerals can be synthesized in the laboratory, including from industrial waste, which guarantees the optimization of their properties. Two residues that have the necessary characteristics for the synthesis are glass powder (PV) and aluminum anodizing mud (LAA). As they demonstrate difficulties in recycling, their use in synthesis is an alternative to reduce their emissions. In this work, an extensive research was developed, demonstrating the properties of zeolites and their efficiency in the removal of different types of effluents are also highlighted. Gaps that still need to be deepened in the adsorption systems analyzed. The synthesis of analcime zeolite of high purity and crystallinity from PV and LAA was also an object of study in this work. The statistical method of Plackett Burman was used to verify the variables of greater statistical relevance in the process. The results demonstrate that it was possible to obtain pure analcime, with a crystallinity of 75%. Scanning electron microscopy images reveal that crystallization occurred incompletely and that the optimization of the most statistically significant variables can lead to analcime synthesis with even higher crystallinity. Thus, the present study demonstrates that the combination of PV and LAA is an alternative in the synthesis of zeolite with high added value, which can contribute to the reduction of solid waste emission, as well as generate effective and low-cost adsorbents for the wastewater treatment.

Keywords: analcime, zeolite, glass powder, aluminum anodizing, synthesis, effluent treatment.

Lista de figuras

Lista de tabelas

Siglas e abreviaturas

PV / GPW Pó de vidro / Glass powder waste

LAA / AAM Lama de anodização de alumínio / Aluminum anodizing mud

BBU Basic Building unit

CBU Composite building unit

CEC Cation Exchange capacity

XRD X-ray diffraction

BET Brunauer-Emmett-Teller

BJH Barret-Joyner-Halenda

TG Thermogravimetry

DTA Differential thermal analysis

CMC Critical micelar conentration

PZC Point of zero charge

FRX X-ray fluorescence

SEM Scanning electron microscope

COD Crystallography open database

FT-IR Fourier transform infrared spectroscopy

Sumário

Estrutura da tese

A presente Tese está dividida em 7 capítulos. O Capítulo 1 apresenta a Introdução, que apresenta uma visão global da temática abordada, assim como a relevância do tema e o conhecimento original ao conhecimento. No Capítulo 2 são apresentados o objetivo geral e os objetivos específicos, apresentados separadamente para cada um dos dois artigos científicos que compõem esta Tese.

O Capítulo 3 apresenta uma breve revisão da literatura, abordando os resíduos industriais que foram utilizados na pesquisa, e sobre uma possibilidade de aplicação de zeólita na indústria mineral.

O Capítulo 4 apresenta um artigo de revisão bibliográfica, abordando as características gerais das zeólitas e sua aplicação como adsorventes para tratamento de cinco tipos de contaminantes.

O Capítulo 5 é formado por um segundo artigo científico, trazendo os resultados da síntese da zeólita analcima a partir dos resíduos apresentados no Capítulo 3.

As conclusões à respeito da pesquisa são mostradas no Capítulo 6, e finalmente, o Capítulo 7 apresenta as sugestões de pesquisas futuras.

CAPÍTULO 1: INTRODUÇÃO

Diariamente, toneladas de resíduos sólidos, líquidos e gasosos são gerados pelos mais diversos setores industriais. A crescente demanda da sociedade por materiais, produtos e serviços faz com que a indústria tenha que intensificar a produção, o que resulta no aumento de resíduos gerados. A questão torna-se um problema para as empresas do ponto de vista financeiro, devido ao custo com transporte para disposição em aterros ou tratamentos necessários para o descarte adequado.

Efluentes líquidos possuem em sua constituição uma infinidade de substâncias químicas, que em sua maioria, são danosas ao meio ambiente. Eventualmente podem atingir os seres humanos, com graves consequências para a saúde. Dentre os elementos químicos que podem estar presentes em efluentes e possuem grande toxicidade, destacam-se os metais pesados. Por serem não-biodegradáveis e por se acumularem no organismo, torna-se vital o tratamento do efluente para descartá-lo de forma segura.

A atividade mineral é um dos segmentos industriais que geram efluentes com a presença de metais pesados. Dos diversos tipos de minérios que podem gerar efluentes contaminados essas espécies químicas, minérios de chumbo merecem destaque. Íons de chumbo são facilmente liberados na água de processo, devido a constituição mineralógica do minério, o que impõe a necessidade do tratamento adequado desse efluente.

Dos diversos tipos de tratamento químico, a técnica da adsorção vem demonstrando destaque, e diversos materiais podem ser utilizados como adsorventes. Minerais pertencentes da família dos tectossilicatos, as zeólitas possuem potencial aplicação como adsorvente. Sua estrutura cristalina única permite com que sejam efetivas na remoção, não só de metais pesados, mas de diversos tipos de contaminantes. Zeólitas ocorrem naturalmente na natureza, mas a ocorrência em depósitos com potencial de explotação são raros. Dessa forma, a síntese desses materiais é uma alternativa para sua obtenção, com propriedades ainda superiores às suas versões naturais, a ponto de serem sintetizadas mais de 130 tipos de zeólitas, com diversas estruturas cristalinas.

Apesar do potencial da síntese desses materiais, sua obtenção é de alto custo, devido aos componentes químicos necessários e características inerentes ao processo. Dessa forma, há um crescente interesse na obtenção de zeólitas sintéticas com o uso de

materiais que são considerados resíduos por outras atividades industriais. O processo torna-se de menor custo e contribui com a economia circular, representando potencial alternativa para a redução de descartes.

Diversos resíduos industriais vêm sendo aplicados para a síntese de zeólitas com resultados promissores, como cinza de casca de arroz, argilominerais, cinzas volantes, lama vermelha, etc. Apesar dos bons resultados obtidos, esses materiais muitas vezes possuem elevado teor de contaminantes, o que resulta na produção de zeólitas com baixa cristalinidade, caso sejam utilizados em seu estado bruto. Também há a questão da razão Si/Al presente no material, que pode não ser adequada para a síntese de determinada zeólita, sendo necessária a adição de reagentes químicos para que o ajuste seja feito, o que acarreta na elevação dos custos. Sendo assim, a utilização de dois resíduos diferentes pode contornar o problema do ajuste da razão Si/Al, caso tenham a composição química adequada.

Nesse contexto, pó de vidro e lama de anodização de alumínio são dois resíduos apresentam características químicas que possibilitam esse ajuste sem a adição de reagentes químicos, além de apresentarem baixo teor de contaminantes, o que em teoria, pode levar à cristalização de zeólitas com cristalinidade elevada em comparação aos demais resíduos. Esses resíduos são gerados em grande quantidade a nível mundial, e possuem baixa possibilidade de reciclagem devido suas características físicas, além de apresentarem baixa biodegradabilidade, elevando o impacto ambiental pelo seu descarte em aterros. Apesar do potencial que o pó de vidro e a lama de anodização apresentam para a síntese de zeólitas, estudos considerando a utilização da combinação desses dois materiais não foram localizados na literatura.

A síntese de zeólitas a partir de resíduos torna-se de grande relevância para o setor industrial, pela possibilidade de redução de suas emissões e agregação de valor a um material que originalmente seria descartado. Essa prática torna-se vantajosa também para as empresas que necessitam de adsorventes eficientes e de baixo custo para o tratamento de seus efluentes, incluindo o setor mineral, que sofre pressões de órgãos ambientais e pela sociedade na gestão dos impactos ambientais gerados por suas atividades.

CAPÍTULO 2: OBJETIVOS

2.1 Objetivo Geral

A presente pesquisa tem como objetivo a obtenção de zeólita analcime de alta pureza e cristalinidade, a partir dos resíduos industriais pó de vidro e lama de anodização de alumínio.

2.2 Objetivos específicos por capítulo

Capítulo 4:

- Levantar informações pertinentes às zeólitas, suas propriedades
- Analisar a aplicação de zeólitas como adsorventes para cinco tipos de contaminantes;
- Levantar informações sobre os mecanismos de adsorção presentes em cada sistema;
- Identificar pontos que ainda necessitam de maior investigação, ou não que ainda não foram analisados na literatura.

Capítulo 5:

- Caracterizar química e mineralogicamente o PV e LAA, de forma a possibilitar a definição das variáveis do processo de síntese;
- Definir as variáveis a serem consideradas no estudo, assim como definir os valores de seus níveis superior e inferior;
- Caracterizar a zeólita obtida, a fim de determinar sua pureza e cristalinidade;
- Definir as variáveis de maior relevância estatística que afetam o processo de síntese, através da metodologia de seleção de variáveis Placket Burman;
- Caracterizar a analcima sintética obtida, para o conhecimento de suas propriedades e que possibilitem sua aplicação como adsorvente.

CAPÍTULO 3: REVISÃO BIBLIOGRÁFICA

3.1 Resíduos industriais

A atividade industrial promove um papel de grande relevância para a sociedade, possibilitando o bem estar e avanço tecnológico da humanidade, através do fornecimento dos mais variados tipos de produtos e materiais. Após a Revolução Industrial a produção aumentou intensamente, para atender a cada vez maior demanda da sociedade [(1)].

Porém, com o aumento da produção, a quantidade de resíduos gerados no processo aumenta proporcionalmente. Efluentes líquidos, emissão de particulados e gases causadores do efeito estufa, e resíduos sólidos vêm se tornando um grave problema ambiental, a nível mundial. Alguns desses resíduos são inertes, e não oferecem riscos, uma vez corretamente descartados. Outros, por outro lado, podem causar efeitos negativos adversos à fauna e a flora, e dependendo do tipo de resíduo, aos seres humanos [(2)].

De acordo com a NBR 10004 [(3)], os resíduos sólidos industriais podem ser classificados em:

Classe I – Resíduos perigosos

Resíduos que apresentam periculosidade em função de suas propriedades físicas, químicas ou infecto-contagiosas e apresentam risco à saúde pública e oferecem riscos ao meio ambiente;

Classe II – Resíduos não perigosos

A) não inertes: aqueles que não se enquadram na classe I nem na classe II B e apresentam propriedades como: biodegradabilidade, combustibilidade ou solubilidade em água;
B) resíduos não perigosos e inertes: resíduos que quando submetidos ao contato com água destilada ou deionizada, à temperatura ambiente, não apresentam nenhum de seus constituintes solubilizados em concentrações superiores aos padrões de potabilidade da água.

3.2 3.2 Lama de anodização de alumínio

O alumínio é o elemento metálico mais abundante na crosta terrestre. É um excelente condutor de calor e eletricidade, possui baixa densidade, maleabilidade e resistência à

corrosão, e devido essas propriedades, seu consumo aumenta cada vez mais por diversos setores industriais. O alumínio é um metal altamente reativo, e normalmente é encontrado na natureza ligado a outros elementos químicos na forma de minerais, geralmente oxigênio [4].

O alumínio metálico, ao entrar em contato com o ar, imediatamente reage com o oxigênio, formando uma fina camada de óxido na superfície, que contribui com o aumento da resistência à corrosão. Entretanto, para determinadas aplicações essa camada é insuficiente para a proteção da peça nas condições de uso, sendo necessário aumentar a espessura da camada de óxido. O processo de anodização cumpre essa função, no qual as peças de alumínio são submetidas processos eletroquímicos controlados, o que força o surgimento de uma camada mais espessa de óxido [5]. O processo tem como finalidade, além de aumentar a resistência à corrosão, dar um melhor acabamento às peças, corrigindo imperfeiçoes superficiais, além de conferir aspecto decorativo, possibilitando a idealização de projetos específicos [6]. A Figura 1 ilustra as etapas básicas do processo de anodização.

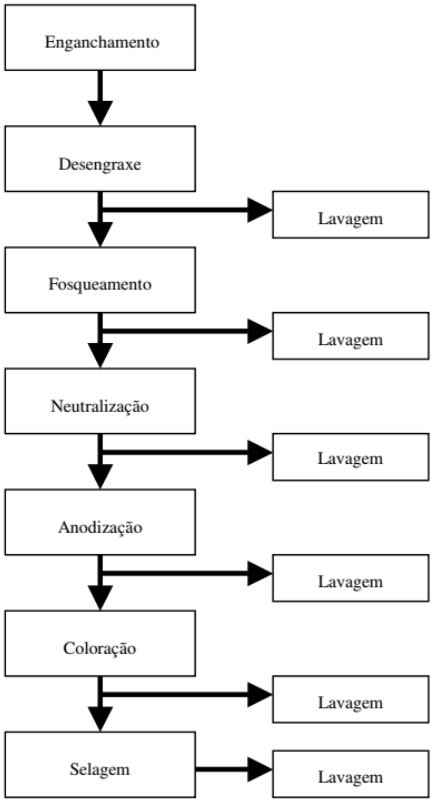

Figure 3.1 - Etapas do processo de anodização de alumínio [7]

Inicialmente as peças são enganchadas em suportes metálicos, de forma permitir a condução de corrente elétrica, e facilitar o processo de limpeza das peças nas etapas

posteriores. Em seguida as peças passam pelo desengraxe, que tem como finalidade remover da superfície das peças óleos e graxas, poeira e outros contaminantes que podem interferir negativamente na anodização. O fosqueamento é realizado promover a homogeneização da superfície, além de promover aspecto fosco às peças. Após a etapa de fosqueamento, as peças são imersas em um banho de ácido sulfúrico, para a neutralização da solução básica presentes nas peças (neutralização), e por fim, o processo de anodização propriamente dito, no qual o alumínio metálico reage com solução de ácido sulfúrico, com a consequente formação de uma camada de óxido de alumínio que possui espessura entre 5 e 30µm [7].

Em cada etapa do processo, as peças passam por uma etapa de lavagem, para eliminar excesso de solução dos banhos, ou resíduos que permanecem sobre as peças após cada etapa. Ao final do processo, as águas de lavagem passam por decantação e posterior remoção do material sólido, a lama de anodização, que possui em média 85% de água [6]. Estima-se que para cada tonelada de alumínio tratado pelo processo de anodização, são gerados cerca de 475kg de resíduo.

Devido à crescente demanda da sociedade por alumínio, a quantidade de resíduos gerados aumentou consideravelmente nas últimas décadas. Em 2002 eram gerados 450.000t de lama de anodização mundialmente, que se elevou para 5.145.000t em 2017 [8]. O aumento expressivo de resíduos gerados traz um forte impacto negativo no aspecto econômico, visto que os gastos com transporte e disposição desse material aumenta consideravelmente. Outro aspecto negativo é com relação ao impacto ambiental. Além da lama de alumínio não possuir biodegradabilidade, o pH final gira em torno de 13-13,5 [1], o que agrava a questão do descarte, que deve ser realizado de forma adequada para a minimização dos impactos ambientais.

Devido as questões levantadas, a possibilidade de reciclagem desse material torna-se atraente, tanto do ponto de vista ambiental quanto econômico. A lama de anodização é composta basicamente de $Al(OH)_3$, apresentando teor de alumínio consideravelmente alto, que pode aumentar ainda mais após calcinação, permitindo que possa ser reutilizado de diversas formas. A Tabela 1 mostra o resultado da composição química LAA utilizado em diversas pesquisas, com a finalidade de reciclagem desse material, verificando-se teores acima de 50%.

Table 3.1 - Composição química de diversas lamas de anodização de alumínio

Composição química (% em peso)	[8]	[4]	[6]	[9]	[7]
SiO_2	0,8	0,5	0,6	1,9	0,4
Al_2O_3	48,5	49,7	55,5	73,6	63,9
Fe_2O_3	0,3	0,2	0,3	0,5	0,2
CaO	0,4	1,6	0,1	0,6	<0,1
MgO	1,6	1,0	0,1	0,3	<0,1
TiO_2	0,4	-	-	-	<0,1
Na_2O	15,8	3,6	2,9	1,2	4,3
K_2O	0,6	-	<0,1	0,2	<0,1
MnO_2	0,1	-	<0,1	<0,1	<0,1
P_2O_5	0,1	-	<0,1	0,5	<0,1
Cr2O3	-	-	-	-	-
SO3	-	7,6	12,1	20,5	-
LOI	29,9	34,7	28,3	-	31,1

3.3 Pó de vidro

O vidro é um material inorgânico amorfo, produzido a partir da fusão da sílica, sendo largamente utilizado nos mais diversos setores industriais, desde a construção civil, automobilismo, indústria de alimentos, dentre outros [10] [11]. Diferentes elementos podem ser adicionados à silica, com a finalidade de modificação de suas propriedades para aplicações específicas, como boro, germânio e alumínio. Porém, o vidro mais consumido é o soda-cal, no qual são adicionados sódio e cálcio, responsáveis por aumentar a resistência e otimizar a cristalização da sílica [2], respectivamente, respondendo por mais de 85% da produção mundial de vidro [12].

Após o processo de fabricação do vidro, é necessário deixá-lo em formatos e tamanhos adequados para sua utilização, especialmente no caso de vidros planos. Durante o tratamento, as peças de vidro são cortadas e lapidadas, para suavizar as bordas da peça após o corte. As peças então seguem para a etapa de polimento, que tem como finalidade de arredondar as partes já lapidadas da peça. Durante todo o processo, a água é utilizada com a função de resfriamento do vidro e equipamentos, evitar a suspensão de pó de vidro e facilitar na remoção dos resíduos gerados [10]. Após a coleta e tratamento do efluente gerado, o pó de vidro é armazenado para posterior descarte.

Durante o processo de fabricação e preparo do vidro são gerados dois tipos de resíduos, na forma de pó e fragmentos. Quando na forma de fragmentos, o vidro é facilmente reciclado, retornando ao processo de fabricação. Porém, na forma de pó o vidro é rejeitado no processo de reciclagem, pois causa danos na parte interna dos fornos devido sua granulometria fina, além de produzir peças com imperfeições [13].

Estima-se que anualmente, sejam produzidos mundialmente cerca de 130 milhões de toneladas de vidro, dos quais pelo menos 10 milhões acabam se tornando resíduos que necessitam de disposição em aterros sanitários [14]. Um único empreendimento é capaz de produzir cerca de 8,5 toneladas por mês [15]. Devido sua baixíssima biodegradabilidade, quando na natureza, o vidro pode demorar até 1 milhão de anos para sua total dissolução. Esses dois fatores contribuem para que o problema do descarte de resíduos de vidro seja foco de esforços mundiais para a reutilização desse material, já que sua reciclagem é inviável tecnicamente [16]. Conforme mostrado na Tabela 2, o vidro possui alto teor de silício, o que torna o pó de vidro um material com características necessárias para utilização em outros segmentos industriais especialmente na construção civil. Porém, o setor não consegue absorver toda a quantidade de resíduos gerada (assim como outros resíduos industriais), e grande parte do material gerado acaba sendo descartado, aumentando a necessidade da busca de novas formas de utilização desse material.

Table 3.2 - Composição química de diversos resíduos de vidro

Composição química (% em peso)	[17]	[18]	[13]	[14]	[19]
SiO_2	69,8	70,6	67,0	71,2	70,5
Al_2O_3	1,4	1,4	0,8	2,2	1,2
Fe_2O_3	0,3	2,5	0,5	0,4	0,4
CaO	10,0	10,9	10,0	10,1	19,7
MgO	0,7	0,7	2,5	1,5	3,4
TiO_2	-	<0,1	-	-	-
Na_2O	12,5	12,8	-	12,9	-
K_2O	-	0,3	-	-	0,4
MnO_2	-	<0,1	-	-	-
P_2O_5	-	<0,1	-	-	-
Cr2O3	-	<0,1	-	-	-
SO3	0,2	0,1	0,3	0,2	4,2
LOI	-	0,1	-	1,6	0,1

3.4 Aplicação de zeólitas no Processamento Mineral

Conforme mencionado anteriormente, a atividade industrial é responsável pela geração de resíduos sólidos e efluentes líquidos, sendo ambos potenciais agentes de contaminação do meio ambiente. No caso de efluentes gerados pela atividade de mineração, é comum a presença de metais pesados, graxas e óleos, coletores, floculantes, espumantes, sólidos em suspensão, entre outros [20, 21]. Torna-se de fundamental importância o tratamento adequado dos efluentes gerados pela indústria, pois apresentam em geral, maior potencial contaminante em comparação aos resíduos

sólidos. Considerando somente metais pesados, a contaminação por esses elementos, cumulativos no organismo e não biodegradáveis, leva a uma série de problemas de saúde, como diversos tipos de câncer, alterações genéticas, paralisia, danos neurológicos, danos a órgãos e sistemas, entre outros [22].

A presença de metais pesados é marcante no caso do beneficiamento de diversos tipos minérios, em especial o de chumbo. Após a cominuição do minério, as partículas encontram-se em granulometria fina, o que aumenta sua área superficial, e consequentemente, sua reatividade e potencial para liberação de íons. Um fator agravante é que o minério de chumbo ocorre em associação com outros minerais sulfetados, como esfarelita, pirita e calcopirita. Uma vez que sulfetos estão em suspensão, tem início uma interação galvânica entre as espécies minerais, no qual o mineral de maior potencial de repouso age como catodo e o de menor potencial age como anodo. No caso da combinação galena/pirita, a galena age como anodo, sendo facilmente oxidada e liberando íons Pb^{2+} na solução [23] [24]. A Figura 2 ilustra a questão da reação galvânica entre esses dois minerais, que se intensifica com o aumento da quantidade de pirita presente no sistema.

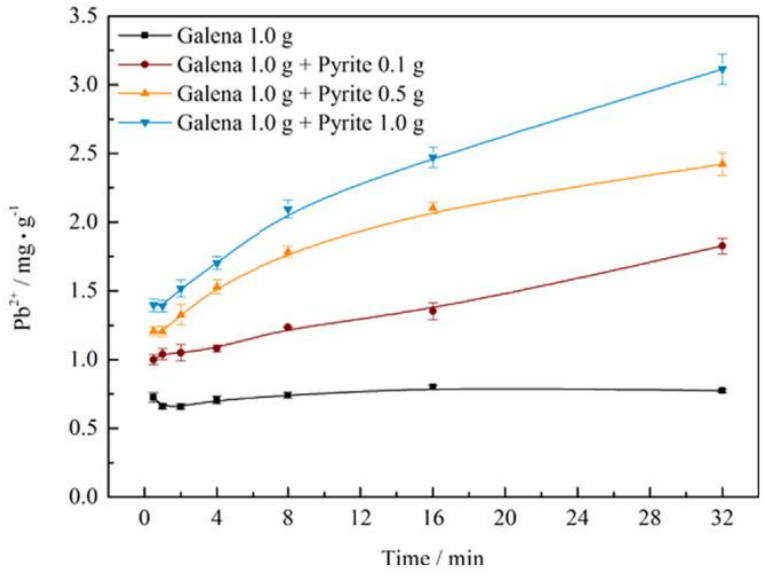

Figure 3.2 - Relação entre liberação de íons Pb2+ e a relação galena/pirita (p/p) [23]

A presença de íons de chumbo na água utilizada durante o processamento do minério tem duas consequências negativas. Em primeiro lugar, cita-se a redução da seletividade, especialmente afetada com a utilização de água de recirculação contendo Pb^{2+}. Os íons de chumbo podem ativar indesejavelmente a pirita e/ou a esfalerita, o que leva a dificuldades na flotação da galena [25] [26] [27]. Em segundo lugar, a água gerada como efluente possui uma concentração muito acima da estabelecida por órgãos de

proteção ambiental. De acordo com a *US Environmental Protection Agency*, o limite estabelecido para chumbo na água destinada ao consumo humano não deve ultrapassar 15ppb. Entretanto, verifica-se que a presença de Pb^{2+} presente na água de processo de minério de chumbo varia entre 76 e 560ppm. Torna-se evidente que a remoção do chumbo é altamente benéfica, tanto no processo de concentração por flotação, quanto na minimização de impactos ambientais.

Diversas são as técnicas de remoção de contaminantes de efluentes, mas a adsorção encontra lugar de destaque. A adsorção é um processo que apresenta grande versatilidade, uma vez que diversos materiais podem ser utilizados como adsorventes, como argilominerais, carvão ativado, e até mesmo alguns resíduos industriais. Outra vantagem da adsorção sobre as demais técnicas é a capacidade de remover contaminantes em concentrações extremamente baixas.

Dentre os materiais que podem ser utilizados como adsorventes, as zeólitas vem atraindo a atenção da comunidade científica. Sua carga elétrica negativa, presença de cátions de compensação trocáveis e a elevada área superficial fazem das zeólitas um material com grande potencial para tal utilização. Diversos tipos de contaminantes podem ser removidos pelas zeólitas, como pigmentos, compostos orgânicos e a base de nitrogênio e fósforo, e no caso de metais pesados, esses materiais possuem uma excelente capacidade de remoção.

REFERÊNCIAS

(1) Marques, D. V., et al. Recycled polyethylene terephthalate and aluminum anodizing sludge-based boards with flame resistance. Waste Manag, 92, 1-14, 2019.

(2) Paiva, O. A. Resíduo industrial de vidro moído em argamassa de cimento Portland. Manaus: Universidade Federal do Amazonas, 2009.

(3) Técnicas, A. B. d. N. NBR 10004 - Resíduos sólidos - Classificação. Rio de Janeiro, 2004, 71.

(4) Souza, M. T., et al. Sustainable cement with Al-anodizing waste: Evaluating reactivity and feasibility as a shrinkage-compensating admixture. Journal of Building Engineering, 30, 2020.

(5) Alvarez-Ayuso, E. Approaches for the treatment of waste streams of the aluminium anodising industry. J Hazard Mater, 164, 2-3, 409-414, 2009.

(6) Moraes, G. G. d., et al. Produção e caracterização de espumas cerâmicas obtidas a partir de lodo de anodização de alumínio. Química Nova, 35, 1, 143-148, 2012.

(7) Sartor, M. N. Utilização do resíduo de anodização do alumínio como matéria prima para o desenvolvimento de produtos cerâmicos. Florianópolis: Universidade Federal de Santa Catarina, 2006. 77.

(8) Mymrin, V., et al. Characterization of construction materials on the base of mortar waste, activated by aluminum anodization sludge and lime production waste. Construction and Building Materials, 212, 202-209, 2019.

(9) Costa, E. B. d. Aproveitamento do resíduo de anodização do alumínio na produção do cimento sulfoaluminanto de cálcio belítico. Porto Alegre: Universidade Federal do Rio Grande do Sul, 2013. 160.

(10) Antônio, A. P. Potencialidades do aproveitamento do resíduo de estação de tratamento de efluentes do processo de lapidação do vidro sodo-cálcico na produção de concretos. Vitória: Universidade Federal do Espírito Santo, 2011.

(11) Barros, L. M. Concreto de alta resistência a partir de matérias-primas amazônicas e vidro reciclado. São Carlos: Universidade de São Paulo, 2016.

(12) Filho, H. C. S. Estabilização de um solo dispersivo com pó de vidro moído e cal de carbureto. Porto Alegre: Universidade Federal do Rio Grande do Sul, 2019.

(13) Ribeiro, U. G. and D. F. Santos. Physical-mechanical potential properties of wastes from glass lapping to produce mortar as partial replacement of the conventional aggregate. Revista IBRACON de Estruturas e Materiais, 13, 1, 142-159, 2020.

(14) Du, Y., et al. Thermal conductivity of cement paste containing waste glass powder, metakaolin and limestone filler as supplementary cementitious material. Journal of Cleaner Production, 287, 2021.

(15)
(16) Khan, M. N. N., et al. Reuse of waste glass as a supplementary binder and aggregate for sustainable cement-based construction materials: A review. Journal of Building Engineering, 28, 2020.

(17) Kalakada, Z., et al. Glass powder as replacement of cement for concrete – an investigative study. European Journal of Environmental and Civil Engineering, 1-18, 2019.

(18) Khan, M. N. N., et al. Effect of waste glass powder as a partial precursor in ambient cured alkali activated fly ash and fly ash-GGBFS mortars. Journal of Building Engineering, 34, 2021.

(19) Alves, J. A. B. L. R., et al. Synthesis of high value added zeolitic materials using glass residue as a silica source. Materials Research, 17, 213-218, 2014.

(20) Melo, V., F., et al. Chumbo e zinco em águas e sedimentos de área de mineração e metalúrgia de metais. Química Nova, 35, 1, 22-29, 2012.

(21) Veras, A. C. M. Análise da contaminação por metais pesados na água e em sedimentos na bacia hidográfica do Rio Doce. Rio de Janeiro: Universidade Federal do Rio de Janeiro, 2020. 151.

(22) Burakov, A. E., et al. Adsorption of heavy metals on conventional and nanostructured materials for wastewater treatment purposes: A review. Ecotoxicology and Environmental Safety, 148, 702-712, 2018.

(23) Wang, X., et al. The influence of galvanic interaction on the dissolution and surface composition of galena and pyrite in flotation system. Minerals Engineering, 156, 2020.

(24) Silvestre, M. O., et al. Dispersion effect on a lead–zinc sulphide ore flotation. Minerals Engineering, 22, 9-10, 752-758, 2009.

(25) Rubio, J., et al. (2010). Aspectos ambientais nos setores mineiro e metalúrgico. Tratamento de minérios. A. B. Luz, J. A. Sampaio and S. C. A. Framça. Rio de Janeiro, CETEM/MCT**:** 753-787.

(26) Smith, R. W. Liquid and Solid Wastes from Mineral Processing Plants. Mineral Processing and Extractive Metallurgy Review, 16, 1, 1-22, 1996.

(27) Basilio, C. I., et al. Lead activation of spharelite during galena flotation. Minerals Engineering, 9, 8, 869-879, 1996.

CAPÍTULO 4: ZEOLITE APPLICATION IN WASTEWATER TREATMENT

ABSTRACT

As a scarce natural resource, the preservation of water quality is of fundamental importance to guarantee its availability for future generations. Due to the increasing industrial activity, effluents are generated with a series of chemical compounds, such as nitrogenous, phosphoric, and organic compounds, heavy metals, and dyes which, if improperly disposed of, contribute to contamination, followed by significant environmental impacts, in addition to the damage to human health. The adsorption technique is an effective approach for removing contaminants from effluents, showing high versatility, due to the use of various materials as adsorbents. Belong to a wide variety of materials, zeolites reveal to be a promising adsorbent. Zeolites are minerals found in nature or which can be synthesized from industrial residues, standing out in the treatment of contaminated effluents. Zeolite removal efficiency depends on the contaminant to be removed and can reach up to 96% for heavy metals, 90% for phosphoric compounds, 96% for dyes, 80% for nitrogen compounds, and 89% for organics. Aiming at the identification of the more relevant findings and research gaps to advance the use of zeolites in the large-scale treatment of industrial effluents, a review on the recent application of zeolites is needed. This paper presents a global view of zeolites, and a review is conducted on several recent studies using zeolites as adsorbents for the contaminants considered, indicating the main characteristics of the various adsorption systems, demonstrating the particularities of each process, aiming to reveal useful information to provide future research, in addition to identifying points that need further investigation.

Keywords: zeolite, wastewater treatment, adsorption, heavy metals, ammonium, dye,

4.1. Introduction

Water is the essential element for life on Earth. Although about 70% of the planet's surface is covered with water, only a small portion of this volume can be consumed as freshwater. Still, much of the freshwater is in the form of glaciers, and therefore, it is not available for consumption [1]. In addition, freshwater is not evenly distributed across continents, with some parts of the world having large reserves, while others suffer from lack. Allied to the problem of the relative scarcity of this limited resource and its irregular distribution, the growing industrial activity has contributed significantly to the contamination of the waters through the disposal, often inadequate, of effluents generated [2].

As society's demand for consumption increases, the food, cosmetics, mining and metallurgy, chemical and pharmaceutical industries, among others, intensified their production, and consequently, greater attention has been paid to the effluents generated. The presence of several contaminating elements present in wastewater is common, such as heavy metals (*e.g.*, lead, arsenic, chromium, mercury, among others) [3], compounds based on nitrogen [4] and phosphorus [5], dyes [6] and various organic compounds [7]. All these elements, if disposed of untreated, contaminate water, soil, plants, and animals, and can eventually reach humans. For the organism, these compounds have high toxicity, and depending on the dosage and time of exposure, a series of disorders can occur. Studies indicate the appearance of several types of cancer, genetic abnormalities, damage to organs and systems, and psychological disorders due to exposure to heavy metals and organic compounds [8, 9]. In addition, the environment can also suffer significant damage when exposed to the inadequate disposal of effluents, especially those rich in dyes, nitrogen, and phosphorus. In the presence of abundance, these elements can cause eutrophication of water bodies, eliminating all aquatic life [10].

Several forms of wastewater treatment have been developed over the decades, to remove contaminating elements from wastewater, before their disposal. Techniques such as chemical precipitation [11], ionic flotation [12], electrodialysis [13], biological treatment [14], among others, are efficient in the treatment of effluents, but they have some disadvantages such as the generation of toxic waste that requires adequate storage, high demand for chemical reagents, high energy cost and limited efficiency to remove contaminants with low concentration [15-18]. In contrast, the adsorption technique is promising and possesses several advantages over other techniques, which justifies its application in the treatment of effluents. One of the great advantages of the

technique is its versatility, as it allows the use of various materials as adsorbents, from activated carbon to industrial wastes [19].

Several materials have been used as adsorbents to remove contaminants from water. Activated carbon, biochar, clay minerals, and advanced materials are among the most studied materials for wastewater decontamination. These materials possess the necessary features to be used for this purpose, *e.g.*, high surface area, negative electric charge (clay minerals), and micro/mesoporous (carbon-based materials) [20,21]. However, some disadvantages limit their use on a large scale. Activated carbon and biochar are products of the calcination of organic matter, *e.g.*, bamboo, corn straw, rice husk, etc., in an anaerobic atmosphere. The properties of the final product can vary in a wide range since it is a function of the precursor used. Another disadvantage is the high cost of production, whereas the calcination temperature can be as high as 900°C [20].

Clays are composed of phyllosilicate minerals. These minerals possess sheet-like structures, exhibiting a high specific area. Furthermore, their atomic structure provides a natural negative charge that is neutralized by a variety of cations. These properties make clays a material with the potential to be used as adsorbents However, they are composed of a wide range of minerals, and their removal potential may be reduced, or present great variation [22]. Their modification can be enhanced by a series of treatments, *e.g.*, thermal, acidic, and surfactant modification, but these treatments increase the process costs [23].

A relatively new class of materials to be used in water treatment are the advanced materials, the nanomaterials, *e.g.*, alumina, silica, titanium oxide, zirconia, etc. These materials possess small size, high specific energy, and high reactivity [24]. Among them, zeolite is a class of material that has attracted the attention of the scientific community and has the potential to be used as an adsorbent in the elimination of contaminating elements in effluents. These minerals, found in nature, or synthesized, have a microporous crystalline structure (with pores opening smaller than 20Å) [25], which guarantee their application for several purposes, such as gas separation [26], water softeners [27], catalyst [28], addition for Portland cement [29] and applications in health and animal food [30]. Exchangeable cations in the microporous structure and negative electrical charge, are two of the properties that allow its application as an adsorbent, for the proper treatment of effluents.

This paper aims to identify the more relevant findings and research gaps on the use of zeolites as adsorbent materials, as well as demonstrate the adsorption mechanisms and particularities of each process, revealing useful information for future research. Review studies, in most cases, bring information about natural or synthetic zeolites, and, in this paper, the reader will find information about both zeolites. A comparison between the two types of zeolites is made, discussing their advantages and disadvantages, their efficiency in wastewater treatment based on their different chemical and physical features, and how the modification of these characteristics can enhance their performance as adsorbents. The next section is dedicated to the discussion about zeolites and their properties, and section 3 presents a review of several recent studies that used zeolites to remove five classes of contaminants. Finally, section 4 presents the conclusions, challenges, and future perspectives to zeolite application in wastewater treatment.

4.2. Microporous materials: zeolites

4.2.1. Zeolite definition

The term zeolite, derived from the Greek words *zein* (boil) and *lithos* (rock), was first used to name a mineral that expanded upon being heated, in 1758 by the Swedish mineralogist Alex Fredrick Cronsted [25, 31]. The reason for this peculiar behavior was only revealed in the year 1857, when it was discovered that these materials have a microporous crystalline structure, capable of storing water inside its pores and releasing it if heated, in theoretically infinite cycles of hydration and dehydration. At this time, it was also discovered the presence of compensation cations in zeolite crystalline structures, and the ability they have to be removed by other ions in solution, through cation exchange [25, 32]. Although these properties were important in several industrial sectors, these minerals remained unused for more than 200 years. Its use on an industrial scale only started in 1905, when economically exploitable sedimentary deposits were discovered, which enabled its application in the detergent industry [33]. The first zeolite synthesis was reported in 1948 [25], during the attempt to recreate the hydrothermal conditions of its formation in nature, and the process has been widely studied since then. Currently, 230 species of zeolites are known, categorized into 133 different crystalline structures, according to rules defined by International Zeolite Association (IZA) [33, 34].

Zeolites belong to the aluminosilicate group, formed by the union of TO_4-type tetrahedrons, or basic building units (BBU), where T represents silicon and/or aluminum

atoms (Figure 1a). The difference in valence between silicon (+4) and aluminum (+3) leads to an excess of negative charge in the crystalline structure, which is neutralized by the presence of compensation cations, usually elements from alkali metal or alkaline earth metal family [32, 34-38]. The basic structure of zeolites can be described by the generic formula $M_{a/b}[(AlO_2)_a(SiO_2)_y].cH_2O$, where *M* represents the compensation cation (M= Na^+, K^+, Li^+, Ca^{2+}, Mg^{2+}, etc.) [34]. The variables *a* and *y* represent the amount of $[SiO_4]^{4-}$ and $[AlO_4]^{5-}$ tetrahedra and *c* is the number of water molecules, parameters which vary between the different zeolite crystalline structures. The water molecules and the compensation cation are not part of the chemical composition of zeolites, and these species are free to enter and exit the crystalline structure without causing structural damage to the crystalline structure [35, 40, 41].

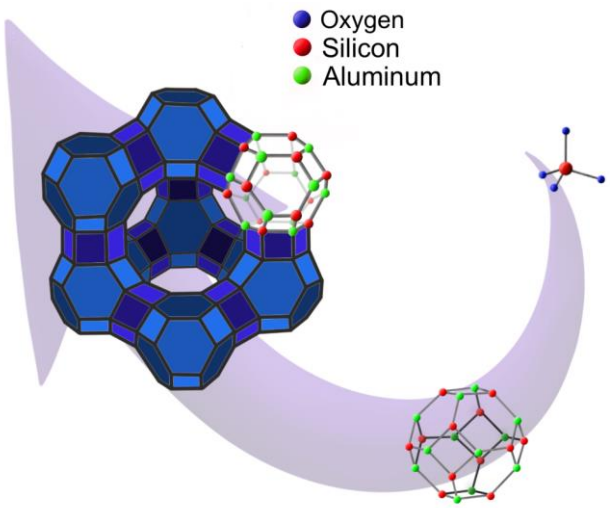

Figure 4.1 - Basic building unit (a), Composite building units (b) in the crystalline structure of FAU-zeolites (c). Oxygen atoms have been omitted for clarity.

The union of $[SiO_4]^{4-}$ and $[AlO_4]^{5-}$ leads to the formation of more complex structures, known as composite building units (CBU), being represented by rings and cages. The rings are named according to the number of oxygen atoms, and rings between 4 and 12 atoms are more common. In the peripheries of the crystal lattice, the rings are called windows and define the effective diameter of the zeolite pores, which limit the entry of certain chemical species into the crystalline structure. This property gives zeolites the ability to be used as molecular sieves and catalysts, in gas separation and the petrochemical industry, respectively. Based on pore diameter, with openings smaller than 20Å, zeolites are classified as microporous materials [25, 38, 42-44]. The union of different types of rings leads to the formation of even more complex structures called cages (Figure 1b). The union of the different types of cages leads to the formation of the

various zeolite structures [45]. As an example, Figure 1c shows the unit cell of a FAU-type zeolite.

Another characteristic of zeolitic materials is the low framework density, which measures the number of T atoms (Si and/or Al) per 1000Å^3. Typically, zeolites have a framework density ranging from 5 to 20, due to the presence of channels and cages in their structure, whereas non-zeolitic materials show values between 20 and 21 [46]. Adsorption is a physical or chemical phenomenon in which molecules accumulate at an interface. This accumulation of molecules is small about the area, and most of the materials used for this purpose are those with high surface area. Due to their microporous structure, zeolites present high surface area per volume, being one of the most used materials for the adsorption of liquid and gaseous substances, achieving complete removal of contaminants in effluents, even at low concentrations [47]. Table 1 summarizes natural and synthetic zeolites' main physicochemical and structural characteristics. In general, synthetic zeolites have a lower framework density, due to their higher degree of crystalline ordering, compared to natural zeolites. Consequently, synthetic zeolites have a greater specific surface area, which increases their efficiency as an adsorbent. Ion exchange occurs in zeolites due to the presence of exchangeable cations inside the crystalline structure. Upon contact with an electrolyte solution, the zeolitic cations are removed from the structure and replaced by the solution cations. The amount of exchangeable cations is called cation exchange capacity (CEC), measured in milliequivalents/g, and is dependent on the chemical and physical properties of the material [48].

4.2.2. Natural zeolites

Zeolites occur in nature typically filling fractures and pores of volcanic rocks, which limits the formation of large deposits. So, this type of mineral deposit is relatively scarce. Volcanic rocks are the main precursor materials in the formation of zeolites, although other minerals such as feldspars, kaolinite, smectite, volcanic glass, or even other zeolites can fulfill this role, depending on the conditions of pressure, temperature, and presence of mineralizing fluids, in a dissolution-precipitation system [59]**.** Only a few countries in the world have exploitable zeolite reserves, exploited exclusively using open-pit methods. The processing of zeolitic ore is relatively simple, involving only comminution steps and grading by particle size ranges [60]. Among the 60 varieties of natural zeolites, only clinoptilolite, analcime, heulandite, laumonite, phillipsite, mordenite, chabazite, erionite, and ferrierite have large known sedimentary reserves, located mainly

in China [32, 59, 60]**.** Zeolitic ore reserves have not been estimated as most producing countries do not disclose this information and only their estimated production is available. In terms of production, the leading countries in 2019 were China (320.000 t), Korea (150.000 t), Slovakia (120.000 t), New Zealand (100.000 t), and the United States (98.000 t) [61]. Natural zeolites, unlike synthetic ones, exhibit a wide range of mineralogical and chemical composition, crystal structure, and pore sizes, which restrain their application if more homogeneous properties are required to guarantee high efficiency. Nevertheless, natural zeolites present a lower cost than synthetic zeolites, ensuring their application in animal feed production, water treatment, odor control, gas adsorption, and pozzolanic addition to Portland cement [62].

Table 4.1 - Structural and Physico-chemical characteristics of most important natural and synthetic zeolites used in effluent treatment.

	Zeolite	Chemical formula	Framework structure	Channel dimensions (Å)	Cation Exchange Capacity (CEC) ($meq.g^{-1}$)	Crystalline system	Space group	Framework density (T/1000 $Å^3$)	References
Natural	Clinoptilolite	$(K_2,Na_2,Ca)_3Al_6Si_{30}O_{72}.21H_2O$	HEU	3.1 x 7.5 + 3.6 x 4.6 [001]; 2.8 x 5.7 [100]	2.2	Monoclinic	*C2/m*	17.5	[49-51]
	Mordenite	$Na_8Al_8Si_{40}O_{96}.24H_20$	MOR	6.5 x 7.0 + 2.6 x 5.7 [001]	2.3	Orthorhombic	*Cmcm*	17.2	[49-51]
	Chabazite	$Ca_6Al_{12}Si_{24}O_{72}.\ 40H_2O$	CHA	3.8 x 3.8	3.8	Rhombohedral	*R3m*	14.5	[49-51]
	Phillipsite	$K_2,(Ca,Na_2)_2Al_6Si_{10}O_{32}.12H_2O$	PHI	3.8 x 3.8 [100]; 3.0 x 4.3 [010]; 3.2 x 3.2 [001]	3.3	Monoclinic	$P2_1/m$	15.8	[49-51]
	Analcime	$Na_{16}Al_{16}Si_{32}O_{96}.\ 16H_2O$	ANA	1.6 x 4.6	4.5	Cubic	*Ia3d*	18.5	[49-51]
	Erionite	$(Ca,Na_2)_{3.5}K_2Al_9Si_{27}O_{72}.27H_2O$	ERI	3.6 x 5.1	3.1	Hexagonal	$P6_3/mmc$	15.7	[49-51]
	Scolecite	$Ca_4Al_8Si_{12}O_{40}.12H_2O$	NAT	2.6 x 3.9 [100]; 2.5 x 4.1 [001]	5.2	Monoclinic	*Cc*	16.2	[59, 50, 52]
	Thomsonite	$Na_4Ca_8Al_{20}Si_{20}O_{80}.24H_2O$	THO	2.3 x 3.9 [100]; 2.2 x 4.0 [010]; 2.2 x 3.0 [001]	-	Orthorhombic	*Pncn*	17.7	[49]
	Sodalite	$Na_8Cl_2Al_6Si_6O_{24}$	SOD	2.8 x 2.8	-	Cubic	*P43n*	17.2	[49]
Synthetic	X	$Na_{58}Al_{58}Si_{134}O_{384}.240H_2O$	FAU	7.4 x 7.4	6.0	Cubic	*Fd-3*	13.3	[49, 53, 54]
	Y	$Na_{58}Al_{58}Si_{134}O_{384}.240H_2O$	FAU	7.4 x 7.4	3.9	Cubic	*Fd-3m*	13.3	[49, 53]
	A	$Na_{96}Al_{96}Si_{96}O_{384}.216H_2O$	LTA	4.1 x 4.5	5.3	Cubic	*Fm3c*	12.9	[49, 55, 56]
	ZSM-5	$Na_nAl_nSi_{96-n}O_{192}.16H_2O$, n<27	MFI	5.3 x 5.6	2.1	Orthorhombic	*Pnma*	17.9	[49, 57]
	ZSM-11	$Na_nAl_nSi_{96-n}O_{192}.16H_2O$, n<16	MEL	5.3 x 5.4	-	Tetragonal	*I4m2*	17.6	[49]
	H-USY	-	FAU	5.5 x 5.1	3.6	Cubic	*Fd-3m*	13.3	[49, 58]
	Beta	$Na_7A_{l7}Si_{57}O_{128}$	*BEA	6.6 x 6.7	1.8	Tetragonal	$P4_122$	15.1	[49, 58]
	ZK-5	$Na_{30}Al_{30}Si_{66}O_{192}.\ _{98}H_2O$	KFI	3.9 x 3.9	-	Cubic	*Im3m*	14.6	[49]

4.2.3. Synthetic zeolites

Crystalline solids can be synthesized using two approaches, whose chemical reactions occur in the solid-state, or the liquid state. The first class of reactions occurs slowly at relatively high temperatures, above 300 °C. In the liquid state, chemical species have greater freedom of movement, and the reaction occurs faster and at lower temperatures [35, 38, 63]. Zeolite synthesis occurs in a liquid state, and several methods can be applied, the main one being the hydrothermal method, considered one of the least costly methods. In the process, water is used as a solvent, along with the sources of silicon and aluminum. Other reagents involved in the process are the mineralizing agent (OH^-, F^-), metal cations, and structure-directing agent (usually an organic surfactant) [39]. Figure 2 illustrates the hydrothermal synthesis process. The reaction takes place in an autoclave reactor under high temperature and autogenous pressure (often up to 15 bar). The reaction product is then washed several times, filtered and oven dried. The solid obtained is the zeolite, which can be used for a variety of applications. The temperature and time for crystallization are critical parameters for synthesis and are dependent on the zeolite to be synthesized [63]. However, the method has some disadvantages, which may limit its application. The water consumption is high, which at the end of the process generates alkaline wastewater, difficult to manage. Besides, the processes may require long reaction times. With advances in zeolite synthesis studies, several other methods were developed, such as non-aqueous methods (solvothermal and ionothermal synthesis, whose solvent is replacing alcohol or hydrocarbons and ionic solutions, respectively), microwave radiation methods, sol-gel methods, ultrasound energy method, among others. Each process has its advantages and disadvantages, and specific types of zeolite crystalline structure can only be synthesized by a certain method, which becomes a limiting factor [35, 38, 39, 64].

The synthesis of zeolites using SiO_2 and Al_2O_3 from chemical reagents is an expensive process due to the cost of manufacturing and purchasing. For this reason, the number of researches focused on locating alternative sources of silica and alumina from cheaper and abundant sources increased in the last decades [35]. Several materials, including those considered waste, have already been successfully used for this purpose. To be used as a precursor, the residue must be cheap, readily available, generated in large quantities, and rich in silica and/or alumina, with low content of contaminating elements [65]. Table 2 shows a few of the most common waste materials used in zeolite synthesis. On the other hand, the quality of these materials is very unstable, which can compromise the quality of the synthesis, requiring a process optimization step [66]. Despite their higher cost, synthetic zeolites have the advantage

of presenting uniform properties, which can guarantee their application in processes that require materials with high purity. Among the properties of synthetic zeolites, the pore size distribution is an important feature to characterize this material. As shown in Table 1, natural zeolites generally present pores with smaller diameters, in addition to varying opening dimensions, depending on the crystallographic direction. On the other hand, a major characteristic of synthetic zeolites is their larger pore diameter, and their uniformity, regardless of the crystallographic direction, which consequently increases their efficiency in certain applications.

Despite advances in the field of zeolite synthesis, the nucleation and crystallization mechanisms are still not deeply understood. A full understanding of this field can lead to the synthesis of new crystalline structures, which can further expand the field of application of these materials. Further developments in the field of synthesis methods are also needed, to reduce the cost of production and bring economic benefits to large-scale production [65].

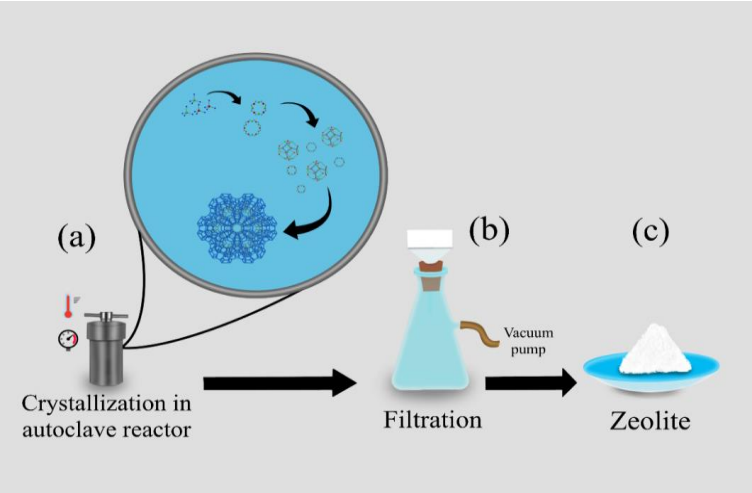

Figure 4.2 - Hydrothermal synthesis process. The crystallization occurs in an autoclave (a). Then the product is filtered and oven dried (b). The remaining solid is the zeolite (c).

Table 4.2 - Common low-cost waste materials used in zeolite synthesis.

Waste material	Oxide provided		Zeolite	References
	SiO_2	Al_2O_3		
Kaolin / Metakaolin	✓	✓	A, Y, 13X, ZSM-5	[31, 56, 67-74]
Glass powder	✓		A, sodalite, LOS-type zeolite, MEL-type zeolite, X, Na-P1, analcime	[75-79]
Aluminum waste		✓	13X, analcime, sodalite, A	[80, 81]
Coal Fly ash	✓	✓	X, A, sodalite, 4A, Na-P1, phillipsite, thomsonite, Y	[82-88]
Fumed silica	✓		A, Na-P	[89, 90]
Red mud		✓	FAU-type zeolite, GIS-type zeolite, magnetic 4A, A, X, ZK-5	[66, 91, 92]
Oil shale ash	✓	✓	X, A	[53, 93]
Bauxite residue		✓	X, A, P	[94-95]
Eletrolitic manganese residue	✓	✓	P, A, chabazite	[97]
Diatomite	✓	✓	X, Y	[98-100]
Rice husk ash	✓		A, ZSM-5, X	[15, 101-103]

4.3.4. Zeolite modification

The effectiveness of zeolite application in certain processes depends directly on their physicochemical and structural properties. In wastewater treatment, the zeolites which present negative electrical charge and compensation cations in their crystal structure ensure the removal of cationic species but can be incompatible with the removal of anionic species and organic compounds. Thus, the modification of zeolites enables the removal of these compounds, in addition to increasing the removal efficiency of cationic species by natural zeolites. Due to the different geological conditions in which zeolites crystallize in nature, the presence of more than one type of compensation cation is common. Modification with a solution of inorganic salts (NaCl, CaCl, NH_4Cl, among others) contributes to uniform the compensation cations present in the crystal structure. Since each cation can be exchanged at different levels of selectivity, standardization leads to optimization of the cation exchange capacity [104].

Another type of modification that has been extensively studied recently is surfactant modification. These chemical species (Figure 3(a)) are described by having a polar head (ionic

or neutral), and a non-polar tail, composed basically of hydrocarbons. Among cationic surfactants used in the modification of zeolites to remove organic compounds, tetramethylammonium, cetyltrimethylammonium (CTMA), hexadecyltrimethylammonium (HDTMA), octadecyldimethylbenzyl ammonium (ODMBA), n-cetylpyridinium (CPD), benzyltetradecyl ammonium (BDTDA), and stearyldimethylbenzylammonium (SDBAC) is the most commonly used [105]. As illustrated in Figure 3(b), unmodified zeolites can electrostatically attract only the cationic species in the solution. When modifying the zeolite with a cationic surfactant, below the critical micellar concentration (CMC), a surfactant monolayer is formed on the zeolite surface, in which the non-polar tails are directed towards the bulk solution, and attracts the organic species through hydrophobic interactions (Figure 3(c)). When surpassing the CMC, a surfactant bilayer is formed, which results in the reversal of the electrical charge of the zeolite surface. Under these conditions, anions in the solution can be removed, as well as organic compounds that can still interact with the hydrophobic regions (Figure 3(d)) [106].

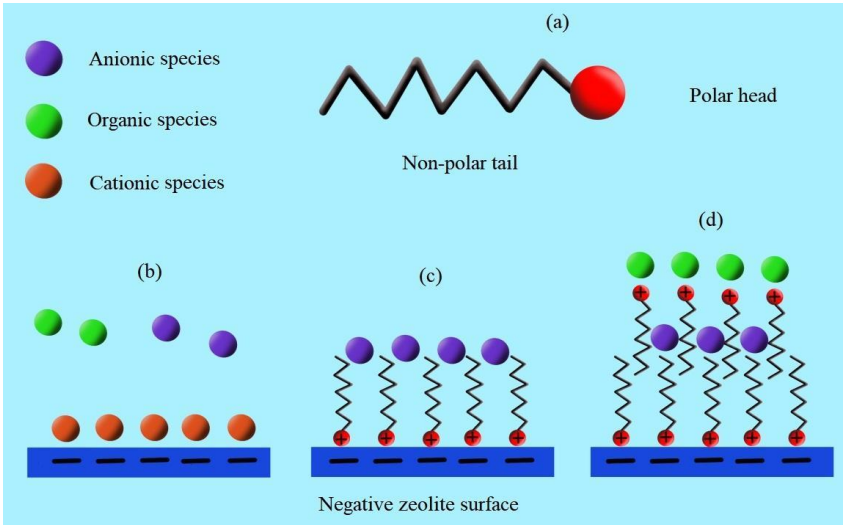

Figure 4.3 - Zeolite can only adsorb cationic species (b). When modified by a cationic surfactant (a), zeolite can also remove anionic (c), and organic species or both (d).

4.3.5. Zeolite characterization for water treatment

The characterization of any material is of great importance for the knowledge of its physical and chemical characteristics, and the prediction of its behavior during its application. In the case of zeolites for the treatment of effluents, some characterization techniques are especially relevant.

The identification of the zeolitic phases can be performed using X-Ray Diffraction (XRD), which is the most used technique for this purpose. In addition to the identification of phases and the quantification by the Rietveld method (particularly in the case of natural zeolites, which present other contaminating minerals), it is also possible to determine their degree of crystallinity (in synthetic zeolites, the presence of non-crystalline material remaining after synthesis negatively affects the material's adsorption capacity) [108].

As mentioned in section 2.1, adsorption is a phenomenon that is surface area-dependent. Furthermore, pore size also affects the efficiency and selectivity for adsorption of molecules and ions by intraparticle diffusion. Such parameters can be determined using gas adsorption-desorption techniques with the aid of the Brunauer-Emmett-Teller (BET) model, to determine the specific surface area, and Barret-Joyner-Halenda (BJH) model, to determine the relative distribution of pore sizes. Once defined, these parameters are used to select the best zeolite to remove a particular contaminant [109].

In the case of removal of organic contaminants, the regeneration of zeolite by temperature is possible, enabling the reuse of the material, which can bring economic benefits to the process. The thermogravimetry (TG) and differential thermal analysis (DTA) techniques help detect the maximum temperature to which the zeolite can be subjected without the destruction of its crystalline structure, with a consequent reduction in its potential for removing contaminants, thus, contributing to the optimization of the regeneration process [109].

Another technique that is relevant in the characterization of zeolite for effluent treatment is the determination of the material's surface electrical properties (zeta potential). Since the electrical charge of zeolites can be modified by changing the pH, the determination of the point of zero charge (pH_{PZC}) at which the reversal of electrical charge occurs contributes especially in the removal of anionic contaminants, in which it is possible to make the surface positively charged by proper pH adjustment [107].

Finally, the determination of the cation exchange capacity (CEC) must be determined, to estimate the amount of contaminant per unit of mass a given zeolite is capable to remove, which implies defining the optimal amount of zeolite for a given process [110]. Although there are other characterization techniques necessary for other applications, the above-mentioned are of greater relevance in the use of zeolites for the treatment of effluents.

4.3. Application of zeolites in wastewater treatment

The quality of industrial effluents has received increased attention due to the concern with environmental impacts in the industrial sector. In this context, an efficient collection and treatment system becomes necessary, as incorrect disposal of water has the potential to cause a series of liabilities to the environment [6, 111-118]. Besides, there is great pressure from environmental policies for the reuse of effluent, to reduce the intake of new water and preserve natural resources [119]. Due to their cationic exchange negative charge characteristics, and relatively low synthesis cost, zeolites have great potential to be used in the removal of a wide variety of substances, such as heavy metals, organic compounds, dyes, and pigments, reagents, nitrogen compounds, among others [105].

4.3.1. Inorganic compounds removal

4.3.1.1. Heavy metals

The application of zeolites for heavy metal sequestration in effluent treatment has found the largest applicability with synthetic zeolites, followed by modified zeolites. Natural varieties, although quite attractive from an economic point of view, show the lowest metal sorption for most heavy metals, as presented in Table 3, because the mineralogical composition of natural zeolites varies greatly from one region to another, and even within the same mineral deposit [60]. In addition, in many cases, more than one variety of zeolite is found in the ore, along with several other minerals which act as contaminants, since they have low metal sorption capacity. Among the contaminating minerals, quartz, albite, biotite, illite, montmorillonite, feldspar, calcite, halite, and heulandite are commonly observed [52, 120, 121]. Synthetic zeolites, constituted in most cases by a single-phase, are adsorbents with high uniformity in their properties, such as pore size distribution, hydrophobicity/hydrophilicity, and the presence of a single compensation cation. The combination of these parameters guarantees their greater capacity for cation exchange compared to natural zeolites.

The modification of natural zeolites concerns a series of chemical treatments that aim to intensify their properties. Chemical treatments, with acids and/or bases, lead to the removal of impurities that clog the pores, resulting in increased cation exchange capacity [105]. Another way of modifying zeolites is by using organic surfactants, which form a monolayer at the zeolite surface. Quaternary amines are the most widely used reagents for this purpose and, as cationic reagents, give the zeolites the ability to adsorb anions [50]. In Table 3, it can be

observed that modified clinoptilolite demonstrated intermediate adsorption capacity between its natural and synthetic forms. The use of hexadecyl pyridinium bromide (a surfactant with the cationic site) in the modification of clinoptilolite enabled the removal of chromium, in the CrO_4^{2-} form, something that would not be possible with natural or synthetic zeolites [122]. Another heavy metal that is present in the form of anions in solution is arsenic. At pH values above 2, this element is found in the forms $HAsO_4^{2-}$, $H_2AsO_4^-$ and AsO_4^{3-}, and its removal is only possible with the use of modified zeolites. In a study using clinoptilolite coated with iron oxide, the removal of arsenic in the anionic solution was possible, due to its affinity for the iron oxide sites at the zeolite surface [123].

Adsorption processes that use zeolites as adsorbents are strongly affected by changes in pH, temperature, and adsorbent/solution mass ratio. When the attractive forces between the surface and the adsorbate overcome the attraction between the adsorbate and the solvent, the ions start to concentrate on the zeolite surface. As a rule, the zeolite metal adsorption process occurs in an endothermic and spontaneous process, presenting higher rates of adsorption with increased temperature [124]. This fact was proved by Dal Bosco et al. [52], who carried out adsorption tests with Cr^{2+}, Ni^{2+}, $Cd^{2+,}$ and Mn^{2+} in zeolite scolecite, at temperatures of 25, 40, and 60 °C. The authors reported greater adsorption of all metals in tests performed at 60 °C, followed by those performed at 40 and 25 °C. In similar experiments, Ćurković *et al*. [121] analyzed the use of natural clinoptilolite to remove Pb^{2+} and Cd^{2+} at different temperatures (20-70 °C). The results also indicated that the increase in temperature favors the adsorption rate in all analyzed scenarios.

The variation in pH also strongly affects the metal adsorption capacity of zeolites. In highly alkaline environments, it can be observed the formation of metal oxides and hydroxides as a precipitated form, reduces the availability of ions to be adsorbed, thus reducing the adsorption rate. In highly acidic environments, the presence of an abundant amount of H^+ in the solution impairs the adsorption due to competition between this chemical species and the metal to be adsorbed, which also reduces the adsorption rate, as verified by Zanin *et al*. [125]. The authors evaluated the removal of Cr^{3+}, $Cu^{2+,}$ and Fe^{3+} using clinoptilolite, in solutions with pH 3, 4, and 5. For chromium, the removal rate was greater at pH 5, with the lowest value observed at pH 3. As for copper and iron, adsorption reached its maximum at pH 4, being slightly lower at pH 5. In solutions with pH 3, 4, and 5, Dal Bosco *et al*. [52] demonstrated that the adsorption density of Cd^{2+}, $Mn^{2+,}$ and Cr^{3+} in zeolite scolecite increased progressively with the increase in pH, whereas for Ni^{2+} the adsorption rate increased rapidly from pH 3 to 4, but showed a significant increase in the transition to pH 5. In a similar study, Alvarez-Ayuso *et al*. [120] varied the pH to values of 3, 4, 5, and 6, in the analysis with Zn^{2+}, Cd^{2+}, Cu^{2+}, $Ni^{2+,}$ and Cr^{3+} using

NaP1 zeolite. The Zn^{2+} adsorption values increased with increasing pH, whereas Cd^{2+}, $Cu^{2+,}$ and Ni^{2+} showed a slight increase in the transition from pH 3 to 4, stabilizing above that value. As for Cr^{3+}, the adsorption increased significantly from pH 3 to 4, again sharply reducing from pH 5 to 6. It is evident the fundamental role of pH in the adsorption of metals in zeolites, as this governs the metal speciation in solution. Preliminary studies of the effect on the solution's pH are needed to evaluate the removal efficiency, especially when the system is multi-element, as each metal has specific pH values at which certain compounds form and precipitate [126]. The pH conditions most used in the application of zeolite in heavy metal removal are close to neutrality or slightly acidic, as can be seen in Table 3.

The solid-liquid ratio is also an important experimental variable when investigating metal adsorption in zeolites. The changes in this parameter can directly or indirectly affect other variables, such as the pH and the solution chemical composition [124]. The increased number of particles raises the specific surface area available for adsorption to occur. In addition, the friction between the particles is more intense than in systems with lower solid percentages. As the particles break down, further increasing the available surface area, greater metal removal can be achieved [124]. It is expected that the adsorption rate will increase with dosage, however, this is not always observed. The high zeolite dosage also increases the amount of the compensation cations in the solution, which can compete with the heavy metal to be removed, leading to a reduction in the adsorption rate [124].

Table 4.3 - Heavy metals removed by different zeolites, along with experimental conditions and adsorption and kinetic models.

Metal ion	Zeolite	T (°C)	Contact time (h)	Metal concentration ($mg.L^{-1}$)	S/L ratio ($g.L^{-1}$)	pH	Metal sorption ($mg.g^{-1}$)	Isotherm model	Kinetics model	References
Pb^{2+}	A	25	5	50-800	1	4	100.0	Langmuir	Pseudo-second order	[91]
	A	25	0,5	100-400	-	7.5	182.0	Langmuir	-	[127]
	X	25	0,5	100-400	-	7.5	213.0			[127]
	Clinoptilolite	70	24	200-2000	10	4.5	78.7	-	-	[121]
	Na-Clinoptilolite	70	24	200-2000	10	4.5	91.2	-	-	[121]
	Faujasite	25	1	70-400	2.5	4.5	25.9	Langmuir	Pseudo-second order	[128]
	Y	26	1	100	1	6	454.5	Langmuir	Pseudo-second order	[129]
	Clinoptilolite	20	6	103.8	100	3	51.6	Langmuir	-	[126]
	HDTMA-Y	25	24	1000.0	4	5	76.0	Langmuir	Pseudo-second order	[130]
Cd^{2+}	A	25	5	50-800	1	4	56,5	Langmuir	Pseudo-second order	[91]
	NaP1	22	6	10-200	2.5	6	50.8	Langmuir	-	[120]
	A	25	0.5	100-400	-	7.5	71.0	Langmuir	-	[127]
	X	25	0.5	100-400	-	7.5	92.0			[127]
	Clinoptilolite	22	6	10-200	10	6	4.6	Langmuir	-	[120]
	Clinoptilolite	70	24	110-1100	10	4.5	13.5	-	-	[121]
	Scolecite	55	24	10-5000	16	6	100.0	Freundlich	Pseudo-second order	[52]
	Na-Clinoptilolite	70	24	110-1100	10	4.5	23.6	-	-	[121]
	Clinoptilolite	20	6	81.5	100	3	7.3	Langmuir	-	[126]
	A	30	-	50-1000	3	8	736.4	Langmuir	Pseudo-second order	[113]
	X	30	-	50-1000	3	8	684.4			
	X	30	2.5	10-160	1	7	38.3	Langmuir	Pseudo-second order	[132]
Cr^{3+}	NaP1	22	6	10-200	2.5	4	43.6	Langmuir	-	[120]
	A+X	25	24	500	5	-	71.1	-	-	[133]

Ni^{2+}	A	25	4	50-300	1	4	41.6	Langmuir	Pseudo-second order	[134]
	Clinoptilolite	22	6	10-200	10	4	4.1	Langmuir	-	[120]
	Mordenite	25	24	500	5	-	3.6	-	-	[133]
	Scolecite	55	24	10-5000	16	6	106.4	Freundlich	Pseudo-second order	[52]
	X	30	2	10-160	1	7	62.1	Langmuir	Pseudo-second order	[132]
	A	25	5	50-800	1	4	41.2	Langmuir	Pseudo-second order	[91]
	A	25	4	50-300	1	4	9.0	Langmuir	Pseudo-second order	[134]
	NaP1	22	6	10-200	2.5	6	20.1	Langmuir	-	[120]
	A	25	1	100-400	-	7.5	24.7	Langmuir	-	[127]
	X	25	1	100-400	-	7.5	24.9			[127]
	Clinoptilolite	22	6	10-200	10	6	2.0	Langmuir	-	[120]
	Scolecite	55	24	10-5000	16	6	122.0	Freundlich	Pseudo-second order	[52]
	13X	40	3	0-100	5	6	6.2	Langmuir	Pseudo-second order	[135]
	HDTMA-Y	25	24	1000	4	5	20.0	-	Pseudo-second order	[130]
Zn^{2+}	A	25	5	50-800	1	4	45.5	Langmuir	Pseudo-second order	[91]
	A	25	4	50-300	1	4	30.8	Langmuir	Pseudo-second order	[134]
	NaP1	22	6	10-200	2.5	6	32.6	Langmuir	-	[120]
	A	25	0.5	100-400	-	7.5	28.6	Langmuir	-	[127]
	X	25	0.5	100-400	-	7.5	41.0			[127]
	Clinoptilolite	22	6	10-200	10	6	3.5	Langmuir	-	[120]
	Clinoptilolite	20	6	98.6	100	3	5.1	Langmuir	-	[126]
	HDTMA-Y	25	24	1000	4	5	26.0	-	Pseudo-second order	[130]
	X	30	2.5	10-160	1	7	45.1	Langmuir	Pseudo-second order	[132]
Cu^{2+}	A	25	5	50-800	1	4	35.6	Langmuir	Pseudo-second order	[91]
	A	25	4	50-300	1	4	50.5	Langmuir	Pseudo-second order	[134]
	NaP1	22	6	10-200	2.5	5	50.5	Langmuir	-	[120]
	A	25	0.5	100-400	-	7.5	41.6	Langmuir	-	[127]
	X	25	0.5	100-400	-	7.5	48.8			[127]
	Clinoptilolite	22	6	10-200	10	5	5.9	Langmuir	-	[120]
	Clinoptilolite	20	6	97.9	100	3	4.8	Langmuir	-	[126]
	HDTMA-Y	25	24	1000	4	5	36.0	-	Pseudo-second order	[130]
	X	30	2	10-160	1	7	64.6	Langmuir	Pseudo-second order	[132]
Mn^{2+}	Clinoptilolite + Mordenite	25	2	5-600	2.5	6	7.1	Langmuir	Pseudo-second order	[136]
	NaOH-activated Clinoptilolite + Mordenite	25	2	5-600	2.5	6	20.9	Langmuir	Pseudo-second order	[136]
	NH_4Cl-activated Clinoptilolite + Mordenite	25	2	5-600	2.5	6	18.5	Langmuir	Pseudo-second order	[136]
	NaCl-activated Clinoptilolite + Mordenite	25	2	5-600	2.5	6	21.3	Langmuir	Pseudo-second order	[136]
	Na_2CO_3-activated Clinoptilolite + Mordenite	25	2	5-600	2.5	6	19.7	Langmuir	Pseudo-second order	[136]
	Manganese oxide-coated Clinoptilolite+mordenite	25	2h	25-600	2.5	6	30.8	Langmuir/ Freundlich	Pseudo-second order	[137]
	Scolecite	55	24	10-5000	16	6	109.9	Freundlich	Pseudo-second order	[52]
As^{5+}	Iron coated clinoptilolite	25	-	2	100	4	0.7	Langmuir	-	[123]
Cr^{6+}	Clinoptilolite	20	24	30-350	25	5	0.9	Langmuir	Pseudo-second order	[122]
	HDPB-Clinoptilolite	20	24	30-350	25	5	2.8	Freundlich	Pseudo-second order	[122]
	Chabazite	20	24	30-350	25	5	1.5	Langmuir	Pseudo-second order	[122]
	HDPB-Chabazite	20	24	30-350	25	5	14.3	Freundlich	Pseudo-second order	[122]
	13X	40	3	0-100	5	6	3.9	Langmuir	Pseudo-second order	[135]

In heavy metal adsorption systems, it is important to consider the presence of more than one species in the solution. In a mixture of heavy metal ions, the increase in the initial concentration leads to a reduction in the adsorption of certain species, due to the greater selectivity presented by some species. Table 4 presents sequences of selectivity for the adsorption of metals in different zeolites, synthetic and natural. Several factors govern the selectivity for metal ions, which must be considered in each system investigated. Among them, it can be cited the

microporous structure and the properties of the element to be removed, such as the ionic radii, hydrated ionic radii, and free hydration energy [134]. As an example, it is noticed the greater ease that lead presents of being adsorbed by zeolites. Among the metals investigated, lead presents the lowest atomic radius when surrounded by water molecules and the lowest hydration energy, which expresses the difficulty to lose the water molecules that surround the ion [134]. Therefore, the metal shows great facility to become a dehydrated ion. Although its dehydrated atomic radius is larger, the other ions tend to remain in hydrated form, which makes the penetration of dehydrated lead ions into the zeolite structure more likely, explaining the greater selectivity in the removal of this metal is present [126].

The adsorption is strongly dependent on factors such as solution pH, temperature, adsorbent dosage, and solution initial concentration. Since these factors varied in the studies analyzed (Table 3), it is difficult to compare the performance of different zeolites. However, in a study verifying the adsorption of a mixture of heavy metals using zeolites A and X, in the same experimental conditions, Ibrahim *et al*. [127] observed greater efficiency in removal using phase X, since this crystalline structure has larger pores (7.4Å), compared to phase A (4.5Å). In a similar study, Shariatinia and Bagherpour [129] also noticed a higher affinity of lead for zeolite NaY (7.4Å) compared to zeolite NaP1 (which has different windows depending on the crystallographic directions: 3.1x4.5Å [100], 2.8x4.8Å [010]). Smaller pores, of dimensions close to those of hydrated ions, limit their entry and impair the diffusion process within the crystalline structure, which compromises the performance of a particular zeolitic phase as an adsorbent.

Table 4.4 - Selectivity in competitive adsorption of heavy metals by different zeolites.

Adsorption selectivity			**Ionic properties**				
Zeolite	**Selectivity**	**References**	**Heavy Metal**	**Hydrated radius (Å)**	**Unhydrated radius (Å)**	**Free energy of hydration (KJ.mol^{-1})**	**References**
FAU-type	$Pb^{2+}>Cu_{2+}>Cd^{2+}>Zn^{2+}>Co^{2+}$	[138]	Pb	4.01	1.32	-1425	[139, 140]
A	$Cu^{2+}>Cr^{3+}>Zn^{2+}>Co^{2+}>Ni^{2+}$	[134]	Cu	4.19	0.72	-2010	
A	$Pb^{2+}>Cd^{2+}>Cu^{2+}>Zn^{2+}>Ni^{2+}$	[127]	Cd	4.26	0.97	-1755	
A	$Pb^{2+}>Cd^{2+}>Zn^{2+}>Ni^{2+}>Cu^{2+}$	[91]	Zn	4.30	0.74	-1955	
NaP1	$Cr^{3+}>Cu^{2+}>Zn^{2+}>Cd^{2+}>Ni^{2+}$	[120]	Co	4.23	0.72	-1915	
X	$Pb^{2+}>Cd^{2+}>Cu^{2+}>Zn^{2+}>Ni^{2+}$	[127]	Cr	4.61	0.64	-4010	
X	$Cr^{3+}>Cu^{2+}>Cd^{2+}>Zn^{2+}$	[132]	Ni	4.04	0.70	-1980	
Scolecite	$Cr^{3+}>Mn^{2+}>Cd^{2+}>Ni^{2+}$	[52]	Mn	4.38	0.80	-1760	
Clinoptilolite	$Pb^{2+}>Zn^{2+}>Cu^{2+}>Cd^{2+}$	[126]					
Clinoptilolite	$Cu^{2+}>Cr^{3+}>Zn^{2+}>Cd^{2+}>Ni^{2+}$	[120]					

4.3.1.2. Nitrogen compounds

As seen in Table 5, zeolites show great potential for application in ammonia removal from effluents. The synthetic versions, due to their larger pore sizes, have a greater affinity for the

ammonia molecules (mean diameter of 0.283nm), which facilitates their entry into the zeolite crystalline structure [141]. Temperature also plays an important role in the removal of ammonia by zeolite, with a reduction in the amount of ammonia removed as the temperature increases, due to the desorption of ammonia from the surface [142]. In contrast, Widiastuti *et al*. [143] demonstrate in their studies that the increase in temperature increases the amount of ammonia adsorbed. These results indicate the influence of temperature on ammonia adsorption onto zeolites are yet not well understood. Despite the importance of temperature in adsorption processes, this variable has not been thoroughly investigated, and further studies are needed to conclude its influence on the ammonia-zeolite adsorption system.

Solution pH strongly affects the adsorption process as well. At very low pH values, competition between H^+ ions makes it difficult to adsorb ammonia molecules, reducing the sorption capacity. In alkaline solutions, NH_4^+ converts to NH_3, which also reduces the adsorption rate, due to the elimination of electrostatic attraction forces between adsorbate and adsorbent. In a study analyzing ammonia adsorption in pH between 4-10, Fu *et al*. [144] observed that the greatest removal of NH_4^+ with a natural clinoptilolite occurs at pH 5-8. In adsorption tests carried out in the pH range between 2-11, Zhao *et al*. [145] verified maximum removal of ammonia by a mixture of zeolite P and analcime, synthesized from red mud, occur at pH 6. In a study analyzing the removal of ammonia by synthetic zeolites, A and X in the pH range between 2 and 10, Moussavi *et al*. [141] demonstrated that the optimum value for the removal of ammonia occurs at pH 7. These results indicate the importance that this variable presents in the removal of ammonia using zeolite as adsorbents, and that the best results can be obtained at pH close to neutrality.

Another factor to be considered in ammonia removal using zeolites is the competition with other ions in the solution. The ionic species readily penetrate the zeolite pores, being easily adsorbed in comparison with molecules. Fu *et al*. [144] analyzed the removal of ammonia using clinoptilolite and clinoptilolite modified with $NaNO_3$ and found that the presence of Na^+, K^+, Mg^{2+}, NO_3^-, SO_4^{2-} and Cl^- negatively affected the NH_4^+ adsorption rate. Zhao *et al*. [145] verified that the removal of NH_4^+ undergoes a significant reduction in the presence of cations such as Na^+, K^+, Ca^{2+}, and Mg^{2+}, due to the zeolite preference to adsorb ions. The order of selectivity in this system was defined as $Na^+ > K^+ > Ca^{2+} > Mg^{2+} > NH_4^+$. Lin *et al*. [146] evaluated the use of chabazite natural zeolite to remove ammonia from swine manure. The chabazite used in the tests had high calcium content and, according to the authors, the exchange rate between calcium and ammonia occurs more slowly than for sodium, due to the higher resistance to the diffusion of Ca^{2+}, something that contributes to the reduction of the adsorption rate. In a study

conducted by Haji *et al*. [4], on the removal of NH_4^+ using zeolite Y with different compensation cations, Na^+ proved to have the highest ammonia removal potential (91.8%), followed by Cs^+ (24.8%), K^+ (24.3%), Mg^{2+} (18.5%) and Ca^{2+} (18.5%). The authors also made a comparison with the performance of zeolite X in the removal of ammonia (both with Na^+ cation), which presented an 83.8% removal. The authors stated that, although zeolite X has a lower Si/Al ratio (which consequently results in a higher CEC), zeolite Y has a greater surface area (980 $m^2.g^{-1}$ vs 527 $m^2.g^{-1}$), which increases its performance as an adsorbent.

Table 5 summarizes several studies utilizing zeolites as adsorbents to remove ammonia. A direct comparison of the efficiency of different zeolite types in the removal of ammonia is difficult, due to the variability of the experimental conditions. Zeolite dosage, ammonia concentration, and contact time are factors that strongly influence adsorption and, as seen in Table 5, these variables were investigated over a wide range. Ideally, it would be necessary to develop standardized tests, under the same conditions, to identify the best zeolite to be used for ammonia removal. However, synthetic zeolites with larger pore openings showed the highest removal capacity, as in the case of zeolites X and A.

Table 4.5 - Zeolites used in ammonium removal, along with experimental conditions and adsorption and kinetic models.

Zeolite	T (°C)	Contact time (h)	concentration ($mg.L^{-1}$)	S/L ratio ($g.L^{-1}$)	pH	NH_4^+ Sorption capacity (mg.L-1)	Isotherm model	Kinetics model	References
Clinoptilolite	25	12	1-20	0-0.6	-	4.3	Langmuir	Pseudo-first order	[144]
$NaNO_3$-modified Clinoptilolite	25	12	1-20	0-0.6	-	8.1	Freundlich	Pseudo-first order	
Zeolite P + Analcime	25	1	5-500	5	6	17.5	Koble-Corrigan	Pseudo-second order	[145]
Zeolite X Zeolite A	25	8	100-400	2	7	89.1 59.3	Freundlich	Pseudo-second order	[141]
Chabazite	25	5	130-2080	75	7	39.3	Langmuir	Pseudo-second order	[146]
Zeolite NaY	25	2	40-615	6.3	--	26.5	Langmuir	Pseudo-second order	[4]
Modified Na-Clinoptilolite	25	24	0-83	-	7.2	14.5	Langmuir	-	[147]
Clinoptilolite + Mordenite	25	8	5-120	10	6	6.3	Freundlich	Pseudo-second order	[143]
Zeolite NaA Magnetic Zeolite NaA	25	0-2	-	-	7.9	10.5 10.4	Freundlich	Pseudo-second order	[142]

4.3.1.3. Phosphoric compounds

As zeolites have low efficiency in removing anionic species in solution, the removal of phosphoric compounds can be especially challenging, as they are present in solution in the anionic form, in a wide pH range. Below pH 2, the predominant species is H_3PO_4, while at pH

between 2-7, 7-12, and above 12, the dominant species are $H_2PO_4^-$, HPO_4^{2-} and PO_4^{3-}, respectively, which result in electrostatic repulsion due to the negative charge. In the acidic pH range, however, sites on the zeolite surface undergo protonation, acquiring a positive electrical charge and attracting phosphate ions, which is followed by chemical interaction between the molecular species and the zeolite surface. This effect was verified by Zhang *et al*. [159], using granular natural zeolite to remove phosphorus from effluent. In removal tests in different pH ranges (1.8-12), it was found that the highest removal rate (close to 100%) occurred at pH 2, reaching close to 0% at pH 7, and increasing slightly in the alkaline pH range. The authors state that alkaline conditions lead to chemical precipitation, which might explain this behavior. In contrast, adsorption is favored by the expansion of the zeolite pores in acidic pH, which contributes to the increase in the surface area available for adsorption. Hamdi and Srasra [160] compared the phosphate adsorption using clay minerals (kaolinite + illite and kaolinite + smectite) and zeolite A. The pH at which the zeolite showed greater adsorption was 5.5, below the PZC of the zeolite A (PZC= 6.7) [154]. The authors explained that the adsorption of phosphate anions in zeolite occurs at positive sites that are protonated at acidic pH. The attraction of negatively charged molecules at these sites is followed by chemical interaction, leading to higher phosphate adsorption.

The modification of the surface of zeolites is a factor that contributes positively to the adsorption of phosphates since the chemical interaction between species and surfaces often exceeds the electrostatic repulsion between them. Goscianska *et al*. [161] evaluated the modification of synthetic zeolites NaP1, NaA, and natural clinoptilolite with lanthanum, aiming at investigating phosphate adsorption. After the modification, the specific surface area and pore volume were reduced in all varieties of zeolites. However, the amount of phosphate adsorbed by the modified zeolites was higher, especially in the case of synthetic zeolites. The authors attributed this increase in adsorption to the fact that lanthanum has a greater affinity to phosphate. X-ray diffraction tests revealed crystallized lanthanum phosphate peaks in the samples after the adsorption tests, which explains why the adsorption increased even with the reduction of the specific surface area and pore volume. Alshameri *et al*. [162] studied the potential of using clinoptilolite zeolite and its modified version with tetra butyl titanate to remove PO_4^{3-}. The authors state that, in this case, it is necessary to modify the surface of the zeolite using inorganic salts or organic surfactants that lead to the appearance of sites with a positive charge. As can be seen in Table 6, the adsorption capacity of natural and synthetic zeolites for phosphate is relatively low, when compared to the other contaminants evaluated in this study. However, the modification is a factor that contributes significantly to increasing the adsorption capacity.

Temperature also presents an important role in phosphate adsorption using zeolite. The increase in temperature positively affects the adsorption capacity. The phosphate molecules move more quickly in the solution, increasing their efficiency in the adsorption of the contaminant. Goscianska *et al*. [161] verified the increase of the adsorption capacity from 10.5 to 16.2 $mg.g^{-1}$ and 57.7 to 63.9 $mg.g^{-1}$, for the synthetic and modified zeolites NaP1 and LaP1, respectively, when the temperature was varied from 25 to 60 ° C, demonstrating the endothermic character of the process.

In the adsorption of anionic species, such as phosphoric compounds, pH control is of fundamental importance. In the case of zeolites, pH below the point of zero charges (PZC) provides the appearance of positive sites at the adsorbent surface, which makes adsorption possible.

Table 4.6 - Phosphate removal by different zeolites, along with experimental conditions and adsorption and kinetic models.

Zeolite	T (°C)	Contact time	Concentration ($mg.L^{-1}$)	S/L ratio ($g.L^{-1}$)	pH	PO_4^{3-} Sorption capacity ($mg.g^{-1}$)	Adsorption isotherm model	Adsorption kinetics model	References
NaP1						11.4			
LaP1						58.2			
NaA	25-60	24h	12.5-200	1	5.3	15.7	Langmuir	-	[161]
LaA						48.9			
Clinoptilolite						20.2			
La-Clinoptilolite						25.5			
Fe-Heulandite	25	3h	1-16	2.4	7	<0.2	Freundlich	-	[163]
Granular zeolite	25	20min	20	25	1.8	3.3	Langmuir	-	[159]
Zeolite A	70	4h	50-1000	6.6	5	52.9	Langmuir	Pseudo-second order	[160]
Clinoptilolite	25	2h	10-100	48	2-4	1.3	Langmuir	-	[162]
TiO_2-modified clinoptilolite				20		34.2			

4.3.2. Organic compounds removal

4.3.2.1. Dyes

The removal of dyes on zeolite surfaces occurs by ion-exchange properties. Table 7 shows the results of several studies using zeolites as adsorbents for dyes. As can be seen, synthetic zeolites have a greater adsorption capacity compared to natural ones, reflecting their greater degree of composition uniformity and physical properties (*e.g.*, crystalline structure, pore size, and compensation cations).

Zeolites exhibit different ion adsorption selectivity and competitive adsorption in multicomponent systems. Ayar *et al*. [148] used natural clinoptilolite and zeolites synthesized from fly ash (analcime + sodalite) to evaluate the removal of safranine O (SO) dye in the presence of Cs^+. The authors noticed that the increase in Cs^+ concentration leads to a reduction in the removal of SO for both zeolites since the Cs^+ ions compete with the SO molecules for the active sites on the surface of the zeolite samples. Due to the difference in the pores sizes of the zeolites used, the results also indicate greater adsorption of SO by clinoptilolite (4.1Å) in comparison with analcime and sodalite (3.2 and 2.3 Å, respectively).

In dye adsorption systems, it is important to consider the size of the molecule to be adsorbed, as this parameter strongly affects the adsorption efficiency. Wang and Zhu [149] carried out a comparative study on the removal of methylene blue and rhodamine B dyes by clinoptilolite zeolite. The larger size of the rhodamine B molecule was indicated to impair the diffusion process in the zeolite pores. The removal capacity verified for this compound, at room temperature, was 9.3 $mg.g^{-1}$, 55% of the capacity verified for methylene blue (16.7 $mg.g^{-1}$). In addition to the adsorption capacity, the relationship between the size of pores and pigment molecules directly affects the adsorption rate. As seen in Table 7, for natural zeolites (*e.g.*: clinoptilolite, analcime, sodalite, and erionite), the equilibrium time is considerably longer, compared to synthetic zeolites (*e.g.*: X and Y), which is explained by the considerably larger pores and greater adsorption capacity, even at shorter contact time [149].

The pH adjustment is also of great importance for the removal of dyes in zeolite adsorption systems. In pH in the basic range, the presence of OH^- causes a deprotonation reaction in the zeolite, inducing an increase in the negative electric charge, which intensifies the adsorption of cationic species. As verified by Oukil *et al*. [150], the adsorption of methylene blue (MB), a cationic dye, reaches its maximum value at pH 8. Lower adsorption was verified at pH 3, due to competition with H^+ ions, in addition to protonation reaction, which makes the zeolite surface charge positive, thus causing electrostatic repulsion between species. Badeenezhad *et al*. [151] found that the pH variation strongly affects the adsorption of clinoptilolite in its natural form, reaching maximum removal of MB in the pH range between 7 and 9. As for the clinoptilolite modified using iron oxide nanoparticles, the adsorption did not show much variation with the pH change, reaching removals greater than 96.4% in the pH range between 3 and 9. The authors state that an alkaline pH, the association of a small amount of available H^+, and the negative surface charge increase the electrostatic attraction of the MB molecules, favoring adsorption. In the case of modified clinoptilolite, the OH^- groups form hydroxy complexes with iron oxide present in the zeolite structure, which contributes to reducing the amount of MB adsorbed. Mittal *et al*. [152] used zeolite Y to remove brilliant green (BG) dye

from the solution. The removal was analyzed in solutions with pH ranging from 2 to 11. In the case of removal of BG by zeolite Y, 78% of dye was removed when the pH of the solution had been adjusted to 6, with no gains in removal being observed at higher pH values, whereas a reduction in the amount of dye removed was observed below pH 6. Cationic dyes are best removed by the zeolite at pH above the point of zero charges (PZC), in which the zeolite surface presents a negative charge. Previous studies indicate that most zeolites present PZC at pH close to neutrality, as verified for zeolites A (PZC= 6.7) [153], Y (PZC = 5.8) [154], NaP1 (PZC = 6.5) [154], sodalite (PZC = 6.5) [155] and clinoptilolite (PZC = 8) [155]. As natural and synthetic zeolites have shown much lower adsorption of anionic dyes compared to cationic ones, due to electrostatic repulsion, pH adjustment becomes of fundamental importance in the removal of these species since zeolites can acquire positive charge in pH< PZC. As verified by Garg *et al*. [156] when studying the adsorption of amido black 10B, an anionic dye, the highest removal rate occurred in the pH range between 2 and 5. Above this pH value, the studied zeolite (synthetic zeolite X) acquires a negative electrical charge, which leads to electrostatic repulsion and consequent reduction in the removal of the contaminant.

Temperature also plays an important role in dye adsorption using zeolites. The temperature increases the mobility of the ions and promotes the expansion of the crystalline structure of the zeolite, which causes an increase in the adsorption rate [157]. Wang and Zhu [149] analyzed the adsorption of MB and rhodamine B in natural clinoptilolite. The increase in temperature positively affected the adsorption, and for both dyes the amount adsorbed was greater at approximately 50°C, showing the endothermic characteristic of the adsorption. On the other hand, the increase in temperature may lead to a reduction in the removal of contaminants, as verified by Garg *et al*. [156], who noted that raising the temperature from 293 K to 333 K resulted in a reduction in the removal of amido black 10B from 73.4% to 48.6%, due to desorption of dye molecules. Temperature becomes a factor that deserves attention, since different zeolite-dye systems can possess endothermic or exothermic behavior, leading to a positive or negative influence on the removal process. As seen in Table 7, the temperature is a parameter that was not investigated in most of the studies analyzed in this review and, as mentioned, it can affect adsorption in different ways. Further in-depth studies on the influence of temperature on dye adsorption using zeolites can provide insightful information.

Table 4.7 - Comparison of dye removal by different zeolites, along with experimental conditions and adsorption and kinetic models.

Dye	Dye type	Zeolite	T (°C)	Contact time	Concentration ($mg.L^{-1}$)	S/L ratio ($g.L^{-1}$)	pH	Sorption capacity ($mg.g^{-1}$)	Adsorption isotherm model	Adsorption kinetics model	References
Safranine O	Cationic	Clinoptilolite Analcime + Sodalite	25	1h-40d	1754.0	5	6.4	34.7 15.7	-	-	[148]
Methylene Blue		H-USY	25	2h	50-150	2	8	59.9	Langmuir	Pseudo-second order	[150]
		Clinoptilolite	30-50	-	3.2-32	0.25	-	16.7-20.2	Langmuir	Pseudo-second order	[149]
		Clinoptilolite Erionite	30	72h	10-1300	2	5	82.0 88.0	Sips	-	[158]
		Magnetic Clinoptilolite	25	45m	25-20	-	7	52.0	Freundlich	-	[151]
Rhodamine B		Clinoptilolite	30-50	-	4.8-47.9	0.25	-	9.3-12.4	Langmuir	Pseudo-second order	[149]
Crystal violet		Zeolite X	50	1h	100	1	9	234.5	Langmuir	Pseudo-second order	[157]
Brilliant green		Zeolite Y	25-55	20min	100-800	0.4	6	409.0	Langmuir	Pseudo-second order	[152]
Basic violet 3		Clinoptilolite Erionite	30	72h	10-1300	2	**5**	98.0 105.0	Sips	-	[158]
Amido black 10B	Anionic	Zeolite X	25	6h	5-50	-	4	1.4	Freundlich	Pseudo-first order	[156]
Acid blue 25		Clinoptilolite Erionite	30	72h	10-1300	2	5	<0.1 <0.1	Sips	-	[158]

4.3.2.2. Organic species

The adsorption of organic compounds using zeolites is significantly dependent on the adsorbent Si/Al ratio. Low-silica zeolites present a greater amount of aluminum content in their composition, resulting in more compensation cations available, which increases their effectiveness in cation exchange. In contrast, high-silica zeolites present greater hydrophobicity, organic compounds removal [164-166]. The adsorption capacity of organics on low-silica zeolites, as well as the affinity for anions, can be amplified with modifications using surfactants. This can be seen in Table 8, which shows studies on the removal of several organic compounds using surfactant-modified zeolites as adsorbents. The modification occurs due to the formation of a surfactant monolayer on the zeolite surface, with the hydrocarbon chain of the molecule facing the solution and making the zeolite hydrophobic. The surfactant concentration is of great importance because if the critical micellar concentration (CMC) is exceeded, a surfactant double layer should be formed, which returns the hydrophilic character to the zeolite [105]. Hosseini Hashemi *et al*. [167] evaluated the use of zeolite Y, modified with hexadecyltrimethylammonium bromide (CTAB), to remove organic pollutants from an olefin plant. Zeolite Y was modified with different concentrations of CTAB, to evaluate the influence

of surfactant concentration on the removal of organic compounds. The best results were obtained with 0.025M CTAB, whereas higher concentrations led to the formation of a double layer, increasing the hydrophilicity of the zeolitic particles, and reducing the adsorption of the organic compounds. The adsorption of organic compounds in CTAB-modified zeolite Y follows the Langmuir model, whose adsorption occurs in monolayer and all sites have the same affinity for adsorbate. As all the analyzed isotherm models (Freundlich, Sips, and Dubinin-Radushkevich) presented acceptable errors, it can also be concluded that the adsorption is favorable and that it occurs basically by physical mechanisms (physisorption) [167].

Jiang *et al*. [165] investigated the adsorption of three organic compounds (triclosan, phenol, and 2,4,6-trichlorophenol) using four synthetic high-silica zeolites, belonging to the FAU, BEA, MFI, and MOR structures. For triclosan adsorption, FAU-type zeolite showed the highest adsorption capacity, followed by MOR and BEA-type. MFI-type zeolite was demonstrated to have a very low adsorption capacity for triclosan. In the case of trichrlorophenol, the adsorption sequence was maintained, again with emphasis on the greater adsorption in the zeolite of the FAU structure. As for phenol, the amount adsorbed by all types of zeolites was lower than for the other compounds. However, the MFI type zeolite stood out in the removal of this chemical compound, followed by the MOR, BEA, and FAU zeolites. The authors associated the adsorption of organic compounds with the size of their hydrocarbon chains and the pore size of zeolites. In the case of FAU-type zeolite, the adsorption of trichlorophenol was greater than triclosan due to the smaller size of the first species, therefore, more molecules could pass through the pores of the FAU zeolite. The adsorption of phenol was shown to be greater in the MFI zeolite, which is the zeolite with the smallest pore size. The authors state that pores with the same order of magnitude as the molecules of organic compounds favor adsorption due to the generation of a greater attraction force between the compound and active sites in the micropores. The organic compound triclosan has been shown to adsorb following the Langmuir model, regardless of the zeolite used. Trichlorophenol followed the Langmuir model only for the FAU zeolite, and adsorbed forming multilayers in the other zeolites, following the Freundlich model. Phenol was adsorbed following the Freundlich model in all the zeolites studied. According to the authors, the hydrophobicity of zeolites has secondary importance. The type and size of organic molecules (which may lead to intermolecular attraction between molecules on the adsorbent), pore size, and crystalline structure of zeolites were more relevant features in the process.

Kuleyin [168] analyzed the removal of phenol and 4-chlorophenol using natural clinoptilolite, modified with hexadecyltrimethyl ammonium (HDTMA). The authors observed that 4-chlorophenol showed the highest adsorption rate in modified clinoptilolite, since the reagent is

more hydrophobic than phenol, showing a greater affinity for zeolites covered by surfactants. In terms of comparison, in the experimental conditions of 20 $g.L^{-1}$ of adsorbent, 20 °C, and initial concentration of 50 $mg.L^{-1}$, natural clinoptilolite showed removal <10% for chlorophenol and <5% for phenol, whereas modified clinoptilolite showed removals of approximately 60% for phenol and 90% for chlorophenol. Vidal *et al*. [169] performed the removal of benzene, ethylbenzene, toluene, o-xylene, and m,p-xylene Y-modified zeolite with HDTMA. The zeolites were modified in different concentrations of HDTMA, using 50, 100, and 200% of the cation exchange capacity (CEC) of the zeolite Y. It was found that the concentration of HDTMA that results in the greatest removal of the analyzed organic compounds was 100% of the CEC. Concentrations of 50 and 200% lead to an incomplete coating of the zeolite surface and the formation of a double layer of surfactant, respectively, which impairs the adsorption of the compounds. The maximum adsorption capacities obtained by the Langmuir model were 150.42, 152.41, 162.22, 175.32, and 164.58 $mg.g^{-1}$ for benzene, toluene, ethylbenzene, m, p-xylene, and o-xylene, respectively. Ghiaci *et al*. [170] used natural clinoptilolite, ZSM-5, and MCM-41 to remove toluene, benzene, and phenol. The zeolites (except MCM-41) were modified with HDTMA bromide and *n*-cetyl pyridinium bromide (CPB), in different concentrations (0.5, 1.8, and 20 $mmol.L^{-1}$). The authors state that the pores of all the zeolites investigated are smaller than the surfactants used in the modification, which would be adsorbed only on the external surface of the particles. It was found that, in all cases, the adsorption of organic compounds on zeolites modified with CPB was greater than in those modified with HDTMA. The authors explained that this is due to the more hydrophobic nature of CPB compared to HDTMA, increasing the interaction of CPB with the organic compounds analyzed. The study revealed the greater adsorption capacity of benzene, toluene, and phenol in zeolite MCM-41, which even without previous treatment, showed adsorption capacities five times greater than those of clinoptilolite and ZSM-5.

Table 4.8 - Zeolites used in organic compounds removal, along with experimental conditions and adsorption and kinetic models.

Organic compound	Zeolite	T (°C)	Contact time	Concentration	S/L ratio ($g.L^{-1}$)	pH	Sorption capacity ($mg.g^{-1}$)	Adsorption isotherm	Adsorption kinetics	References
Toluene Styrene Indene Hexadecane Octadecane Dioctyl phthalate	CTAB- zeolite Y	-	8h	43ppm	1	-	30.9	Langmuir	-	[167]
Triclosan	FAU-type BEA-type MOR-type	25	24h	0.3-17.4	30	-	377.6 119.0 153.2	Langmuir	-	[165]
Phenol	HDTMA-clinoptilolite	20	4h	10-50ppm	20-100	-	0.8	Freundlich	-	[168]
	BDTDA- clinoptilolite						1.3			
	HDTMA-ZSM-5	-	24h	0.0816-1.2mmol/L	5	-	6.2	Langmuir/ Freundlich/ Redlich-Peterson	-	[170]
	CPB-ZSM-5						9.4			
	HDTMA-Clinoptilolite						11.4			
	CPB-Clinoptilolite						11.9			
	MCM-41						59.4			
4-chlorophenol	HDTMA-clinoptilolite	20	4h	10-100ppm	20-100	-	12.7	Freundlich	-	[168]
	BDTDA- clinoptilolite	20	4h	10-100ppm	20-100	-	6.41			
2,4,6-trichlorophenol	FAU-type	25	24h	1-60µmol/L	30	-	314.5	Langmuir		[165]
Toluene	HDTMA-Y	28	6h	1-60mg/L	30	-	152.4	Temkin	Pseudo-second order	[169]
	HDTMA-ZSM-5	-	24h	0.0816-1.2mmol/L	5	-	9.3	Langmuir/ Freundlich/ Redlich-Peterson	-	[170]
	CPB-ZSM-5	-	24h	0.0816-1.2mmol/L	5	-	16.4			
	MCM-41	-	24h	0.0816-1.2mmol/L	5	-	145.2			
Benzene	HDTMA-Y	28	6h	1-60mg/L	30	-	150.4	Temkin	Pseudo-second order	[169]
	HDTMA-ZSM-5	-	24h	0.0816-1.2mmol/L	5	-	7.7	Langmuir/ Freundlich/ Redlich-Peterson	-	[170]
	CPB-ZSM-5						15.0			
	HDTMA-Clinoptilolite						16.6			
	CPB-Clinoptilolite						23.1			
	MCM-41						112.3			
Ethylbenzene	HDTMA-Y	28	6h	1-60mg/L	30	-	162.2	Temkin	Pseudo-second order	[169]
m,p-xylene	HDTMA-Y						175.3			
o-xylene	HDTMA-Y						164.6			

4.3.3. Kinetic studies

The adsorption kinetic models help to understand the mass transfer adsorption mechanisms, in addition to providing information about adsorption rate and general performance of the adsorbent [125]. Ideally, an ideal adsorbent should possess a high adsorption capacity allied with a rapid adsorption rate. The mass transfer mechanism includes three steps. The first is the external diffusion, in which the adsorbate is transferred to the solid through a liquid film layer. The concentration of adsorbate governs the driving force, and the external diffusion occurs faster in the case of higher concentrations. The second step is the internal diffusion when the adsorbate penetrates the pores. Finally, the third step is the interaction of the

adsorbate with the active sites in the adsorbent [171]. Table 9 shows the equations of the most widely used adsorption isotherm and adsorption kinetics models applicable for adsorption systems, including zeolites as adsorbents. The pseudo-second order model best fits the experimental data in the studies analyzed in this review (as verified in Tables 3-8). This model, adequate for solutions with low concentration, indicates that the material utilized as adsorbent possesses a large number of active sites. Low silica zeolites possess a high amount of aluminum in their crystallographic structure, each one representing an active point for adsorption, which is why the second-order model is the one that best represents the phenomenon. Despite being widely applied in adsorption kinetics studies, pseudo-first and pseudo-second order models cannot explain the mass transfer mechanism, being considered empirical models. Thus, the mechanism is better explained by internal diffusion models such as the intraparticle diffusion model. This model assumes that the diffusion of adsorbate into the pores of the adsorbent is the slowest step in the adsorption process. Graphically, the process is represented by a straight line that may pass through the origin. In this case, intraparticle diffusion is the only mechanism that limits the process, and the adsorption on the outer layer takes place instantaneously. Otherwise, there is an indication that more than one mechanism is controlling the adsorption process [171].

In the case of heavy metals adsorption, the intraparticle diffusion model has also shown adherence in some studies, as verified by Jin *et al*. [135], indicating that the adsorption occurs initially on the external surface of the particles, followed by adsorption within the pores in the crystalline structure of the particles. Since metallic ions present dimensions of the same order of magnitude of the pores, the adsorption occurs quickly, regardless of the zeolite used or the heavy metal to be removed.

For ammonia, results of adsorption experiments performed by Zhao *et al*. [145] e Lin *et al*. [146] indicated that in the first 5 minutes of contact, ammonia removal reached 56.4% for analcime and P zeolites, and 50% for chabazite zeolite, respectively. Although the intraparticle diffusion model did not present a good correlation with the experimental data, it is believed that the diffusion was the main adsorption mechanism acting in the first 30 minutes of contact [146].

Considering the adsorption of dyes, the data demonstrate that, for the zeolites and dyes analyzed, adsorption on the external surface occurs quickly. However, the intraparticle diffusion rate is quite reduced, reflecting the difficulty that the molecules present in entering the pores of the zeolite, due to its size. At this point, the more uniform chemical composition (greater stability of the Si/Al ratio) and pore size of synthetic zeolites show greater adsorption potential for dyes. Once again, it is important to consider the relationship between the size of

the dye molecule and the pore dimensions of the zeolite to assess the time required for the adsorption to occur, this information being essential to design the processes for removing this type of contaminant.

As for kinetics of phosphoric compounds adsorption, Hamdi and Srasra [160] verified that most of the phosphorus was removed within a 2h interval, with no further removals being verified after this time. This suggests that adsorption occurs only on the surface, and the entry of molecules into the interior of the zeolite pores was impaired. However, adsorption kinetics has not been investigated in most studies. Further studies on the kinetics of phosphoric compounds removal using zeolites are necessary to have a better understanding of the adsorption process, in addition to allowing the determination of the optimal contact time for the design of treatment systems for this type of effluent.

The adsorption of organic compounds onto zeolites differs from the process of removal of other contaminants because hydrophobic interactions between adsorbent/adsorbate are of greater importance. The modification of zeolites using surfactants makes this interaction possible by the appearance of a hydrophobic monolayer at the zeolite surface. However, the surfactant molecules are too compared to the pore sizes, and the coating only occurs on the surface of the particles. Studies carried out by Kuleyin [168] demonstrate that removal occurs within the first 30 minutes of contact, and quickly stabilizes, indicating that the diffusion in the zeolite pores is a limiting factor for adsorption. The process did not fit well with the intraparticle diffusion model, which confirms the external character of the adsorption of organic molecules. Since adsorption occurs on the surface of the particles, it is expected that the particle size of the zeolite used may influence the efficiency of the process. Considering natural zeolites, the comminution process can be optimized with prior knowledge of this parameter. However, granulometry is not among the physical parameters of the adsorbents used in the analyzed studies. Another factor that may influence the adsorption process, which has not been investigated, is pH. The variation of this variable can affect the ionization state of the molecules, both the surfactant and the adsorbate, which can strongly influence the process.

Table 4.9 - Most used models to describe the adsorption isotherm and kinetics of zeolites in wastewater treatment systems.

Adsorption isotherm models	Model equation	Variables	References
Langmuir	$q_e = q_m \frac{K_L C_e}{1+K_L C_e}$ (1)	C_e: equilibrium concentration (mg/L);	[126]
Freundlich	$q_e = K_F C_e^{\frac{1}{n}}$ (2)	q_e: equilibrium adsorption capacity (mg/g);	[134]
Sips	$q_e = \frac{q_s a_s C_e^{n_s}}{1+a_s C_e^{n_s}}$ (3)	K_L: Langmuir constant (L/mg);	[158]
Koble-Corrigan	$q_e = \frac{a C_e^{n}}{1+b C_e^{n}}$ (4)	q_m: maximum adsorption capacity (mg/g);	[145]
Dubinin-Radushkevich	$q_e = q_m e^{(\beta \varepsilon^2)}$ (5)	n: empirical parameter for adsorption intensity;	[167]
Redlich-Peterson	$q_e = \frac{K_{RP} C_e}{1+B C_e^{g}}$ (6)	K_F: Freundlich constant (mg/g)(mg/L)$^{(-1/n)}$;	[170]
Temkin	$q_e = \frac{RT}{b_T} ln\ (A_T C_e)$ (7)	q_s: theoretical maximum adsorption capacity (mg/g);	[172]
Adsorption kinetics models	Model equation	a_s, n_s: Sips parameters;	
Pseudo-first order	$q_t = q_e(1 - e^{(-k_1 t)})$ (8)	a,b: Koble-Corrigan parameters;	[173]
Pseudo-second order	$q_t = \frac{k_2 q_e^2 t}{1+k_2 q_e t}$ (9)	β: constant related to adsorption energy;	[173]
Intraparticle diffusion	$q_t = k_i t^{1/2}$ (10)	ε: Polanyi adsorption potential;	[93,171]
		K_{RP}, B: equilibrium constants;	
		g: exponencial constant value (0-1);	
		A_T, b_T: equilibrium Temkin constants;	
		R: gas constant (J/mol.K);	
		T: temperature (K);	
		q_e, q_t: amount of adsorbed species at equilibrium at any time (mg/g);	
		k_1: pseudo-first order constant (h^{-1});	
		k_2: pseudo-second order constant (g/mg.h);	
		k_i: intraparticle diffusion constant (mg/g.$h^{0.5}$);	
		t: time (h)	

4.3.4. Adsorption isotherms

The analysis of adsorption isotherms reveals important information, such as maximum adsorption capacity (mg/g) and the adsorption mechanism, which can be used in the development of adsorption systems for wastewater treatment [50]. The isotherm models are represented by curves that relate the amount of adsorbate at the adsorbent surface and the concentration of the adsorbate in the liquid phase, at a constant temperature. Table 9 shows the existing adsorption isotherm models in the literature used to characterize the adsorption on microporous materials. The models most commonly adopted to represent the adsorption isotherms are the Langmuir and Freundlich models, which assume a uniform distribution in monolayers at the adsorbent surface, and the multilayer adsorption on a heterogeneous

surface of the adsorbent, respectively [50]. Temkin's model assumes the existence of an adsorbate-adsorbate interaction, which confirms that the presence of hydrophobic tails groups interaction is a dominant factor in the process. The Redlich-Peterson model is similar to the Langmuir and Freundlich models, but it is more suitable for wider ranges of contaminant concentration, also fitting well in processes with this characteristic [169].

According to data collected in Table 3, the Langmuir model was the one that best fitted the experimental data of the studies analyzed, indicating that the adsorption to the heavy metals system using zeolites as adsorbents occurs with the formation of a monolayer on the surface of the particles. The adsorption rate is higher in the first minutes of contact, at which more active sites are available for adsorption. As the sites on the surface are occupied, the ions migrate into the pores within the crystalline structure [135]. In addition to adsorption, ion exchange is also present as a mechanism for removing heavy metals in solution, as indicated by Bai *et al*. [132] and Hui *et al*. [134], who verified an increase in sodium concentration in solution after the equilibrium time is reached.

For ammonia adsorption, among the studies analyzed in Table 5, the Langmuir isotherm model showed the best adherence to experimental data, indicating that the adsorption of these molecules occurs with the formation of a monolayer. The Freundlich model also showed good applicability, indicating the heterogeneity of the adsorbent surface, in addition to the fact that the process occurs spontaneously [142].

Comparably to nitrogenous compounds and heavy metals, the dye adsorption process occurs mainly by cationic exchange and electrostatic interactions. The process is favored for zeolites with a lower Si/Al ratio, in which the largest amount of aluminum atoms contributes to a greater negative charge. As each negative site is capable of adsorbing only one dye molecule, a monolayer is formed. As shown in Table 7, most studies indicate that the Langmuir isotherm best represents the adsorption process, which confirms this theory.

For phosphoric compounds, the process occurs by electrostatic attraction and, as in the previous cases, each site can adsorb only one molecule, leading to the formation of a monolayer. The Langmuir isotherm illustrates this phenomenon well and this model best fitted the experimental data available for the investigation on the use of zeolites as adsorbents.

In the case of organic compounds, the Langmuir model fits well with the experimental data, indicating that the hydrophobic interaction process allows the formation of a monolayer of contaminant molecules over the surfactant layer, and the process occurs spontaneously, as

indicated by the good fitting of the Freundlich isotherm. As seen in Table 8, there is also an indication of good adjustment by the Temkin and Redlich-Peterson isotherms, demonstrating the hydrophobic interaction between que adsorbate and the surfactant modified zeolite.

4.4. Conclusions, challenges, and future perspectives

Based on investigations conducted by several authors, it can be seen that synthetic zeolites have greater adsorption capacity for the various compounds analyzed, due to high degree ordering in the crystalline structure and, consequently, standardization of pore sizes and cation exchange capacity. Natural zeolites are less efficient since the presence of contaminating minerals reduces adsorption efficiency. Therefore, modification of natural zeolites is an alternative to enhancing their properties for application in wastewater treatment.

As for contaminants, heavy metals, dyes, and ammonium are readily adsorbed by zeolites, with fast kinetic rates. However, for anionic species, such as phosphoric compounds and some heavy metals (*e.g.*, chromium and arsenic), adsorption is impaired, due to electrostatic repulsion, but possible at specific pH ranges. Organic compounds, which are predominantly hydrophobic, have been removed using zeolites by modifying them with surfactants, creating a hydrophobic layer on the surface of the zeolite, which increases its affinity for these compounds. In this case, the dosage of the surfactant becomes an important variable to be considered.

Despite a large number of bench-scale researches which show the effectiveness of zeolites as contaminant adsorbents, further studies on adsorption kinetics (phosphoric compounds), temperature (dyes), granulometry, and pH (organic compounds), desorption, and pilot-scale investigations are necessary. Furthermore, synthetic solutions are used in the research, which does not reflect the characteristics of real wastewater. The presence of other chemical species in this scenario could affect the adsorption mechanisms in different ways and is important to consider the presence of these elements to apply zeolite in large-scale industrial applications.

REFERENCES

[1] Thorsteinsson T, Jóhannesson T, Snorrason Á. Glaciers and ice caps: Vulnerable water resources in a warming climate. *Current Opinion in Environmental Sustainability*, vol. 5, pp. 590-598, 2013.

[2] Bogardi JJ, Dudgeon D, Lawford R, Flinkerbusch E, Meyn A, Pahl-Wostl C, *et al*. Water security for a planet under pressure: interconnected challenges of a changing world call for sustainable 4solutions. *Current Opinion in Environmental Sustainability*, vol. 5, pp. 35-43, 2012.

[3] Jaishankar M, Tseten T, Anbalagan N, Mathew BB, Beeregowda KN. Toxicity, mechanism, and health effects of some heavy metals. *Interdiscip Toxicol*, vol. 7, pp. 60-72, 2014.

[4] Haji S, Al-Buqaishi BA, Bucheeri AA, Bu-Ali Q, Al-Aseeri M, Ahmed S. The dynamics and equilibrium of ammonium removal from aqueous solution by Na-Y zeolite. *Desalination and Water Treatment*, vol. 57, article 18922-9001, 2015.

[5] Bacelo H, Pintor AMA, Santos SCR, Boaventura RAR, Botelho CMS. Performance and prospects of different adsorbents for phosphorus uptake and recovery from water. *Chemical Engineering Journal*, vol. 381, 2020.

[6] Hassan MM, Carr CM. A critical review on recent advancements of the removal of reactive dyes from dyehouse effluent by ion-exchange adsorbents. *Chemosphere*, vol. 209, pp. 201-219, 2018.

[7] Trojanowicz M. Removal of persistent organic pollutants (POPs) from waters and wastewaters by the use of ionizing radiation. *Sci Total Environ*, vol. 718, article134425, 2020.

[8] Zhao W, Liang Y, Wu Y, Wang D, Zhang B. Removal of phenol and phosphoric acid from wastewater by microfiltration carbon membranes. *Chemical Engineering Communications*, vol. 205, pp. 1432-1441, 2018.

[9] Wu MN, Wang XC, Ma XY. Phytotoxicity comparison of organic contaminants and heavy metals usingChlorella Vulgaris. *Desalination and Water Treatment*, pp. 1-8, 2015.

[10] Kroeze C, Hofstra N, Ivens W, Löhr A, Strokal M, van Wijnen J. The links between global carbon, water, and nutrient cycles in an urbanizing world — the case of coastal eutrophication. *Current Opinion in Environmental Sustainability*, vol. 5, pp. 566-572, 2013.

[11] Wei T, Guizhen L, Tianli W, Min Y, Jinhui P, Barrow CJ, *et al*. Preparation and adsorption of phosphorus by new heteropolyacid salt–lanthanum oxide composites. *Desalination and Water Treatment*, vol. 57, pp. 7874-7880, 2015.

[12] Zouboulis AI, Goetz L. Ion flotation as a tool for speciation studies selective separation in the system Cr3+/Cr6+. *Toxicological & Environmental Chemistry*, vol. 31, pp. 539-547, 1991.

[13] Muisa N, Nhapi I, Ruziwa W, Manyuchi MM. Utilization of alum sludge as adsorbent for phosphorus removal in municipal wastewater: A review. *Journal of Water Process Engineering*, vol. 35, 2020.

[14] Shahidi D, Roy R, Azzouz A. Advances in catalytic oxidation of organic pollutants – Prospects for thorough mineralization by natural clay catalysts. *Applied Catalysis B: Environmental*, vol. 174, pp. 277-292, 2015.

[15] Wang Y, Du T, Jia H, Qiu Z, Song Y. Synthesis, characterization and CO2 adsorption of NaA, NaX, and NaZSM-5 from rice husk ash. *Solid-State Sciences*, vol. 86, pp. 24-33, 2018.

[16] Schlichter B, Mavrov V, Erwe T, Chmiel H. Regeneration of bonding agents loaded with heavy metals by electrodialysis with bipolar membranes. *Journal of Membrane Science*, vol. 232, pp. 99-105, 2004.

[17] Dabrowski A, Hubicki Z, Podkoscielny P, Robens E. Selective removal of the heavy metal ions from waters and industrial wastewaters by ion-exchange method. *Chemosphere*, vol. 56, pp. 91-106, 2004.

[18] Marchioretto MM, Bruning H, Rulkens W. Heavy Metals Precipitation in Sewage Sludge. *Separation Science and Technology*, vol. 40, pp. 3393-3405, 2005.

[19] Chakraborty R, Asthana A, Singh AK, Jain B, Susan ABH. Adsorption of heavy metal ions by various low-cost adsorbents: a review. *International Journal of Environmental Analytical Chemistr*y, pp. 1-38, 2020.

[20] Arif, M., *et al*., *Synthesis,* characteristics and mechanistic insight into the clays and clay minerals-biochar surface interactions for contaminants removal-A review*.* Journal of Cleaner Production, vol. 310, 2021.

[21] Lazaratou, C.V., D.V. Vayenas, and D. Papoulis, The role of clays, clay minerals and clay-based materials for nitrate removal from water systems: A review. *Applied Clay Science*, vol. 185,2020.

[22] Otunola, B.O. and O.O. Ololade, A review on the application of clay minerals as heavy metal adsorbents for remediation purposes. *Environmental Technology & Innovation*, vol. 18, 2020.

[23] Zhang, T., et al., Removal of heavy metals and dyes by clay-based adsorbents: From natural clays to 1D and 2D nano-composites. *Chemical Engineering Journal*, vol. 420, 2021.

[24] Basheer, A.A., New generation nano-adsorbents for the removal of emerging contaminants in water. *Journal of Molecular Liquids*, vol. 261, pp. 583-593, 2018.

[25] Lima RC, Bieseki L, Melguizo PV, Pergher SBC. Environmentally friendly zeolites - Synthesis and source materials: *Springer*; 2019.

[26] Iulianelli A, Drioli E. Membrane engineering: Latest advancements in gas separation and pre-treatment processes, petrochemical industry, and refinery, and future perspectives in emerging applications. *Fuel Processing Technology*, vol. 206, 2020.

[27] Koohsaryan E, Anbia M, Maghsoodlu M. Application of zeolites as non-phosphate detergent builders: A review. *Journal of Environmental Chemical Engineering*, vol. 8, 2020.

[28] Kianfar E, Hajimirzaee S, mousavian S, Mehr AS. Zeolite-based catalysts for methanol to gasoline process: A review. *Microchemical Journal*, vol. 156, 2020.

[29] Paris JM, Roessler JG, Ferraro CC, DeFord HD, Townsend TG. A review of waste products utilized as supplements to Portland cement in concrete. *Journal of Cleaner Production*, vol. 121, pp. 1-18, 2016.

[30] Bacakova L, Vandrovcova M, Kopova I, Jirka I. Applications of zeolites in biotechnology and medicine - a review. *Biomater Sci*, vol. 6, pp. 978-989, 2018.

[31] Johnson EBG, Arshad SE. Hydrothermally synthesized zeolites based on kaolinite: A review. *Applied Clay Science*, vol. 97, pp. 215-221, 2014.

[32] Masters AF, Maschmeyer T. Zeolites – From curiosity to the cornerstone. *Microporous and Mesoporous Materials*, vol. 142, pp. 423-438, 2011.

[33] Guisnet M, Gilson J-P. Introduction to zeolite science and technology. In: Guisnet M, Gilson J-P, (editors). Zeolites for cleaner technologies. Vol. 3. London: *Imperial College Press*; 2002.

[34] Li Y, Li L, Yu J. Applications of Zeolites in Sustainable Chemistry. *Chem*, vol. 3, pp. 928-949, 2017.

[35] MgBemere HE, Ekpe IC, Lawal GI. Zeolite synthesis, characterizations, and application areas - A review. *International Research Journal of Environmental Sciences*, vol. 6, pp. 45-59, 2017.

[36] Yoldi M, Fuentes-Ordoñez EG, Korili SA, Gil A. Zeolite synthesis from industrial wastes. *Microporous and Mesoporous Materials*, vol. 287, pp. 183-191, 2019.

[37] Diaz I, Mayoral A. TEM studies of zeolites and ordered mesoporous materials. *Micron*, vol. 42, pp. 512-527, 2011.

[38] Xu R, Pang W, Yu J, Huo Q, Chen J. Chemistry of zeolites and related porous materials synthesis and structure. Singapore: *John Wiley & Sons Pte Ltd*; 2007.

[39] Liu J, Yu J. Toward greener and designed synthesis of zeolite materials. In: Sels BF, Sels LF, (editors). Zeolites and zeolite-like materials. Amsterdam: *Elsevier*; 2016.

[40] Payra P, dutta PK. Zeolites: a primer. In: Auerbach SM, Carrado KA, Dutta KP, (editors). Handbook of zeolite science and technology. New York: Marcell Dekker, Inc.; 2003. Chapter 1283.

[41] Dong J, Xu Z, Yang S, Murad S, Hinkle KR. Zeolite membranes for ion separations from aqueous solutions. *Current Opinion in Chemical Engineering*, vol. 8, pp. 15-20, 2015.

[42] Ghobarkar H, Schäf O, Guth U. Zeolites—from kitchen to space. *Progress in Solid State Chemistry*, vol. 27, pp. 27-73, 1999.

[43] Silaghi M-C, Chizallet C, Raybaud P. Challenges on molecular aspects of dealumination and desilication of zeolites. *Microporous and Mesoporous Materials*, vol. 191, pp. 82-96, 2014.

[44] Broach RW. Zeolite types and structures. In: Kulprathipanja S, (editor). Zeolites in industrial separation and catalysis. Weinheim: *WILEY-VCH*; 2010.

[45] Lobo RF. Introduction to the structural chemistry of zeolites. In: Auerbach SM, Carrado KA, Dutta PK, (editors). Handbook of zeolite science and technology. New York: *Marcel Dekker, Inc.*; 2003. p. 1283.

[46] Baerlocher C, McCuster LB, Olson DH. Atlas of zeolite framework types. 6 ed. Amsterdam: *Elsevier*; 2007.

[47] Rashed MN, Palanisamy PN. Introductory Chapter: Adsorption and Ion Exchange Properties of Zeolites for Treatment of Polluted Water. Zeolites and Their Applications. 2018. Chapter Chapter 1.

[48] Colella C. Ion exchange equilibria in zeolite minerals. Mineralium Deposita. 1996;31:554-62.

[49] Barelocher C, McCuster LB, Olson DH. Atlas of zeolite framework types. 6 ed. Amsterdam: *Elsevier*; 2007.

[50] Yuna Z. Review of the Natural, Modified, and Synthetic Zeolites for Heavy Metals Removal from Wastewater. *Environmental Engineering Science*, vol. 33, pp. 443-454, 2016.

[51] Yu J. Synthesis of zeolites. In: Čejka J, Bekkum Hv, Corma A, Schüth F, (editors). Introduction to zeolite science and practice. Vol. 168. 3 ed: *Elsevier*; 2007. Chapter 3.

[52] Dal Bosco SM, Jimenez RS, Carvalho WA. Removal of toxic metals from wastewater by Brazilian natural scolecite. *J Colloid Interface Sci*, vol. 281, pp. 424-431, 2005.

[53] Fernandes Machado NRC, Malachini Miotto DM. Synthesis of Na–A and –X zeolites from oil shale ash. *Fuel*, vol. 84, pp. 2289-2294, 2005.

[54] Barros MASD, Zola AS, Arroyo PA, Souza-Aguiar EF, Tavares CRG. Binary ion exchange of metal ions in Y and X zeolites. Brazilian *Journal of Chemical Engineering*, vol. 20, pp. 4113-4421, 2003.

[55] Drioli E, Giorno L. Encyclopedia of Membranes. Elsevier, 2016.

[56] Ayele L, Pérez-Pariente J, Chebude Y, Díaz I. Synthesis of zeolite A from Ethiopian kaolin. *Microporous and Mesoporous Materials*, vol. 215, pp. 29-36, 2015.

[57] Garcia-Sosa I, Solache-Rios M. Cation-exchange capacities of zeolites A, X, Y, ZSM-5, and Mexican erionite compared with the retention of cobalt and cadmium. *Journal of Radioanalytical and Nuclear chemistry*, vol. 250, pp. 205-206, 2001.

[58] Zola AS, Barros MASD, Sousa-Aguiar EF, Arroyo PA. Determination of the maximum retention of cobalt by ions exchange in H-zeolites. *Brazilian Journal of Chemical Engineering*, vol. 29, pp. 285-392, 2012.

[59] Ray RL, Sheppard RA. Occurrence of zeolites in sedimentary rocks: an overview. In: Bish DL, Ming DW, (editors). Natural zeolites: occurrence, properties, applications. Vol. 45. New Mexico: *Reviews in Mineralogy and Geochemistry*; 2001.

[60] Marantos I, E. Christidis G, Ulmanu M. Zeolite Formation and Deposits. *Handbook of Natural Zeolites.* 2012. p. 28-51.

[61] U.S. Geological Survey. Mineral commodity summaries 2020: *U.S. Geological Survey*; 2020. p. 200.

[62] Flanagan DM. Zeolites - U, S. *Geological Survey Minerals Yearbook* - 2016. 2018.

[63] Morris RE. Ionothermal synthesis of zeolites and other porous materials. In: Cejka J, Corma A, Zones S, (editors). Zeolites and catalysis, synthesis, reactions, and applications. Vol. 1. Weinheim: *Wiley-VCH*; 2010.

[64] He Y, Tang S, Yin S, Li S. Research progress on green synthesis of various high-purity zeolites from natural material-kaolin. *Journal of Cleaner Production*, vol. 306, 2021.

[65] Khaleque A, Alam MM, Hoque M, Mondal S, Haider JB, Xu B, et al. Zeolite synthesis from low-cost materials and environmental applications: A review. *Environmental Advances*, vol. 2, 2020.

[66] Belviso C, Kharchenko A, Agostinelli E, Cavalcante F, Peddis D, Varvaro G, et al. Red mud as an aluminum source for the synthesis of magnetic zeolite. *Microporous and Mesoporous Materials*, vol. 270, pp. 24-29, 2018.

[67] Maia AÁB, Dias RN, Angélica RS, Neves RF. Influence of an aging step on the synthesis of zeolite NaA from Brazilian Amazon kaolin waste. *Journal of Materials Research and Technology*, vol. 8, pp. 2924-2929, 2019.

[68] Krongkrachang P, Thungngern P, Asawaworarit P, Houngkamhang N, Eiad-Ua A. Synthesis of Zeolite Y from Kaolin via hydrothermal method. *Materials Today: Proceedings*, vol. 17, pp. 1431-1436, 2019.

[69] Ma Y, Yan C, Alshameri A, Qiu X, Zhou C, li D. Synthesis and characterization of 13X zeolite from low-grade natural kaolin. *Advanced Powder Technology*, vol. 25, pp. 495-499, 2014.

[70] Wang J-Q, Huang Y-X, Pan Y, Mi J-X. New hydrothermal route for the synthesis of high purity nanoparticles of zeolite Y from kaolin and quartz. *Microporous and Mesoporous Materials*, vol. 232, pp. 77-85, 2016.

[71] Wang J-Q, Huang Y-X, Pan Y, Mi J-X. Hydrothermal synthesis of high purity zeolite A from natural kaolin without calcination. *Microporous and Mesoporous Materials*, vol. 199, pp. 50-56, 2014.

[72] Ayele L, Pérez-Pariente J, Chebude Y, Díaz I. Conventional versus alkali fusion synthesis of zeolite A from low-grade kaolin. *Applied Clay Science*, vol. 132, pp. 485-490, 2016.

[73] Kovo AS, Holmes SM. Effect of Aging on the Synthesis of Kaolin-Based Zeolite Y from Ahoko Nigeria Using a Novel Metakaolinization Technique. *Journal of Dispersion Science and Technology*, vol 31, pp. 442-448, 2010.

[74] Kovo AS, Hernandez O, Holmes SM. Synthesis and characterization of zeolite Y and ZSM-5 from Nigerian Ahoko Kaolin using a novel, lower temperature, metakaolinization technique. *Journal of Materials Chemistry*, vol. 19, 2009.

[75] Kim J-C, Choi M, Song HJ, Park JE, Yoon J-H, Park H-S, et al. Synthesis of uniform-sized zeolite from windshield waste. *Materials Chemistry and Physics*, vol. 166, pp. 20-25, 2015.

[76] Tsujiguchi M, Kobashi T, Oki M, Utsumi Y, Kakimori N, Nakahira A. Synthesis and characterization of zeolite A from crushed particles of aluminoborosilicate glass used in LCD panels. *Journal of Asian Ceramic Societies*, vol. 2, pp. 27-32, 2014.

[77] Vinaches P, Alves JABLR, Melo D, M. A., Pergher SBC. Raw powder glass as a silica source in the synthesis of colloidal MEL zeolite. *Materials Letters*, vol. 178, pp. 217-220, 2016.

[78] Alves JABLR, Dantas ERS, Pergher SBC, A. MDM, Melo MAF. Synthesis of high-value-added zeolitic materials using glass residue as a silica source. *Materials Research*, vol. 17, 213-218, 2014.

[79] Majdinasab AR, Manna PK, Wroczynskyj Y, van Lierop J, Cicek N, Tranmer GK, et al. Cost-effective zeolite synthesis from waste glass cullet using energy-efficient microwave radiation. *Materials Chemistry and Physics*, vol. 221, pp. 272-287, 2019.

[80] Dufour J, González V, Iglesia AL. Synthesis of 13X zeolite from alkaline waste streams in the aluminum anodizing industry. *Industrial and Engineering Chemistry Research*, vol. 40, pp. 1140-1145, 2001.

[81] Abdelrahman EA. Synthesis of zeolite nanostructures from waste aluminum cans for efficient removal of malachite green dye from aqueous media. *Journal of Molecular Liquids*, vol. 252, pp. 72-82, 2018.

[82] Shigemoto N, Hayashi H, Miyaura K. Selective formation of na-x zeolite from coal fly ash by fusion with sodium hydroxide prior to hydrothermal reaction. *Journal of Materials Science*, vol. 28, pp. 4781-4786, 1993.

[83] Somerset VS, Petrik LF, White RA, Klink MJ, Key D, Iwuoha EI. Alkaline hydrothermal zeolites synthesized from high SiO2 and Al2O3 co-disposal fly ash filtrates. *Fuel*, vol. 84, pp. 2324-2329, 2005.

[84] Ferrarini SF, Cardoso AM, Alban L, Pires MJR. Evaluation of the sustainability of integrated hydrothermal synthesis of zeolites obtained from waste. *Journal of Brazilian Chemistry Society*, vol. 29, pp. 1464-1479, 2018.

[85] Fukasawa T, Horigome A, Karisma AD, Maeda N, Huang A-N, Fukui K. Utilization of incineration fly ash from biomass power plants for zeolite synthesis from coal fly ash by microwave hydrothermal treatment. *Advanced Powder Technology*, vol. 29, pp. 450-456, 2018.

[86] Itskos G, Koutsianos A, Koukouzas N, Vasilatos C. Zeolite development from fly ash and utilization in lignite mine-water treatment. *International Journal of Mineral Processing*, vol. 139, pp. 43-50, 2015.

[87] Belviso C. Ultrasonic vs hydrothermal method: Different approaches to convert fly ash into the zeolite. How do they affect the stability of synthetic products over time? Ultrasonics *Sonochemistry*, vol. 43, pp. 9-14, 2018.

[88] Zhao XS, Lu QQ, Zhu HY. Effects of ageing and seeding on the formation of zeolite Y from coal fly ash. *Journal of Porous Materials*, pp. 245-251, 1997.

[89] Ismail AA, Mohamed RM, Ibrahim IA, Kini G, Koopman B. Synthesis, optimization and characterization of zeolite A and its ion-exchange properties. *Colloids and Surfaces A: Physicochemical and Engineering Aspects*, vol. 366, pp. 80-87, 2010.

[90] Zhang J, Li X, Liu J, Wang C. A Comparative Study of MFI Zeolite Derived from Different Silica Sources: Synthesis, Characterization and Catalytic Performance. *Catalysts*, vol. 9, 2018.

[91] Xie W-M, Zhou F-P, Bi X-L, Chen D-D, Li J, Sun S-Y, et al. Accelerated crystallization of magnetic 4A-zeolite synthesized from red mud for application in removal of mixed heavy metal ions. *Journal of Hazardous Materials*, vol. 358, pp. 441-449, 2018.

[92] Belviso C, Agostinelli E, Belviso S, Cavalcante F, Pascucci S, Peddis D, et al. Synthesis of magnetic zeolite at low temperature using a waste material mixture: Fly ash and red mud. *Microporous and Mesoporous Materials*, vol. 202, pp. 208-216, 2015.

[93] Bai S-x, Zhou L-m, Chang Z-b, Zhang C, Chu M. Synthesis of Na-X zeolite from Longkou oil shale ash by alkaline fusion hydrothermal method. *Carbon Resources Conversion*, vol. 1, pp. 245-250, 2018.

[94] Qiang Z, Shen X, Guo M, Cheng F, Zhang M. A simple hydrothermal synthesis of zeolite X from bauxite tailings for highly efficient adsorbing CO2 at room temperature. *Microporous and Mesoporous Materials*, vol. 287, pp. 77-84, 2019.

[95] Wang C, Zhou J, Wang Y, Yang M, Li Y, Meng C. Synthesis of zeolite X from low-grade bauxite. *Journal of Chemical Technology & Biotechnology*, vol. 88, pp. 1350-1357, 2013.

[96] Ma D, Wang Z, Guo M, Zhang M, Liu J. Feasible conversion of solid waste bauxite tailings into highly crystalline 4A zeolite with valuable application. *Waste Manag*, vol. 34, pp. 2365-2372, 2014.

[97] Li C, Zhong H, Wang S, Xue J, Zhang Z. A novel conversion process for waste residue: Synthesis of zeolite from electrolytic manganese residue and its application to the removal of heavy metals. *Colloids and Surfaces A: Physicochemical and Engineering Aspects*, vol. 470pp. 258-267, 2015.

[98] Yao G, Lei J, Zhang X, Sun Z, Zheng S, Komarneni S. Mechanism of zeolite X crystallization from diatomite. *Materials Research Bulletin*, vol. 107, pp. 132-138, 2018.

[99] Sanhueza V, Kelm U, Cid R, López-Escobar L. Synthesis of ZSM-5 from diatomite: a case of zeolite synthesis from a natural material. *Journal of Chemical Technology & Biotechnology*, vol. 79, pp. 686-690, 2004.

[100] Garcia G, Cardenas E, Cabrera S, Hedlund J, Mouzon J. Synthesis of zeolite Y from diatomite as silica source. *Microporous and Mesoporous Materials*, vol. 219, pp. 29-37, 2016.

[101] Mukherjee S, Barman S, Halder G. Fluoride uptake by zeolite NaA synthesized from rice husk: Isotherm, kinetics, thermodynamics, and cost estimation. *Groundwater for Sustainable Development*, vol. 7, pp. 39-47, 2018.

[102] Wang Y, Du T, Qiu Z, Song Y, Che S, Fang X. CO2 adsorption on polyethylenimine-modified ZSM-5 zeolite synthesized from rice husk ash. *Materials Chemistry and Physics*, vol. 207, pp. 105-113, 2018.

[103] Wang Y, Du T, Fang X, Jia H, Qiu Z, Song Y. Synthesis of CO2-adsorbing ZSM-5 zeolite from rice husk ash via the colloidal pretreatment method. *Materials Chemistry and Physics*, vol. 232, pp. 284-293, 2019.

[104] Margeta K, Zabukovec N, Siljeg M, Farkas A. Natural Zeolites in Water Treatment – How Effective is Their Use. *Water Treatmen*t. 2013. Chapter Chapter 5.

[105] Wang S, Peng Y. Natural zeolites as effective adsorbents in water and wastewater treatment. *Chemical Engineering Journal*, vol. 156, pp. 11-24, 2010.

[106] de Gennaro B. Surface modification of zeolites for environmental applications. *Modified Clay and Zeolite Nanocomposite Materials*, pp. 57-85, 2019.

[107] Morais S, e Costa FG, Lourdes Pereir Md. Heavy Metals and Human Health. *Environmental Health - Emerging Issues and Practice*2012. Chapter Chapter 2.

[108] Lv XM, Li J, Chen H, Tang HJ. Copper wastewater treatment with a high concentration in a two-stage crystallization-based combined process. Environ Technol, vol. 39, pp. 2346-2352, 2018.

[109] Kadhom M, Albayati N, Alalwan H, Al-Furaiji M. Removal of dyes by agricultural waste. *Sustainable Chemistry and Pharmacy*, vol. 16, 2020.

[110] Pavithra KG, P SK, V J, P SR. Removal of colorants from wastewater: A review on sources and treatment strategies. *Journal of Industrial and Engineering Chemistry*, vol. 75, pp. 1-19, 2019.

[111] Aljerf L. High-efficiency extraction of bromocresol purple dye and heavy metals as chromium from industrial effluent by adsorption onto a modified surface of zeolite: Kinetics and equilibrium study. *Journal of Environmental Management*, vol. 225, pp. 120-132, 2018.

[112] Ozkan A, Sener AG, Ucbeyiay H. Investigation of coagulation and electrokinetic behaviors of clinoptilolite suspension with multivalent cations. *Separation Science and Technology*, vol. 53, pp. 823-832, 2017.

[113] Iqbal, A., et al., Synthesis and characterization of pure phase zeolite 4A from coal fly ash. *Journal of Cleaner Production*, vol. 219, pp. 258-267, 2019.

[114] Samanta, N.S., et al., Preparation and characterization of zeolite from waste Linz-Donawitz (LD) process slag of steel industry for removal of Fe3+ from drinking water. *Advanced Powder Technology*, vol. 32, pp. 3372-3387, 2021.

[115] Szerement, J., et al., Contemporary applications of natural and synthetic zeolites from fly ash in agriculture and environmental protection. *Journal of Cleaner Production*, vol. 311, 2021.

[116] Basiuk M, Brown RA, Cartwright D, Davison R, Wallis PM. Trace organic compounds in rivers, streams, and wastewater in southeastern Alberta, Canada. *Inland Waters*, vol. 7, pp. 283-296, 2017.

[117] Awad AM, Shaikh SMR, Jalab R, Gulied MH, Nasser MS, Benamor A, et al. Adsorption of organic pollutants by natural and modified clays: A comprehensive review. *Separation and Purification Technology*, vol. 228, 2019.

[118] Villarin MC, Merel S. Paradigm shifts and current challenges in wastewater management. *J Hazard Mater*, vol. 390, 2020.

[119] Bennett A. Legislation and market forces: regulators and wastewater reuse. *Filtration & Separation*, vol. 46, pp. 16-21, 2009.

[120] Alvarez-Ayuso E, Garcia-Sanchez A, Querol X. Purification of metal electroplating wastewaters using zeolites. *Water Research*, vol. 37, pp. 4855-4862, 2003.

[121] Ćurković L, Cerjan-Stefanović Š, Filipan T. Metal ion exchange by natural and modified zeolites. *Water Research*, vol. 31, pp. 1379-1382, 1997.

[122] Zeng Y, Woo H, Lee G, Park J. Adsorption of Cr(VI) on hexadecylpyridinium bromide (HDPB) modified natural zeolites. *Microporous and Mesoporous Materials*, vol. 130, pp. 83-91, 2010.

[123] Jeon C-S, Baek K, Park J-K, Oh Y-K, Lee S-D. Adsorption characteristics of As(V) on iron-coated zeolite. *Journal of Hazardous Materials*, vol. 163, pp. 804-808, 2009.

[124] USEPA. Batch-type adsorption procedures for estimating soil attenuation of chemicals. In: *Agency USEP,* (editor). Ohio: National Technical Information Service; 1992.

[125] Zanin E, Scapinello J, de Oliveira M, Rambo CL, Franscescon F, Freitas L, et al. Adsorption of heavy metals from wastewater graphic industry using clinoptilolite zeolite as adsorbent. *Process Safety and Environmental Protection*, vol. 105, pp. 194-200, 2017.

[126] Batjargal T, Yang J-S, Kim D-H, Baek K. Removal Characteristics of Cd(II), Cu(II), Pb(II), and Zn(II) by Natural Mongolian Zeolite through Batch and Column Experiments. *Separation Science and Technology*, vol. 46, pp. 1313-1320, 2011.

[127] Ibrahim HS, Jamil TS, Hegazy EZ. Application of zeolite prepared from Egyptian kaolin for the removal of heavy metals: II. Isotherm models. *Journal of Hazardous Materials*, vol. 182, pp. 482-847, 2010.

[128] Xing P, Wang C, Ma B, Chen Y. Removal of Pb(II) from aqueous solution using a new zeolite-type absorbent: Potassium ore leaching residue. *Journal of Environmental Chemical Engineering*, vol 6, pp. 7138-7143, 2018.

[129] Shariatinia Z, Bagherpour A. Synthesis of zeolite NaY and its nanocomposites with chitosan as adsorbents for lead(II) removal from aqueous solution. *Powder Technology*, vol. 338, pp. 744-763, 2018.

[130] Huang F-C, Han Y-L, Lee C-K, Chao H-P. Removal of cationic and oxyanion heavy metals from water using hexadecyltrimethylammonium-bromide-modified zeolite. *Desalination and Water Treatment*, vol. 57, article 17870-9, 2015.

[131] Santasnachok C, Kurniawan W, Hinode H. The use of synthesized zeolites from power plant rice husk ash obtained from Thailand as adsorbent for cadmium contamination removal from zinc mining. *Journal of Environmental Chemical Engineering*, vol. 3, pp. 2115-2126, 2015.

[132] Bai S, Chu M, Zhou L, Chang Z, Zhang C, Liu B. Removal of heavy metals from aqueous solutions by X-type zeolite prepared from a combination of oil shale ash and coal fly ash. *Energy Sources, Part A: Recovery, Utilization, and Environmental Effects*, pp. 1-11, 2019.

[133] Covarrubias C, García R, Arriagada R, Yánez J, Garland MT. Cr(III) exchange on zeolites obtained from kaolin and natural mordenite. *Microporous and Mesoporous Materials*, vol. 88, pp. 220-230, 2006.

[134] Hui KS, Chao CY, Kot SC. Removal of mixed heavy metal ions in wastewater by zeolite 4A and residual products from recycled coal fly ash. *Journal of Hazardous Materials*. 2005;127:89-101.

[135] Jin Y, Wu Y, Cao J, Wu Y. Adsorption behavior of Cr(VI), Ni(II), and Co(II) onto zeolite 13x. *Desalination and Water Treatment*, vol. 54, pp. 511-524, 2014.

[136] Taffarel SR, Rubio J. On the removal of Mn2+ ions by adsorption onto natural and activated Chilean zeolites. *Minerals Engineering*, vol. 22,m pp. 336-343, 2009.

[137] Taffarel SR, Rubio J. Removal of Mn2+ from aqueous solution by manganese oxide coated zeolite. *Minerals Engineering*, vol. 23, pp. 1131-1138, 2010.

[138] Joseph IV, Tosheva L, Doyle AM. Simultaneous removal of Cd(II), Co(II), Cu(II), Pb(II), and Zn(II) ions from aqueous solutions via adsorption on FAU-type zeolites prepared from coal fly ash. *Journal of Environmental Chemical Engineering*, vol. 8, 2020.

[139] Nightngale ER. Phenomenological theory of ion solvation. Effective radii of hydrated ions. *The Journals of Physical Chemistry*, vol. 63, pp. 1381-1387, 1959.

[140] Marcus Y. Thermodynamics of solvation of ions - Gibbs free energy of hydration at 298.15K. *Journal of Chemical Society, Faraday Transactions*, vol. 87, pp. 2995-2999, 1991.

[141] Moussavi G, Talebi S, Farohki M, Mojtabaee Sabouti R. Removal of ammonium from water by adsorption onto synthetic zeolites NaA and NaX: a comparative parametric, kinetic, and equilibrium study. *Desalination and Water Treatment*, vol. 51, pp. 5710-5720, 2013.

[142] Liu H, Peng S, Shu L, Chen T, Bao T, Frost RL. Effect of Fe3O4 addition on the removal of ammonium by zeolite NaA. *J Colloid Interface Sci*, vol. 390, pp. 204-210, 2013.

[143] Widiastuti N, Wu H, Ang HM, Zhang D. Removal of ammonium from greywater using natural zeolite. *Desalination*, vol. 277, pp. 15-23, 2011.

[144] Fu H, Li Y, Yu Z, Shen J, Li J, Zhang M, et al. Ammonium removal using a calcined natural zeolite modified with sodium nitrate. *J Hazard Mater*, vol. 393, article 122481, 2020.

[145] Zhao Y, Niu Y, Hu X, Xi B, Peng X, Liu W, et al. Removal of ammonium ions from aqueous solutions using zeolite synthesized from red mud*. Desalination and Water Treatment*, pp. 51-12, 2015.

[146] Lin H, Wu X, Zhu J. Kinetics, equilibrium, and thermodynamics of ammonium sorption from swine manure by natural chabazite. *Separation Science and Technology*, vol. 51, pp. 202-213, 2015.

[147] Beler-Baykal B, Allar AD. Upgrading fertilizer production wastewater effluent quality for ammonium discharges through ion exchange with clinoptilolite. *Environ Technol*, vol. 29, pp. 665-672, 2008.

[148] Ayar N, Keçeli G, Kurtoğlu AE, Atun G. Cationic dye adsorption onto natural and synthetic zeolites in the presence of Cs+and Sr2+ions. *Toxicological & Environmental Chemistry*, vol. 97, pp. 11-21, 2014.

[149] Wang S, Zhu ZH. Characterization and environmental application of an Australian natural zeolite for basic dye removal from aqueous solution. J Hazard Mater, vol. 136, pp. 946-952, 2006.

[150] Oukil S, Bali F, Halliche D. Adsorption and kinetic studies of methylene blue on modified HUSY zeolite and an amorphous mixture of γ-alumina and silica. *Separation Science and Technology*, pp. 1-17, 2019.

[151] Badeenezhad A, Azhdarpoor A, Bahrami S, Yousefinejad S. Removal of methylene blue dye from aqueous solutions by natural clinoptilolite and clinoptilolite modified by iron oxide nanoparticles. *Molecular Simulation*, vol. 45, pp. 564-571, 2019.

[152] Mittal H, Babu R, Dabbawala AA, Stephen S, Alhassan SM. Zeolite -Y incorporated karaya gum hydrogel composites for highly effective removal of cationic dyes. *Colloids and Surfaces A: Physicochemical and Engineering Aspects*, vol. 19, 2019.

[153] Kraljević Pavelić S, Micek V, Filošević A, Gumbarević D, Žurga P, Bulog A, et al. Novel, oxygenated clinoptilolite material efficiently removes aluminum from aluminum chloride-intoxicated rats in vivo. *Microporous and Mesoporous Materials*, vol. 249, pp. 146-156, 2017.

[154] Roy P, Pal P, Sensharma S, Das N, Bandyopadhyay A. Performance of zeolite powder and a tubular membrane having different Si/Al ratio for removing As(III) in the aqueous phase. International *Journal of Applied Ceramic Technology*, vol. 14, pp. 461-473, 2017.

[155] Makgabutlane B, Nthunya LN, Musyoka N, Dladla BS, Nxumalo EN, Mhlanga SD. Microwave-assisted synthesis of coal fly ash-based zeolites for removal of ammonium from urine. *RSC Advances*, vol. 10, pp. 2416-2427, 2020.

[156] Garg A, Mainrai M, Bulasara VK, Barman S. Experimental Investigation on Adsorption of Amido Black 10b Dye onto Zeolite Synthesized from Fly Ash. *Chemical Engineering Communications*, vol 202, pp. 123-130, 2014.

[157] Sivalingam S, Sen S. Efficient removal of textile dye using nanosized fly ash derived zeolite-x: Kinetics and process optimization study. *Journal of the Taiwan Institute of Chemical Engineers*, vol. 96, pp. 305-314, 2019.

[158] Hernandez-Montoya V, Perez-Cruz MA, Mendoza-Castillo DI, Moreno-Virgen MR, Bonilla-Petriciolet A. Competitive adsorption of dyes and heavy metals on zeolitic structures. *J Environ Manage*, vol. 116, pp. 213-221, 2013.

[159] Zhang Y, Kou X, Lu H, Lv X. The feasibility of adopting zeolite in phosphorus removal from aqueous solutions. *Desalination and Water Treatment*, vol. 52, pp. 4298-4304, 2013.

[160] Hamdi N, Srasra E. Removal of phosphate ions from aqueous solution using Tunisian clays minerals and synthetic zeolite. *Journal of Environmental Sciences*, vol. 24, pp. 617-623, 2012.

[161] Goscianska J, Ptaszkowska-Koniarz M, Frankowski M, Franus M, Panek R, Franus W. Removal of phosphate from water by lanthanum-modified zeolites obtained from fly ash*. J Colloid Interface Sci*., vol. 513, pp. 72-81, 2018.

[162] Alshameri A, Yan C, Lei X. Enhancement of phosphate removal from water by TiO2/Yemeni natural zeolite: Preparation, characterization and thermodynamic. *Microporous and Mesoporous Materials*, vol. 196, 145-57, 2014.

[163] Gao L, Zhang C, Sun Y, Ma C. Effect and mechanism of modification treatment on ammonium and phosphate removal by ferric-modified zeolite. *Environ Technol*, vol. 40, pp. 1959-1968, 2019.

[164] Jiang N, Shang R, Heijman SGJ, Rietveld LC. High-silica zeolites for adsorption of organic micro-pollutants in water treatment: A review. *Water Res,* vol. 144, pp. 145-161, 2018.

[165] Jiang N, Shang R, Heijman SGJ, Rietveld LC. Adsorption of triclosan, trichlorophenol, and phenol by high-silica zeolites: Adsorption efficiencies and mechanisms. *Separation and Purification Technology*, vol. 235, 2020.

[166] Chen F, Li Y, Huang A. Hydrophilicity reversal by post-modification: Hydrophobic zeolite FAU and LTA coatings on stainless-steel-net for oil/water separation. *Colloids and Surfaces A: Physicochemical and Engineering Aspects*, vol. 601, 2020.

[167] Hosseini Hashemi MS, Eslami F, Karimzadeh R. Organic contaminants removal from industrial wastewater by CTAB treated synthetic zeolite Y. *J Environ Manage*, vol. 233, 785-792, 2019.

[168] Kuleyin A. Removal of phenol and 4-chlorophenol by surfactant-modified natural zeolite. *J Hazard Mater*, vol. 144, pp. 307-315, 2007.

[169] Vidal CB, Raulino GS, Barros AL, Lima AC, Ribeiro JP, Pires MJ, et al. BTEX removal from aqueous solutions by HDTMA-modified Y zeolite. *J Environ Manage*, vol. 112, pp. 178-185, 2012.

[170] Ghiaci M, Abbaspur A, Kia R, Seyedeyn-Azad F. Equilibrium isotherm studies for the sorption of benzene, toluene, and phenol onto organo-zeolites and as-synthesized MCM-41. *Separation and Purification Technology*, vol. 40, pp. 217-229, 2004.

[171] Wang J, Guo X. Adsorption kinetic models: Physical meanings, applications, and solving methods. *J Hazard Mater*, vol. 390, article 122156, 2020.

[172] Vidal CB, Barros AL, Moura CP, de Lima AC, Dias FS, Vasconcellos LC, et al. Adsorption of polycyclic aromatic hydrocarbons from aqueous solutions by modified periodic mesoporous organosilica. *J Colloid Interface Sci*., vol. 357, pp. 466-473, 2011.

[173] Shubair T, Eljamal O, Tahara A, Sugihara Y, Matsunaga N. Preparation of new magnetic zeolite nanocomposites for removal of strontium from polluted waters. *Journal of Molecular Liquids*, vol. 288, article 111026, 2019.

CAPÍTULO 5: SYNTHESIS OF HIGH PURITY ANALCIME ZEOLITE FROM GLASS POWDER WASTE AND ALUMINUM ANODIZING WASTE

ABSTRACT

The advance of population growth necessarily intensifies the activities in the industrial sector, which increases the generation of wastes with high potential for environmental impact. The reuse of solid wastes is an alternative for the development of materials with greater added value, which also contributes to the reduction of disposal in sanitary landfills. The present work aimed to synthesize analcime zeolite ($Na_{16}Al_{16}Si_{32}O_{96}.16H_2O$) of high purity and crystallinity, from two industrial residues that present difficulty to be recycled: glass powder waste (GPW) and aluminum anodizing mud (AAM). Plakett Burman statistical design was used to identify the variables of greater statistical relevance in the process, aiming at future optimization. The results reveal pure analcime formation, reaching a crystallinity of up to 75%, confirmed by XRD and XRF analysis. The analcime obtained has a low contaminant level, approximately 3% of calcium oxide, and the SEM analysis indicated the presence of particles with incomplete crystallization, which indicates that the optimization of the more relevant variables can lead to the formation of products with higher crystallinity. It was also observed the formation of zeolite NaP1, indicating that the combination GPW and AAM can be used to obtain other zeolitic phases. Consequently, a product with greater added value can be obtained, contributing for the sustainability in the aluminum and glass industries.

Keywords: analcime, glass powder waste, aluminum anodizing mud, Plackett Burman, zeolite synthesis

5.1 Introduction

Discovered in 1758 by the Swedish mineralogist Alex Fredrick Cronsted, zeolites are materials with microporous crystalline structures, which nowadays find application in several industrial sectors. These minerals, belonging to the class of aluminosilicates, are formed from the union of TO_4-type tetrahedrons, where T can be represented by the elements silicon and/or aluminum (Sivalingam and Sen, 2018; Yao *et al.*, 2018). The difference in valence between these two elements generates a crystal structure with an excess of negative electrical charge. During its formation, this is counterbalanced by compensation cations, usually elements of the alkali or alkaline earth metal family (Alves *et al.*, 2014). Another peculiarity of these minerals is observed in their microporous structure, which presents openings smaller than 20Å, consequently resulting in a solid that possesses a high surface area. The combination of these properties makes zeolites an attractive option for application as adsorbents (Chen *et al.*, 2021; Vidal *et al.*, 2012; Xie *et al.*, 2018), water softener (Cardoso *et al.*, 2015; Koohsaryan *et al.*, 2020), catalysts in the petrochemical industry (Collins *et al.*, 2020; Li *et al.*, 2017), gas separation (Kosinov *et al.*, 2016; Kumar *et al.*, 2020; Qiang *et al.*, 2019), medical applications (Khodaverdi *et al.*, 2016; Vilaca *et al.*, 2013), civil construction, as an addition to Portland cement (Das *et al.*, 2021; Kaplan *et al.*, 2021; Tran *et al.*, 2019), and many others.

Currently, more than 60 natural zeolite varieties are known, but large mineral deposits are relatively scarce. With the increasing demand, studies indicated the feasibility of artificially replicating the conditions of zeolite formation in nature, and, from 1905 onwards, the mineral began to be synthesized on a large scale. More than 230 different types of zeolites are currently known, being classified into 133 distinct crystal structures. Among them, analcime is a naturally occurring zeolite that can also be synthesized. This zeolitic phase presents the chemical formula $Na_{16}Al_{16}Si_{32}O_{96}.16H_2O$, with a Si/Al ratio of 1.5-3.0. The crystalline structure of analcime is compact compared to other zeolites, exhibiting pore sizes of 2.6Å (Vereshchagina *et al.*, 2018). The crystal unit cell is composed of 24 cavities, and among them, 16 are filled with water molecules (Vigil de la Villa Mencía *et al.*, 2020). Even showing a small opening size, analcime still finds application in heavy metals adsorption, *e.g.* lead, nickel, zinc, and copper (Hsiao *et al.*, 2017), gas separation, as a molecular sieve, and nuclear waste immobilization (Bortolini *et al.*, 2020). In any case, synthetic analcime possesses higher efficiency compared to the natural variety due to the absence of other minerals that act as contaminants (Bejar *et al.*, 2014).

Despite the possibility of producing synthetic zeolites, the process is costly, especially due to the chemical reagents used as a source of silicon and aluminum. An alternative green

synthesis method is to use raw materials with a high amount of silicon and aluminum as a precursor. In this way, the synthesis gains economic benefits, and for this reason, the search for low-cost precursor materials became a necessity (He *et al.*, 2021; Ma *et al.*, 2014; Vereshchagina *et al.*, 2018). In theory, any material rich in Si and Al can be used as a precursor in the synthesis, even those considered residues from other industrial activities. Among the various industrial residues that can be used as sources of silicon and aluminum in the synthesis of analcime, glass powder waste (GPW) and aluminum anodizing mud (AAM) stand out for their chemical composition.

The glass powder is the waste generated during the cutting and polishing step in the production of glass pieces. Due to its fine particle size, this material is difficult to recycle, as it generates bubbles and imperfections in new pieces (Khan *et al.*, 2021). It is estimated that the production of GPW accounts for approximately 5% of the total solid waste generated globally (Dadsetan *et al.*, 2021). The disposal of GPW in landfills becomes a common activity, and due to the low biodegradability of glass, this practice is considered harmful to the environment (Du *et al.*, 2021; Kalakada *et al.*, 2019; Ramteke *et al.*, 2021; Salzmann *et al.*, 2020).

Aluminum anodizing mud is the residue generated during the electrochemical process responsible for the formation of an oxide layer on the surface of aluminum pieces, aiming at protection against corrosion. The process takes place by immersing the parts in a bath of NaOH or H_2SO_4, which removes part of the aluminum from the surface into the solution. It is estimated that for every 1 ton of aluminum treated by anodizing, 475kg of sludge is generated, consisting mostly of aluminum hydroxide (Mymrin *et al.*, 2018; Souza *et al.*, 2020). After removing the water, this residue, which is considered non-toxic and non-inert, is disposed of in landfills, significantly contributing to environmental impact (Souza *et al.*, 2019).

This research aims to obtain a single-phase analcime zeolite, with high crystallinity, using the above-mentioned industrial residues as precursors. The use of such residues can bring economic benefits to the synthesis process, and contributes to a circular economy, reducing the environmental impacts of landfill disposal, adding value to the residues. To reach the purity and crystallinity desired, the Placket Burman method was applied to evaluate which variables present greater statistical relevance, enabling future optimization.

5.2 Materials and methods

5.2.1 *Precursor Materials*

Glass powder waste (GPW) and aluminum anodizing mud (AAM) was used as precursor materials as sources of silicon and aluminum, respectively, being supplied by Akrominas - Comercio de Aluminio LTDA and Bend Glass Comercio e Industria LTDA, located in Contagem-MG, Brazil. The materials were oven dried at 100°C for 48h and deagglomerated in a porcelain ball mill for 30min. As a source of alkali, P.A. sodium hydroxide in micropellets was used. During the synthesis, reverse osmosis treated water (conductivity <1.5μS.cm) was used.

5.2.2 *Materials characterization*

The chemical composition of GPW, AAM, and synthetic analcime powder samples were determined via FRX analysis using a Rayny EDX-720 spectrometer (Shimadzu, US). The identification of crystalline phases in the samples of precursor materials was performed in a Philips X-ray diffractometer (Panalytical, UK), operating with Cu k-alpha radiation (40kV, 30mA), 2q ranging from 5 to 90º, at 0.06°/s. The crystalline phases were identified using the Match! Software, with Crystallography Open Database, revision. 184238. The identification of the zeolitic product was made in the same equipment used for mineral characterization of the precursor materials. Only the 2q and step were modified. For zeolitic samples, the 2q range was set from 3 to 50°, at 0.02°/s step, since the characteristic peaks of zeolites occur in low 2q angles. The zeolitic phases were identified using Match3! software, followed by quantification using Rietveld method. The patterns used for peak identification was obtained from the International Zeolite Association Database. The crystallinity determination was performing by measuring the relation between the peaks area and the total area under the sample diffractogram, according to Equation 1 (Iqbal *et al.*, 2019).

$$\%crystallinity = \frac{Sum\ of\ cristalline\ peaks\ area}{Total\ area} * 100 \quad (1)$$

The FT-IR analysis was performed in an Alpha Spectrometer (Bruker, DE) in Attenuated Total Reflectance (ATR) mode, with a nominal resolution of 4 cm^{-1}. The spectra were recorded from 4000 to 400 cm^{-1}, and an average of 32 scans was taken. The size distribution of precursor materials was measured by Lase Particle Analyzer (Cilas 1064, FR). The samples were deagglomerated in an ultrasonic bath for 200s. Zeta potential measurements were performed using a Zetasizer 3000 HS 1256 (Panalytical, UK). The suspensions were prepared by adding 0.01g of analcime in 25mL of KCl 10^{-3}M solution (supporting electrolyte). Then, the pH was

adjusted using dilute solutions of NaOH and HCl and measurements were performed in triplicate.

Secondary electron scanning electron microscopy (SE-SEM) was performed using a Quanta 200 FEI microscope (Thermofisher, US), with a resolution of 1.6nm, operating with 10 to 15kV. The sample undergone metallization before the analysis. The thermogravimetry analysis was performed in a DTA60H thermogravimetric analyzer (Shimadzu, US), using an aluminum crucible, a heating rate of 10°C.min$^{-1,}$ and 50mL.min^{-1} nitrogen flow, from 25 to 900°C.

5.2.3 *Zeolite synthesis*

The synthesis of analcime zeolite from GPW and AAM was conducted in a 2-step process (alkaline fusion followed by hydrothermal synthesis). First, a given mass of GPW, AAM, and NaOH was measured on an analytical digital balance and then calcined in a porcelain crucible. The material resulting from the alkaline fusion was dissolved in ultra-pure water and stirred for 1h. Then, 20ml of the solution was transferred to a Teflon-lined stainless-steel autoclave, remaining in an oven for crystallization. At the end of the process, the solid obtained was filtered and washed several times until pH 9 was reached, to remove excess Na^+ ions. Finally, the solid was oven dried at 60°C for 72h.

5.2.4 *Plackett-Burman methodology*

For the development of this research, 7 experimental variables were considered, based in previous studies, and shown in Table 1. However, with the increase in the number of variables to be investigated, a high number of tests are necessary. The Plackett-Burman methodology was applied for an initial assessment to identify which variables have greater statistical relevance in the synthesis process, allowing for a small number of tests (Plackett and Burman, 1946). Recent researchers have used this methodology in their studies, obtaining consistent results (Caroca *et al.*, 2021; Paul *et al.*, 2020; Silva *et al.*, 2021). Thus, 7 real and 4 dummy variables were combined in a 12-run non-geometric experimental design, as shown in Table 2. The Crystallinity (%) and Analcime content (%) in the products obtained from the synthesis were defined as response variables. The experimental design was conducted in duplicate, and the mean values of Crystallinity (%) and Analcime (%) were taken.

Table 5.1 - Variables in the synthesis and their low/high levels.

Factors	Symbol	Unit	Levels	
			Low (-1)	High (+)
Calcination temperature	C_{temp}	°C	500	700
Calcination time	C_{time}	h	2	3
SiO_2/Al_2O_3 ratio	SiO_2/Al_2O_3	-	2.5	8
Na_2O/SiO_2 ratio	Na_2O/SiO_2	-	6	15
H_2O/Na_2O ratio	H_2O/Na_2O	-	20	300
Crystallization temperature	Cr_{temp}	°C	90	110
Crystallization time	Cr_{time}	h	4	24
Dummy 1	A	-	-	-
Dummy 2	B	-	-	-
Dummy 3	C	-	-	-
Dummy 4	D	-	-	-

Table 5.2 - Placket Burman design and values of the response variables.

Test number	**Run order**	**A**	**C_{temp}**	**C_{time}**	**B**	**SiO_2 / Al_2O_3**	**Na_2O / SiO_2**	**C**	**H_2O / Na_2O**	**D**	**Cr_{temp}**	**Cr_{time}**	**Crystallinity (%)**	**Analcime (%)**
1	3	+	700	2	+	8	15	-	200	-	110	24	74.9	100.0
2	6	+	500	3	+	8	6	-	200	+	90	24	74.5	85.2
3	5	-	700	3	+	2,5	6	-	300	-	110	24	72.0	93.0
4	9	+	700	3	-	2,5	6	+	200	+	110	4	61.9	92.6
5	11	+	700	2	-	2,5	15	-	300	+	90	24	65.8	97.1
6	7	+	500	2	-	8	6	+	300	-	110	24	65.5	100.0
7	12	-	500	2	+	2,5	15	+	200	+	110	24	75.4	100.0
8	1	-	500	3	-	8	15	-	300	+	110	4	65.9	100.0
9	4	-	700	2	+	8	6	+	300	+	90	4	12.2	0.0
10	10	+	500	3	+	2,5	15	+	300	-	90	4	52.8	0.0
11	2	-	700	3	-	8	15	+	200	-	90	4	60.7	100.0
12	8	-	500	2	-	2,5	6	-	200	-	90	4	54.8	0.0

5.3 Results and discussion

5.3.1 Characterization of GPW and AAM

Figure 1 shows the mineralogical composition of the AMM and GPW samples. The AMM sample (Figure 1(a)) exhibits the absence of amorphous halo, and high-intensity peaks, revealing the crystalline nature of this material. The peaks are related to the minerals Gibbsite (COD 9015976) and Bayerite (COD 1000061), isomorphic forms of aluminum hydroxide. The crystalline form of AAM implicates in high chemical stability, which impairs the dissolution of the material, and consequently, limits the amount of Al^{3+} in solution. The GPW diffractogram reveals the presence of an amorphous halo (Figure 1(b)). Low-intensity peaks of fluorite (COD

9007064) can be seen in the diffractogram, as this material acts as fondant for silica fusion in the glass fabrication process. Besides, the absence of peaks characterizes GPW as an amorphous material. Even though amorphous materials can present high chemical reactivity, glass hardly solubilizes.

As the two materials are characterized by their extremely low solubility, it is necessary to subject them to the alkaline fusion method. In this process, the materials are fused with an alkaline base, *e.g.,* sodium hydroxide, in temperatures ranging from 500 to 700ºC. The products of this reaction are sodium aluminate and sodium silicate, both soluble species (Akın *et al.*, 2021).

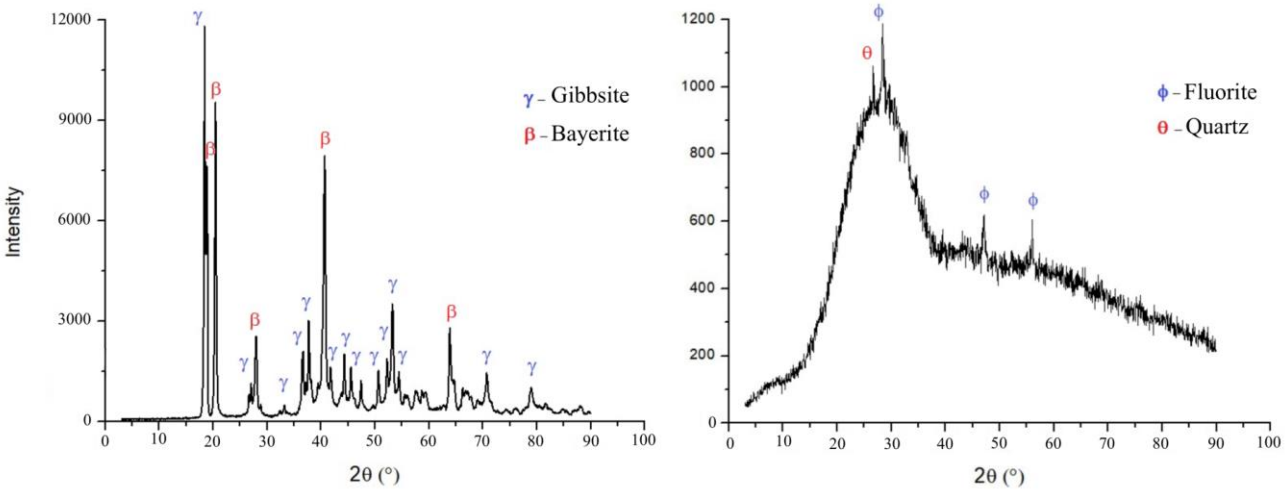

Figure 5.1 - Mineral phase identification of AAM (a) and GPW (b).

The GPW and AAM chemical composition and size distribution are described in Table 2. AAM is mainly composed of Al_2O_3 and shows a low percentage of contaminant elements. The loss on ignition represents 33.7% of the sample, but the alkaline fusion volatilizes these compounds. Consequently, loss of ignition does not represent a great source of contaminant elements. The GPW is composed of 70.5% of silica, and approximately 22% of calcium and sodium oxides, used in the glass fabrication process. The sodium present in GPW is another Na^+ source, which reduces the amount of NaOH needed in the synthesis.

The fact that the materials are sources of silica and alumina separately ensures that the Si/Al ratio required for crystallization is obtained with only these two materials, without the need to add chemical compounds for stoichiometric adjustment, which brings economic benefits to the process.

Some residues that are frequently used in the synthesis of the zeolite may have a high percentage of contaminants. In the case of GPW and AAM, the low contaminant content

guarantees that the entire mass of the materials is used in the synthesis, without the generation of sub-waste, making the process environmentally friendly.

Table 2 also shows the size distribution of GPW and AAM. The medium diameter (D_m) measured for GPW and AAM were 8.96 and 25.4µm, respectively. The materials fineness is a consequence of their generation (abrasion and precipitation). This fact can represent two benefits. First, it is not necessary to grind the material to obtain this size distribution (grinding is required only to deagglomerate the materials after drying). And secondly, because of the fineness, the materials present a high surface area, which favors the chemical reactions in the alkali fusion step.

Table 5.3 - Physico-Chemical properties of GPW and AAM.

Chemical composition (%wt)	GPW	AAM	Synthetic Analcime
SiO_2	70.55	0.20	50.55
Al_2O_3	1.06	64.61	31.65
CaO	10.38	0.01	3.01
Cr_2O_3	<0.01	<0,01	0.01
Fe_2O_3	0.25	0,26	0.52
K_2O	0.24	<0,01	0.26
MgO	0.80	-	0.79
MnO	<0.01	<0,01	0.02
Na_2O	11.88	1,14	11.49
P_2O_5	0.26	<0,01	0.26
TiO_2	0.09	0,01	0.04
PPC	4.11	33,71	-
Particle size distribution (µm)			
D_m	8.96	25.36	-
D_{10}	1.43	4.58	-
D_{50}	7.84	25.19	-
D_{90}	21.35	43.36	-

5.3.2 Main variables in Analcime synthesis

Figure 3 shows Pareto charts for the response variables, *i.e*., Crystallinity (%) and Analcime (%). Crystallization time and temperature are the variables with the greatest statistical significance for both responses. As verified in Table A1, the tests reaching greater crystallinity are those conducted at the high-level values of time and temperature. In tests which used a lower temperature (90°C), the products obtained showed lower crystallinity, because the energy supplied is relatively low for the analcime zeolite to crystallize properly. At high-level crystallization temperature and low-level crystallization time, crystallinity is also impaired, as nuclei begin to form, but there is not enough time for the crystals to grow (Qiang *et al.*, 2019). In Figure 2, it is possible to verify in the Pareto chart that both, the crystallization time and

crystallization temperature, when changing from the lower to the upper level, strongly increases the responses.

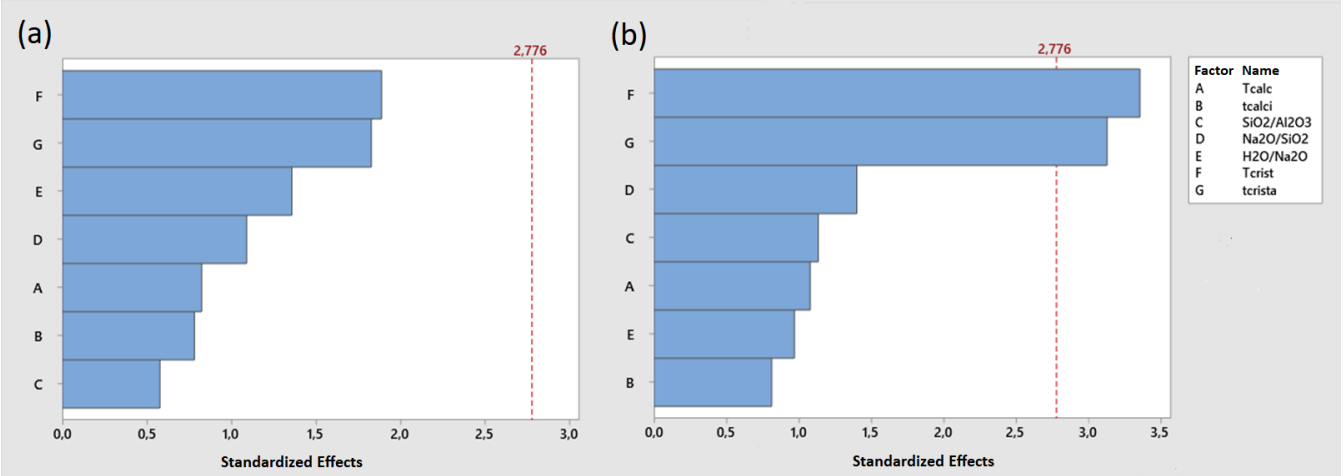

Figure 5.2 - Pareto chart of standardized effects for Crystallinity (%) (a) and Analcime (%) (b) with 95% confidence.

The Na_2O/SiO_2 ratio has greater statistical significance for Analcime (%) compared to Crystallinity (%). The amount of Na^+ ions have a strong influence on crystallization, impairing analcime crystallization when present in low concentration in solution. In research verifying the influence of different mineralizing agents, (Hsiao et al., 2017) concluded that the absence of Na^+ prevents the crystallization of analcime. Na^+ ions are located in the interior of the small cavities of the analcime crystalline structure, and their presence is necessary for the structure to crystalize adequately (Yuan *et al.*, 2016).

The SiO_2/Al_2O_3 ratio is the variable that has the least statistical relevance for Crystallinity (%) since a wide range of values allows the crystallization of several zeolitic phases. However, the SiO_2/Al_2O_3 ratio is more relevant for Analcime (%), as a specific range of SiO_2/Al_2O_3 is required for this phase to form. Consequently, for the synthesis of any zeolite, this is an important variable to be considered when seeking the production of a pure phase (Iqbal *et al.*, 2019).

The H_2O/Na_2O ratio has no significant relevance for the crystallization of analcime, but it affects Crystallinity (%) more pronouncedly. In this case, increasing values of this variable negatively affect both responses. The greater amount of water in the system leads to a lower concentration of Na^+ ions in the solution (Bai *et al.*, 2018), which, as discussed earlier, inhibits the formation of analcime. In the case of crystallization, the greater dilution of the solution makes the monomers more difficult to nucleate (Lin and Chen, 2021).

Among all the variables considered in this study, the calcination time and the calcination temperature showed low relevance for both responses. The melting point of sodium hydroxide is around 500°C, and the conversion of GPW and AAM into soluble Na-salts is possible in this temperature (Mori, 2003; Rahman *et al.*, 2013). Thus, it is suggested to use the values presented in the lower levels, for energy saving, which contributes to reducing the process cost. As indicated in Figure 3, the normal distribution graphs show the adherence of experimental results to the Placket Burman statistical design, indicating that the results fit the model adequately. It is important to mention that these variables were considered statistically relevant only in the levels considered in this research, and should not be extended for other ranges.

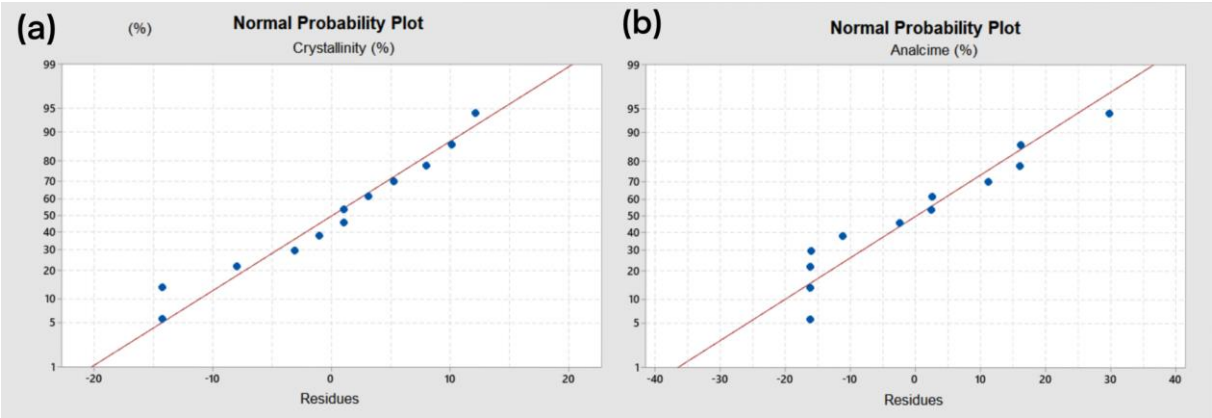

Figure 5.3 - Normal probability plot of standardized effects for Crystallinity (%) (a) and Analcime (%) (b).

5.3.3 Analcime characterization

Figure 4 shows the XRD results for all tests, in order of crystallinity. The objective of synthesizing high purity analcime zeolite was achieved in the majority of tests, especially run 7-12, 1-3, and 11-2, which in addition to purity, showed high crystallinity. The analcime, cancrinite, sodalite, and NaP1 phases are phases that compete during crystallization, and consequently, the definition of limits for the experimental variables is of great importance to obtain high purity zeolite. It is reported in the literature that the optimum crystallization time for analcime is approximately 24h (Jiménez *et al.*, 2021). Although the temperature indicated to be set at 200°C (Robson, 2016), in this research it was possible to obtain high purity analcime at a temperature of 100°C. In runs 12-8 and 10-10, there were no peaks related to analcime. The conditions of these two tests led to the formation of sodalite and NaP1, with emphasis on the 10-10 run, which showed high purity of NaP1 (although with low crystallinity). Despite the objective of crystallizing only analcime zeolite in this work, this result can be considered

positive, since it reveals the potential of the combination between GPW and AAM for the crystallization of other zeolite phases, which increases the possibility of using these materials as precursors. For runs 9-4, the experimental conditions were inadequate for the crystallization of any type of zeolite, and the product showed very low crystallinity.

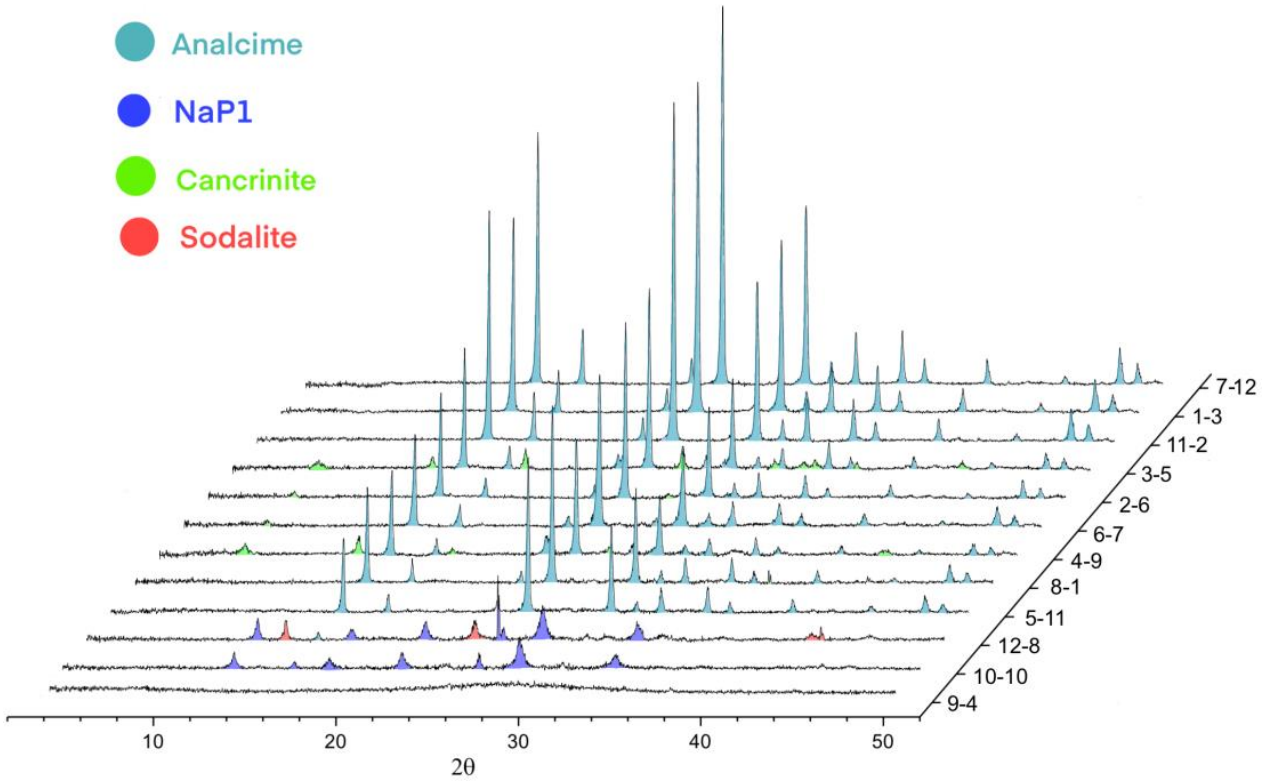

Figure 5.4 - XRD results of the experimental runs.

The FT-IR spectrum of the Synthesized analcime is shown in Figure 5. The bands located at 436 cm-1, 615 cm-1 and 436 cm-1 indicate the T-O-T bending vibration, where T represents Si and/or Al (Abdelrahman *et al.*, 2020; Jiménez *et al.*, 2021). Symetric streching is represented by the band at 730 cm-1 (Jiménez *et al.*, 2021). It can be observed, the spectra exhibit an intense peak in the 950-1250 cm-1 range, a striking feature of zeolitic materials, representing asymmetric stretching vibration of T-O-T bonds (Iqbal *et al.*, 2019). It can also be seen a low-intensity peak at 1636 cm-1, which is related to the bending vibration of O-H bonds, of water molecules in the micropores (Azizi *et al.*, 2016; Iqbal *et al.*, 2019). The FT-IR spectrum is in agreement with the DRX and FRX results, confirming that the material is composed mainly of silicon, aluminum, and oxygen.

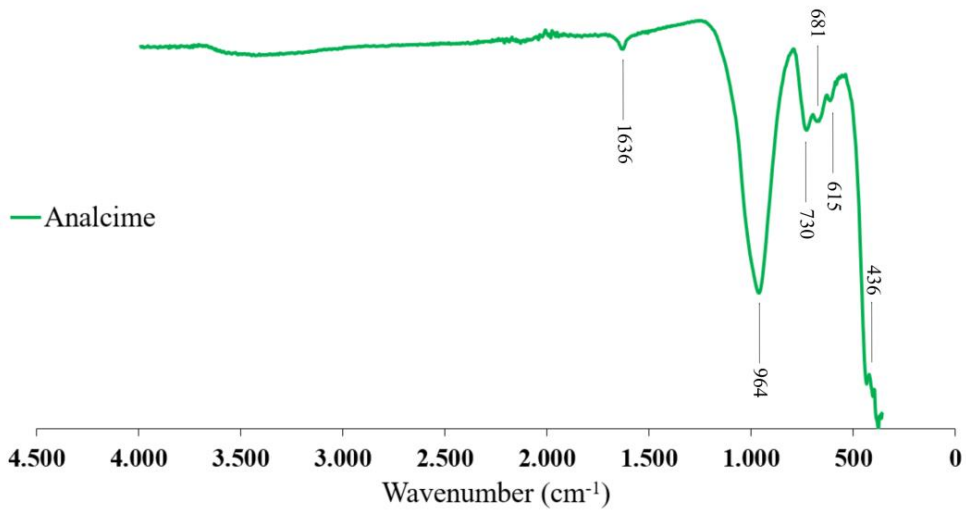

Figure 5.5 - FT-IR spectra of the synthesized analcime.

The chemical composition of the analcime sample is presented in Table 2. The Si/Al ratio of synthesized analcime is 1.4, which is close to the values observed in previous studies (1.5-3) (Hegazy *et al.*, 2010; Vereshchagina *et al.*, 2018). FRX analysis also report 74.25% of $Na_{16}Al_{16}Si_{32}O_{96}$, a value which agrees with the calculated crystallinity from DRX data. The sample also presents 3% of calcium oxide, the major contaminant present in the precursor materials.

Figure 6 illustrates the results of zeta potential for the analcime sample in pH range from 1 to 9. The analcime zeolite displays a negative electrical charge in a wide pH range. The natural negative charge is higher in the basic solution due to the presence of an excess of OH^- (Pugazhenthi and Vinoth Kumar, 2017), with a maximum value of -47,3mV at pH 9.0. The point of zero charge (PZC) is observed at approximately pH 2.6. Below this pH, in a strongly acidic solution, the analcime particles became positively charged, due to excess of H^+ (Pugazhenthi and Vinoth Kumar, 2017), with a maximum value of 37.6mV at pH 1,0. The PZC determination is of great importance in the application of zeolite in contaminant removal from wastewater. Zeolites can readily remove cationic species due to electrostatic attraction (*e.g.*, heavy metals, ammonia, and dyes), but the removal of anionic species is not possible. However, pH values below PZC can enable the removal of anionic species due to induced positive electrical charge (Adam *et al.*, 2018; Arslan and Veli, 2012; Khanmohammadi *et al.*, 2019; Nekhunguni *et al.*, 2017; Sivalingam and Sen, 2019). Hence, the determination of PCZ is of fundamental importance for the treatment of effluents contaminated by anionic species.

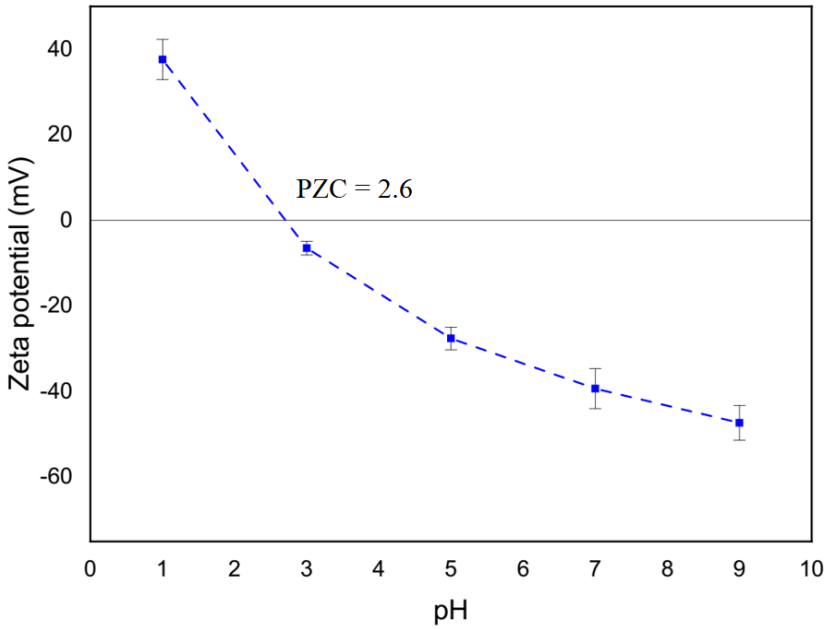

Figure 5.6 - Zeta potential of analcime.

SE-SEM images of the precursor materials and analcime are shown in Figure 7. The AAM particles (Fig. 7a) present rough surfaces, that may be related to precipitation of $Al(OH)_3$ in the formation of the anodizing mud. As for GPW (Fig. 7b), the cutting and polishing of glass pieces result in the formation of sharped edges particles. Both materials exhibit a wide size distribution, also verified in size distribution analysis in terms of their D_{90} and D_{10} (Table 2), with very large and small particles. On the other hand, analcime particles present a relatively uniform particle size distribution (Fig. 7c), with particles size around 10µm. The presence of well-crystallized particles can be observed, in the form of tetrahedrons, characteristic of analcime (Jiménez *et al.*, 2021; Vigil de la Villa Mencía *et al.*, 2020). However, the majority of particles exhibit incomplete crystallization (Fig. 7d), since the particles are trapezoidal, but without well-defined edges. It can also be seen the presence of uncrystallized material in the upper region of Fig. 7d. According to Table 2, the analcime sample is composed of approximately 94% of silicon, aluminum and sodium oxides, and the incomplete crystallization was observed, suggesting that the optimization of the variables in the process, especially those of greater statistical relevance for Crystallization (%), can enables the synthesis of analcime to reach crystallinity above 75%, which was the maximum value obtained in this work.

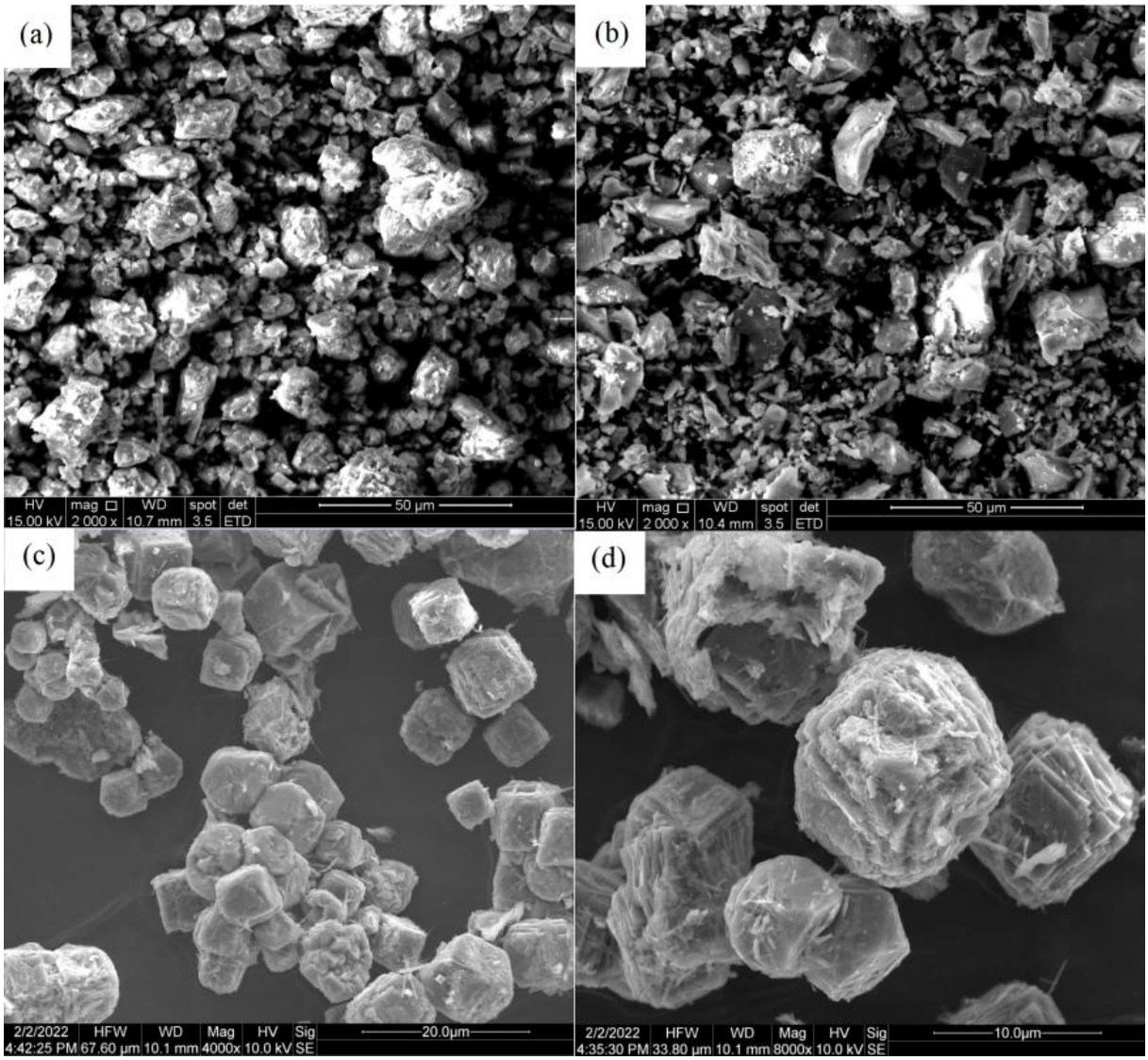

Figure 5.7 - SE-SEM image of the precursor materials AAM (a) and GPW (b), and the synthesized analcime zeolite (c) and (d).

The thermogravimetric curve of analcime is shown in Figure 8. In the range from 25 to 200°C, there is a slight mass loss of 3%, related to the water adsorbed on the surface of the particles, followed by an intense mass loss, about 8% up to about 400°C. The mass loss in this range is related to the elimination of water molecules present in the analcime pores and agrees with values obtained by recent studies (Jiménez *et al.*, 2021; Jing *et al.*, 2017; Vereshchagina *et al.*, 2018). The authors also verified that the mass loss stabilizes after 400°C. However, an additional mass loss of approximately 3% up to 900°C is noted, which may be related to the decomposition of calcium oxide present in the sample (Bilton *et al.*, 2012), as verified by XRF analysis. In any case, analcime shows high thermal stability, which is advantageous in processes that demand high-temperature rates.

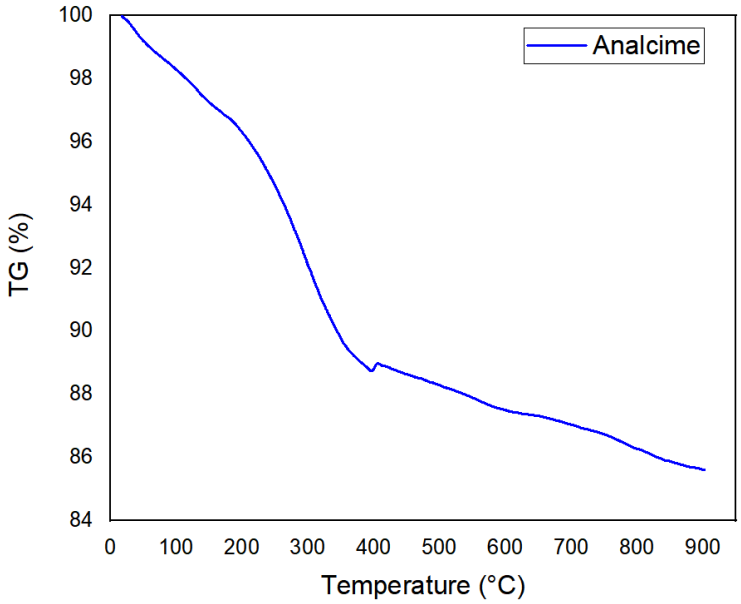

Figure 5.8 - Analcime thermogravimetric (TG) curve.

5.4 Conclusions

In this work, analcime of high purity and crystallinity was synthesized from the combination of glass powder waste and aluminum anodizing mud. Due to their high chemical stability, a 2-step approach was used, *i.e.,* alkaline fusion followed by hydrothermal synthesis. From the results obtained by the statistical Plackett Burman methodology, temperature and crystallization time were observed to be the variables with the greatest statistical relevance in the synthesis, while alkaline fusion temperature and time are the ones with the least relevance. The zeolite obtained showed high crystallinity, but according to the results, it is expected that the optimization of the variables can lead to the formation of pure analcime with crystallinity higher than 75%, the maximum crystallinity obtained in this work. The results indicate that obtaining analcime for application in various industrial sectors is an alternative for the reuse of GPW and AAM, contributing to sustainability and circular economy.

APPENDIX

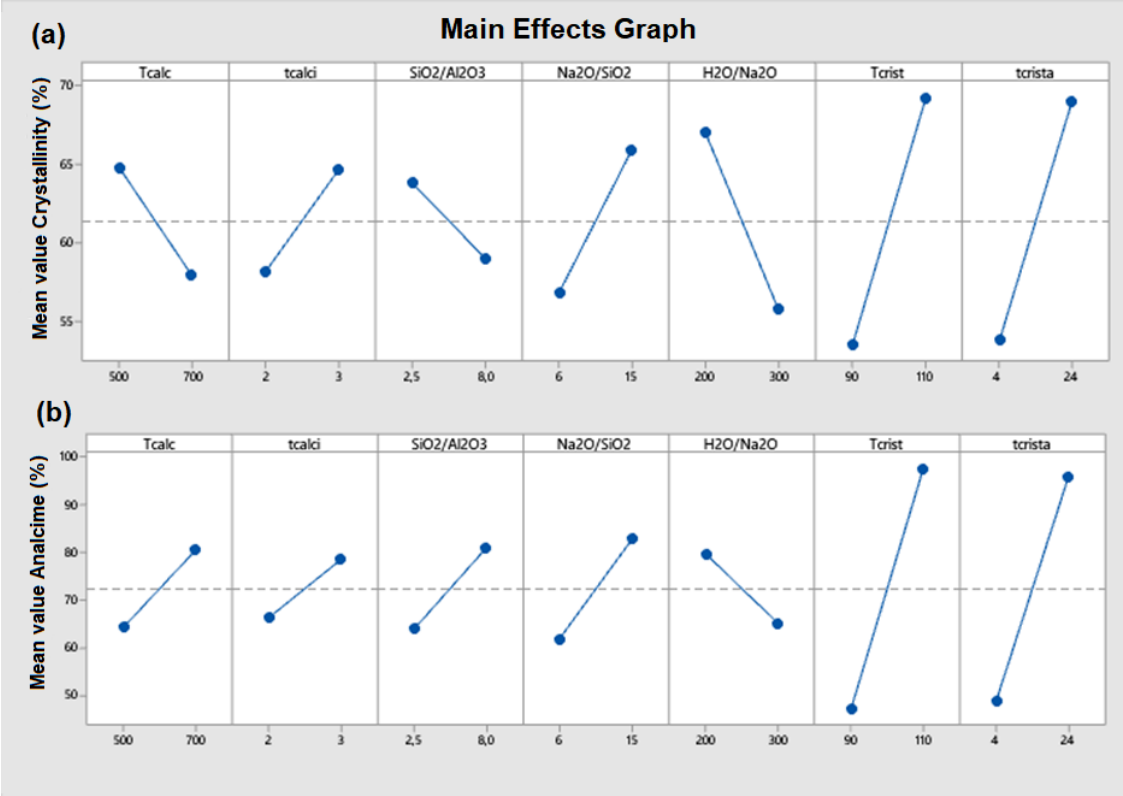

Figure A1 – Main effect plots of standardized effects for Crystallinity (%) (a) and Analcime (%) (b).

REFERENCES

Abdelrahman, E.A., Alharbi, A., Subaihi, A., Hameed, A.M., Almutairi, M.A., Algethami, F.K., Youssef, H.M., 2020. Facile fabrication of novel analcime/sodium aluminum silicate hydrate and zeolite Y/faujasite mesoporous nanocomposites for efficient removal of Cu(II) and Pb(II) ions from aqueous media. Journal of Materials Research and Technology 9(4), 7900-7914.

Adam, M.R., Salleh, N.M., Othman, M.H.D., Matsuura, T., Ali, M.H., Puteh, M.H., Ismail, A.F., Rahman, M.A., Jaafar, J., 2018. The adsorptive removal of chromium (VI) in aqueous solution by novel natural zeolite based hollow fibre ceramic membrane. Journal of Environmental Management 224, 252-262.

Akın, S.Ş., Kirdeciler, S.K., Kazanç, F., Akata, B., 2021. Critical analysis of zeolite 4A synthesis through one-pot fusion hydrothermal treatment approach for class F fly ash. Microporous and Mesoporous Materials 325.

Alves, J.A.B.L.R., Dantas, E.R.S., Pergher, S.B.C., A., M.D.M., Melo, M.A.F., 2014. Synthesis of high value added zeolitic materials using glass residue as a silica source. Materials Research 17, 213-218.

Arslan, A., Veli, S., 2012. Zeolite 13X for adsorption of ammonium ions from aqueous solutions and hen slaughterhouse wastewaters. Journal of the Taiwan Institute of Chemical Engineers 43(3), 393-398.

Azizi, S.N., Ghasemi, S., Derakhshani-mansoorkuhi, M., 2016. The synthesis of analcime zeolite nanoparticles using silica extracted from stem of sorghum Halepenesic ash and their application as support for electrooxidation of formaldehyde. International Journal of Hydrogen Energy 41(46), 21181-21192.

Bai, S.-x., Zhou, L.-m., Chang, Z.-b., Zhang, C., Chu, M., 2018. Synthesis of Na-X zeolite from Longkou oil shale ash by alkaline fusion hydrothermal method. Carbon Resources Conversion 1(3), 245-250.

Bejar, A., Ben Chaabene, S., Jaber, M., Lambert, J.-F., Bergaoui, L., 2014. Mn-analcime: Synthesis, characterization and application to cyclohexene oxidation. Microporous and Mesoporous Materials 196, 158-164.

Bilton, M., Brown, A.P., Milne, S.J., 2012. Investigating the optimum conditions for the formation of calcium oxide, used for CO2sequestration, by thermal decomposition of calcium acetate. Journal of Physics: Conference Series 371.

Bortolini, H.R., Lima, D.S., Perez-Lopez, O.W., 2020. Hydrothermal synthesis of analcime without template. Journal of Crystal Growth 532.

Cardoso, A.M., Horn, M.B., Ferret, L.S., Azevedo, C.M., Pires, M., 2015. Integrated synthesis of zeolites 4A and Na-P1 using coal fly ash for application in the formulation of detergents and swine wastewater treatment. J Hazard Mater 287, 69-77.

Caroca, E., Serrano, A., Borja, R., Jimenez, A., Carvajal, A., Braga, A.F.M., Rodriguez-Gutierrez, G., Fermoso, F.G., 2021. Influence of phenols and furans released during thermal pretreatment of olive mill solid waste on its anaerobic digestion. Waste Manag 120, 202-208.

Chen, J., Huang, R., Ouyang, H., Yu, G., Liang, Y., Zheng, Q., 2021. Utilization of dredged river sediments to synthesize zeolite for Cd(II) removal from wastewater. Journal of Cleaner Production 320.

Collins, F., Rozhkovskaya, A., Outram, J.G., Millar, G.J., 2020. A critical review of waste resources, synthesis, and applications for Zeolite LTA. Microporous and Mesoporous Materials 291.

Dadsetan, S., Siad, H., Lachemi, M., Sahmaran, M., 2021. Evaluation of the tridymite formation as a technique for enhancing geopolymer binders based on glass waste. Journal of Cleaner Production 278.

Das, M., Adhikary, S.K., Rudzionis, Z., 2021. Effectiveness of fly ash, zeolite, and unburnt rice husk as a substitute of cement in concrete. Materials Today: Proceedings.

Du, Y., Yang, W., Ge, Y., Wang, S., Liu, P., 2021. Thermal conductivity of cement paste containing waste glass powder, metakaolin and limestone filler as supplementary cementitious material. Journal of Cleaner Production 287.

He, Y., Tang, S., Yin, S., Li, S., 2021. Research progress on green synthesis of various high-purity zeolites from natural material-kaolin. Journal of Cleaner Production 306.

Hegazy, E.Z., El Maksod, I.H.A., El Enin, R.M.M.A., 2010. Preparation and characterization of Ti and V modified analcime from local kaolin. Applied Clay Science 49(3), 149-155.

Hsiao, Y.-H., Ho, T.-Y., Shen, Y.-H., Ray, D., 2017. Synthesis of analcime from sericite and pyrophyllite by microwave-assisted hydrothermal processes. Applied Clay Science 143, 378-386.

Iqbal, A., Sattar, H., Haider, R., Munir, S., 2019. Synthesis and characterization of pure phase zeolite 4A from coal fly ash. Journal of Cleaner Production 219, 258-267.

Jiménez, A., Misol, A., Morato, Á., Rives, V., Vicente, M.A., Gil, A., 2021. Synthesis of pollucite and analcime zeolites by recovering aluminum from a saline slag. Journal of Cleaner Production 297.

Jing, Z., Cai, K., Li, Y., Fan, J., Zhang, Y., Miao, J., Chen, Y., Jin, F., 2017. Hydrothermal synthesis of pollucite, analcime and their solid solutions and analysis of their properties. Journal of Nuclear Materials 488, 63-69.

Kalakada, Z., Doh, J.-H., Chowdhury, S., 2019. Glass powder as replacement of cement for concrete – an investigative study. European Journal of Environmental and Civil Engineering, 1-18.

Kaplan, G., Coskan, U., Benli, A., Bayraktar, O.Y., Kucukbaltacı, A.B., 2021. The impact of natural and calcined zeolites on the mechanical and durability characteristics of glass fiber reinforced cement composites. Construction and Building Materials 311.

Khan, M.N.N., Kuri, J.C., Sarker, P.K., 2021. Effect of waste glass powder as a partial precursor in ambient cured alkali activated fly ash and fly ash-GGBFS mortars. Journal of Building Engineering 34.

Khanmohammadi, H., Bayati, B., Rahbar- Shahrouzi, J., Babaluo, A.-A., Ghorbani, A., 2019. Molecular simulation of the ion exchange behavior of Cu2+, Cd2+ and Pb2+ ions on different zeolites exchanged with sodium. Journal of Environmental Chemical Engineering 7(3), 103040.

Khodaverdi, E., Soleimani, H.A., Mohammadpour, F., Hadizadeh, F., 2016. Synthetic Zeolites as Controlled-Release Delivery Systems for Anti-Inflammatory Drugs. Chem Biol Drug Des 87(6), 849-857.

Koohsaryan, E., Anbia, M., Maghsoodlu, M., 2020. Application of zeolites as non-phosphate detergent builders: A review. Journal of Environmental Chemical Engineering 8(5).

Kosinov, N., Gascon, J., Kapteijn, F., Hensen, E.J.M., 2016. Recent developments in zeolite membranes for gas separation. Journal of Membrane Science 499, 65-79.

Kumar, S., Srivastava, R., Koh, J., 2020. Utilization of zeolites as CO2 capturing agents: Advances and future perspectives. Journal of CO2 Utilization 41.

Li, Y., Li, L., Yu, J., 2017. Applications of Zeolites in Sustainable Chemistry. Chem 3(6), 928-949.

Lin, Y.-J., Chen, J.-C., 2021. Resourcization and valorization of waste incineration fly ash for the synthesis of zeolite and applications. Journal of Environmental Chemical Engineering 9(6).

Ma, Y., Yan, C., Alshameri, A., Qiu, X., Zhou, C., li, D., 2014. Synthesis and characterization of 13X zeolite from low-grade natural kaolin. Advanced Powder Technology 25(2), 495-499.

Mori, H., 2003. Extraction of silicon dioxide from waste colored glasses by alkali fusion using potassium hydroxide. Journal of Materials Science(38), 3461-3468.

Mymrin, V., Pedroso, D.E., Pedroso, C., Alekseev, K., Avanci, M.A., Winter, E., Cechin, L., Rolim, P.H.B., Iarozinski, A., Catai, R.E., 2018. Environmentally clean composites with hazardous aluminum anodizing sludge, concrete waste, and lime production waste. Journal of Cleaner Production 174, 380-388.

Nekhunguni, P.M., Tavengwa, N.T., Tutu, H., 2017. Investigation of As(V) removal from acid mine drainage by iron (hydr) oxide modified zeolite. Journal of Environmental Management 197, 550-558.

Paul, T., Sinharoy, A., Pakshirajan, K., Pugazhenthi, G., 2020. Lipid-rich bacterial biomass production using refinery wastewater in a bubble column bioreactor for bio-oil conversion by hydrothermal liquefaction. Journal of Water Process Engineering 37.

Plackett, R.L., Burman, J.P., 1946. The design of optimum multifactorial experiments. Biometrika 33, 305-325.

Pugazhenthi, G., Vinoth Kumar, R., 2017. Removal of chromium from synthetic wastewater using MFI zeolite membrane supported on inexpensive tubular ceramic substrate. Journal of Water Reuse and Desalination 7(3), 365-377.

Qiang, Z., Shen, X., Guo, M., Cheng, F., Zhang, M., 2019. A simple hydrothermal synthesis of zeolite X from bauxite tailings for highly efficient adsorbing CO2 at room temperature. Microporous and Mesoporous Materials 287, 77-84.

Rahman, M.A., Gafur, M.A., Kurny, A.S.W., 2013. Kinetics of recovery of alumina from coal fly ash through fusion with sidoum hydroxide. American Journal of Materials Engineering and Technology 1(3), 54-58.

Ramteke, D.D., Hujova, M., Kraxner, J., Galusek, D., Romero, A.R., Falcone, R., Bernardo, E., 2021. Up-cycling of 'unrecyclable' glasses in glass-based foams by weak alkali-activation, gel casting and low-temperature sintering. Journal of Cleaner Production 278.

Robson, H., Lillerud, K. P., 2016. Verified synthesis of zeolitic materials. International Zeolite Association.

Salzmann, R.D., Ackerman, J.N., Cicek, N., 2020. Pilot-scale, on-site investigation of crushed recycled glass as tertiary filter media for municipal lagoon wastewater treatment. Environ Technol, 1-9.

Silva, J.A.D., A, F.M.B., Fermoso, F.G., Zaiat, M., Silva, G.H.R., 2021. Evaluation of the influence of trace metals on methane production from domestic sewage, using the Plackett-Burman experimental design. J Environ Manage 294, 113002.

Sivalingam, S., Sen, S., 2018. Optimization of synthesis parameters and characterization of coal fly ash derived microporous zeolite X. Applied Surface Science 455, 903-910.

Sivalingam, S., Sen, S., 2019. Efficient removal of textile dye using nanosized fly ash derived zeolite-x: Kinetics and process optimization study. Journal of the Taiwan Institute of Chemical Engineers 96, 305-314.

Souza, M.T., Onghero, L., Repette, W.L., Raupp Pereira, F., de Oliveira, A.P.N., 2020. Sustainable cement with Al-anodizing waste: Evaluating reactivity and feasibility as a shrinkage-compensating admixture. Journal of Building Engineering 30.

Souza, M.T., Simao, L., Montedo, O.R.K., Raupp Pereira, F., de Oliveira, A.P.N., 2019. Aluminum anodizing waste and its uses: An overview of potential applications and market opportunities. Waste Manag 84, 286-301.

Tran, Y.T., Lee, J., Kumar, P., Kim, K.-H., Lee, S.S., 2019. Natural zeolite and its application in concrete composite production. Composites Part B: Engineering 165, 354-364.

Vereshchagina, T.A., Kutikhina, E.A., Solovyov, L.A., Vereshchagin, S.N., Mazurova, E.V., Chernykh, Y.Y., Anshits, A.G., 2018. Synthesis and structure of analcime and analcime-zirconia composite derived from coal fly ash cenospheres. Microporous and Mesoporous Materials 258, 228-235.

Vidal, C.B., Raulino, G.S., Barros, A.L., Lima, A.C., Ribeiro, J.P., Pires, M.J., Nascimento, R.F., 2012. BTEX removal from aqueous solutions by HDTMA-modified Y zeolite. J Environ Manage 112, 178-185.

Vigil de la Villa Mencía, R., Goiti, E., Ocejo, M., Giménez, R.G., 2020. Synthesis of zeolite type analcime from industrial wastes. Microporous and Mesoporous Materials 293.

Vilaca, N., Amorim, R., Machado, A.F., Parpot, P., Pereira, M.F., Sardo, M., Rocha, J., Fonseca, A.M., Neves, I.C., Baltazar, F., 2013. Potentiation of 5-fluorouracil encapsulated in zeolites as drug delivery systems for in vitro models of colorectal carcinoma. Colloids Surf B Biointerfaces 112, 237-244.

Xie, W.-M., Zhou, F.-P., Bi, X.-L., Chen, D.-D., Li, J., Sun, S.-Y., Liu, J.-Y., Chen, X.-Q., 2018. Accelerated crystallization of magnetic 4A-zeolite synthesized from red mud for application in removal of mixed heavy metal ions. Journal of Hazardous Materials 358, 441-449.

Yao, G., Lei, J., Zhang, X., Sun, Z., Zheng, S., Komarneni, S., 2018. Mechanism of zeolite X crystallization from diatomite. Materials Research Bulletin 107, 132-138.

Yuan, J., Yang, J., Ma, H., Liu, C., 2016. Crystal structural transformation and kinetics of NH4+/Na+ ion-exchange in analcime. Microporous and Mesoporous Materials 222, 202-208.

CAPÍTULO 6: CONCLUSÃO

Zeólitas são minerais microporosos que possuem elevada eficiência no tratamento de efluentes. Apesar de ser extensivamente investigada na literatura para esta finalidade, a maioria dos estudos analisa o processo em escala de bancada, sendo necessário estender os esforços para escala piloto, de modo a determinar a viabilidade técnico-econômica de sua aplicação em larga escala. Além disso, diversos pontos que precisam de maior aprofundamento em determinados sistemas de adsorção foram identificados, sendo sua investigação necessária para a total compreensão dos mecanismos de adsorção presentes em tais sistemas.

O pó de vidro e a lama de anodização de alumínio são materiais que demonstraram possuir as características necessárias para a síntese da zeólita analcima pura, com alta cristalinidade. A otimização das variáveis do processo consideradas pode elevar a cristalinidade da analcima, aumentando ainda mais sua eficiência na aplicação como adsorvente. Dessa forma, a produção de zeólitas sintéticas contribui com redução da emissão de resíduos sólidos pela sua conversão em adsorventes de baixo custo que podem beneficiar indústrias que devem tratar seus efluentes antes do descarte, inclusive o setor da mineração.

CAPÍTULO 7: SUGESTÕES PARA TRABALHOS FUTUROS

Pelos resultados obtidos no desenvolvimento desta pesquisa, foram levantados alguns pontos que podem investigados:

- Otimização das variáveis consideradas estatisticamente relevantes, para elevação da cristalinidade da analcima sintética;

- Avaliar a remoção de íons de chumbo, visando aplicação no tratamento de efluentes do processo de beneficiamento de minérios de chumbo;

- Avaliar o impacto na seletividade de flotação da galena pela remoção de Pb^{2+} pela analcima;

- Avaliar a síntese de outras fases zeolíticas a partir do PV e LAA.